

Analysis, detection and control of secure and safe cyber-physical control systems in a unified framework

Linlin Li, Steven X. Ding, Maiying Zhong, Dong Zhao, Yang Shi

Abstract—This paper deals with analysis, simultaneous detection of faults and attacks, fault-tolerant control and attack-resilient of cyber-physical control systems. In our recent work, it has been observed that an attack detector driven by an input residual signal is capable of reliably detecting attacks. In particular, observing system dynamics from the perspective of the system input-output signal space reveals that attacks and system uncertainties act on different system subspaces. These results motivate our exploration of secure and safe cyber-physical control systems in the unified framework of control and detection. The unified framework is proposed to handle control and detection issues uniformly and in subspaces of system input-output data. Its mathematical and control-theoretic basis is system coprime factorizations with Bezout identity at its core. We firstly explore those methods and schemes of the unified framework, which serve as the major control-theoretic tool in our work. It is followed by re-visiting and examining established attack detection and resilient control schemes. The major part of our work is the endeavours to develop a control-theoretic paradigm, in which analysis, simultaneous detection of faults and attacks, fault-tolerant and attack-resilient control of cyber-physical control systems are addressed in a unified manner.

Index Terms—Attack detection, fault detection, fault-tolerant control, resilient control, stealthy attacks, system vulnerability, system privacy-preserving, unified framework

I. INTRODUCTION

TODAY'S automatic control systems as the centerpiece of industrial cyber-physical systems (CPSs) are fully equipped with intelligent sensors, actuators and a modern information infrastructure. It is a logic consequence of ever increasing demands for system performance and production efficiency that today's automatic control systems are of an extremely high degree of integration, automation and complexity [1]. Maintaining reliable and safe operations of cyber-physical control systems (CPCSSs) are of elemental importance for optimally managing industrial CPSs over the whole operation

This work has been supported by the National Natural Science Foundation of China under Grants 62322303, and 62233012.

L. Li is with School of Automation and Electrical Engineering, University of Science and Technology Beijing, Beijing 100083, P. R. China, Email: linlin.li@ustb.edu.cn

S. X. Ding is with the Institute for Automatic Control and Complex Systems (AKS), University of Duisburg-Essen, Germany. Email: steven.ding@uni-due.de

M. Zhong is with the College of Electrical Engineering and Automation, Shandong University of Science and Technology, Qingdao 266590, China. Email: mzhong@buaa.edu.cn

D. Zhao is with School of Cyber Science and Technology, Beihang University, Beijing 100191, China. E-mail: dzhao@buaa.edu.cn

Y. Shi is with Department of Mechanical Engineering, University of Victoria, Victoria, BC, V8W 2Y2, Canada. E-mail: yshi@uvic.ca

life-cycle. As an indispensable maintenance functionality, real-time monitoring, fault detection (FD) and fault-tolerant control (FTC) [1]–[5] are widely integrated in CPCSSs and run parallel to the embedded control systems. In a traditional automatic control system, FD and FTC are mainly dedicated to maintaining functionalities of sensors and actuators as these key components become defective [1], [6].

Recently, a new type of malfunctions, the so-called cyber-attacks on CPSs, have drawn attention to the urgent need for developing new monitoring, diagnosis and resilient control strategies [7]–[13]. Cyber-attacks can not only considerably affect functionalities of sensors and actuators, but also impair communications among the system components and subsystems. Differing from technical faults, cyber-attacks are artificially created. As the main categories of malicious attacks, denial-of-service (DoS) attacks [8], [14] and deception attacks [8], attract major research attention. By blocking the communication links of system components over networks, DoS attacks can degrade system performance [15]. The deception attacks are usually designed to cause system performance degradation through modifying data packets without being detected and may lead to immense damages during system operations [8], [10], [16]. In particular, it was shown that attackers with model knowledge can exploit specified system dynamics to construct perfectly stealthy sensor and actuator attacks that evade classical Luenberger or Kalman-filter-based residuals [17], [18]. These results revealed intrinsic vulnerabilities of passive observer-based detectors and provided a unifying framework linking cyber-attack detection to classical concepts from fault detection. Building on this foundation, a large body of work like observer-based FD methods, unknown-input observers, parity relations, and structured observer banks have been proposed to detect the so-called replay, zero dynamics, covert attacks, false data injection attacks, also called integrity stealthy attacks [7], [8], [19]–[23]. Complementary to it, active detection approaches such as dynamic watermarking inject designed excitation signals into the control inputs, rendering attacks statistically detectable [24].

As a response to the security issues of CPSs, resilient control, where the objective is to maintain closed-loop stability and acceptable performance despite ongoing attacks, has received increasing attention from both the research and application domains. As appropriate countermeasures, the so-called resource-aware secure control methods [9], [25], like event-triggered control algorithms or switching control mechanisms, are prevalent resilient control schemes. These methods make

the CPSs highly resilient against attacks by means of optimal management of data communications among subsystems in the CPS. Beyond detection, observer-based methods also play a key role in resilient control. Typical architectures integrate attack detection with controller reconfiguration or compensation mechanisms, e.g. via switching observers and controllers or attack-tolerant state estimators [26]. Further methods include model predictive control [27], adaptive control [28], and sliding mode control [29].

The argument that a detailed understanding of attack mechanisms is fundamental for assessing CPS vulnerabilities and informing the development of defense strategies has spurred significantly recent interest in attack design [23], [30]–[36]. Attack design presupposes that attackers are in the possession of partial or full system knowledge. In this context, a further type of cyber-attacks, the so-called eavesdropping attacks, play a key role [8], [13]. Although such attacks do not cause changes in system dynamics and performance degradation, they enable adversary to gain system knowledge, which is especially critical when an attacker uses such knowledge for designing stealthy attacks. This shift has revealed new and fundamental privacy risks that motivated recent research on privacy preserving and protection issues [13], [37]–[39].

In our recent work, we observed that an observer-based attack detector with an output residual generator is less capable than an attack detector driven by an input residual signal [40]. Stimulated by this observation, our further exploration revealed meaningful evidence [41], [42] that

- attacks can be equivalently expressed by an unknown input in the system input, which is exactly the input residual signal, and
- attacks and system uncertainties, including faults, affect the system dynamics in a dual manner.

In particular, when the system dynamics are examined from the perspective of the system input-output signal space, it is plainly seen that attacks and system uncertainties act on different subspaces. This prospect is strongly obscured, as viewing a CPCS from the perspective of a classic closed-loop configuration. From that point of view, the influences of attacks and system uncertainties on the system dynamic are fully corrupted, which considerably hinder a reliable attack detection and even simultaneous detection of attacks and faults. These results have motivated us to explore secure and safe CPCSs in the unified framework of control and detection [41], [42].

On account of the cognition that both feedback control and fault detection systems are driven by (output) residual signal, the unified framework has been initially proposed to manage control and detection issues uniformly, in which control and detection problems are handled in subspaces of system input-output data, rather than in a closed-loop configuration. Its groundwork is the output-input residual signals, serving as indicators that fully characterize the system nominal behavior and uncertain dynamics, including uncertainties induced by faults and cyber-attacks. The mathematical and control-theoretic basis of the framework is coprime factorizations of plant models and feedback controllers, where the Bezout identity, defining

a unimodular linear isomorphism between the input-output signals and the residual signals, is at its core [42].

Inspired by these observations, the main objective of this paper is to leverage the unified framework of control and detection to study issues of analysis, simultaneous detection, fault-tolerant and resilient control of cyber-physical control systems under attacks and faults. Our work comprises three steps. We will firstly explore those methods and schemes in the unified framework, which serve as the major control-theoretic tool to deal with the related issues. It is followed by re-visiting and examining state of the art methods of the relevant techniques, in particular attack detection and resilient control schemes. The last step, the major part of our work, is the endeavours to develop a control-theoretic paradigm, in which analysis, simultaneous detection of faults and attacks, fault-tolerant and attack-resilient control of CPCSs are unified addressed. Our work will deliver the following contributions:

- Establishment of control-theoretic setting for the subsequent work on secure CPCSs with system image and residual subspaces in its core (Definitions 1-3), gap metric as the distance between two subspaces, Bezout identities and the associated transformations, and coprime factorizations of the plant and controllers (Theorem 1 and Corollary 1) as the basic mathematical and control-theoretic tool;
- Exploration of secure CPCS configurations, particularly the Plug-and-Play (PnP) structure that builds the basic system configuration for the proposed fault-tolerant and attack-resilient control scheme (Subsection III-C1);
- Alternative and enhanced forms of three well-established attack detection and resilient control schemes, the MTD and watermark methods (Subsections III-C2-III-C3), the auxiliary system-based detection method (Subsection V-A2), and characterization of zero dynamics attacks in the unified framework (Subsection III-C4);
- Introduction of the concept of attack information potential between the plant and control station that builds the basis for attack detection and resilient control study (IV-B1), and proof of two elementary forms of the system dynamic under cyber-attacks, (i) on the plant side (Theorem 5), and (ii) on the control station side (Theorem 6);
- Demonstration of the duality between the faulty dynamic and attack dynamic (Subsection IV-B3);
- Introduction of the concepts of attack detectability, as a general and detection method-independent definition of stealthy attacks, the actuability of attacks that is overlooked in the literature, but important for addressing attack design issues, and proof of the existence conditions (Subsection IV-C1);
- Exploration of image attacks as a general form of undetectable (stealthy) attacks that simplifies (stealthy) attacks design (Subsection IV-C1);
- Introduction of attack stability margin as a measure of the system vulnerability (Subsection IV-C2) and proof of a sufficient condition of the system vulnerability under image attacks (Theorem 10);
- Exploration of three schemes of simultaneous detection

- of faults and attacks (Subsection V-A);
- Exploration of a fault-tolerant and attack-resilient control system (V-B) with a performance analysis (Theorems 12-13) and a proof of the stability condition (Theorem 14);
- Exploration of a subspace-based privacy-preserving scheme whose core is a privacy filter generating an auxiliary signal (V-C);
- Introduction of the concepts of system-level privacy and \mathcal{L}_2 -privacy based on the similarity of two system subspaces and measured by gap metric (Definitions 8-9);
- Formulation and solution of the \mathcal{L}_2 -privacy-filter design as an optimization problem (Theorem 16).

Notations. Throughout this paper, standard notations known in control theory and linear algebra are adopted. In addition, ℓ_2 is the space of square-summable sequences over $(-\infty, \infty)$, $\ell_2([0, \infty))$ is its subspace of causal sequences. \mathcal{H}_2 is the Hardy space of z -transforms of sequences in $\ell_2([0, \infty))$. \mathcal{RH}_∞ (\mathcal{RL}_∞) denotes the space of real-rational, proper transfer functions with poles in the unit disk (without poles on $|z| = 1$). $G^*(z) = G^T(z^{-1})$ is the conjugate of $G(z)$.

II. PRELIMINARIES AND PROBLEM FORMULATION

A. Configuration of feedback control systems

The linear discrete-time invariant (LDTI) feedback control systems are considered in this work and modelled by

$$\begin{cases} y(z) = G(z)u(z) + r_{y,0}(z) \\ u(z) = K(z)y(z) + r_{u,0}(z), \end{cases} \quad (1)$$

where $u \in \mathbb{R}^p$ and $y \in \mathbb{R}^m$ represent the plant input and output vectors, respectively. $G(z)$ is the transfer function matrix with the minimal state space realisation (A, B, C, D) described by

$$\begin{cases} x(k+1) = Ax(k) + Bu(k) \\ y(k) = Cx(k) + Du(k) + r_{y,0}(k). \end{cases} \quad (2)$$

Here, $x \in \mathbb{R}^n$ is the state vector, matrices A, B, C, D are known and of appropriate dimensions. The transfer function matrix $K(z)$ denotes an LDTI control system that will be described in the next subsection, and $(r_{u,0}, r_{y,0})$ model a given control command and uncertainties in the plant, respectively, and will be specified in the sequel.

B. System coprime factorizations

Coprime factorizations of transfer function matrices [43], [44] play an essential role in our subsequent study and serves as a basic tool. Given the plant model G , the factorizations

$$G(z) = N(z)M^{-1}(z) = \hat{M}^{-1}(z)\hat{N}(z), \quad (3)$$

$M(z), N(z), \hat{M}(z), \hat{N}(z) \in \mathcal{RH}_\infty$, are called right coprime factorization (RCF) and left coprime factorization (LCF) of $G(z)$, respectively, if there exist $X(z), Y(z), \hat{X}(z), \hat{Y}(z) \in \mathcal{RH}_\infty$ such that

$$[X(z) \ Y(z)] \begin{bmatrix} M(z) \\ N(z) \end{bmatrix} = I, \quad [-\hat{N}(z) \ \hat{M}(z)] \begin{bmatrix} -\hat{Y}(z) \\ \hat{X}(z) \end{bmatrix} = I. \quad (4)$$

Note that $(X(z), Y(z))$ and $(\hat{X}(z), \hat{Y}(z))$ are left- and right coprime pairs (LCP and RCP), respectively. It is known that

$$[X(z) \ Y(z)] \begin{bmatrix} -\hat{Y}(z) \\ \hat{X}(z) \end{bmatrix} = 0 \iff X(z)\hat{Y}(z) = Y(z)\hat{X}(z). \quad (5)$$

The double Bezout identity [43], [44] gives a compact form of (3)-(4),

$$\begin{bmatrix} X(z) & Y(z) \\ -\hat{N}(z) & \hat{M}(z) \end{bmatrix} \begin{bmatrix} M(z) & -\hat{Y}(z) \\ N(z) & \hat{X}(z) \end{bmatrix} = I. \quad (6)$$

The Bezout identity (6) plays an essential role in our subsequent work. In particular, the state space realizations of the eight transfer functions in (6) and the associated alternative system representations build the cornerstone of our work.

The RCF $(M(z), N(z))$ is a state feedback control system given by

$$\begin{cases} x(k+1) = A_Fx(k) + BVv(k), A_F = A + BF \\ \begin{bmatrix} u(k) \\ y(k) \end{bmatrix} = \begin{bmatrix} Fx(k) + Vv(k) \\ C_Fx(k) + DVv(k) \end{bmatrix}, C_F = C + DF, \end{cases} \quad (7)$$

$$\begin{bmatrix} u(z) \\ y(z) \end{bmatrix} = I_G(z)v(z), I_G(z) = \begin{bmatrix} M(z) \\ N(z) \end{bmatrix}, \quad (8)$$

$$M = (A_F, BV, F, V), N = (A_F, BV, C_F, DV). \quad (9)$$

The system (7)/(8) is also called stable image representation (SIR). As the dual system of the SIR, the LCF $(\hat{M}(z), \hat{N}(z))$ is an **observer-based residual generator** described by

$$\begin{cases} \hat{x}(k+1) = A_L\hat{x}(k) + B_K \begin{bmatrix} u(k) \\ y(k) \end{bmatrix}, A_L = A - LC \\ r_y(k) = C_K\hat{x}(k) + D_K \begin{bmatrix} u(k) \\ y(k) \end{bmatrix}, C_K = WC \\ B_K = [B_L \ -L], B_L = B - LD, D_K = [WD \ W], \end{cases} \quad (10)$$

$$r_y(z) = K_G(z) \begin{bmatrix} u(z) \\ y(z) \end{bmatrix}, K_G(z) = [-\hat{N}(z) \ \hat{M}(z)], \quad (11)$$

$$\hat{M} = (A_L, -L, C_K, W), \hat{N} = (A_L, B_L, C_K, WD), \quad (12)$$

which is called stable kernel representation (SKR). The RCP and LCP, $(\hat{X}(z), \hat{Y}(z))$ and $(X(z), Y(z))$, are **observer-based state feedback control and input residual generator systems**, respectively, and modelled by

$$\begin{cases} \hat{x}(k+1) = A_F\hat{x}(k) + LW^{-1}r_y(k), \\ \begin{bmatrix} u(k) \\ y(k) \end{bmatrix} = \begin{bmatrix} F \\ C_F \end{bmatrix}\hat{x}(k) + \begin{bmatrix} 0 \\ W^{-1} \end{bmatrix}r_y(k), \end{cases} \quad (13)$$

$$\begin{bmatrix} u(z) \\ y(z) \end{bmatrix} = \begin{bmatrix} -\hat{Y}(z) \\ \hat{X}(z) \end{bmatrix}r_y(z), \quad (14)$$

$$\hat{Y} = (A_F, -LW^{-1}, F, 0), \hat{X} = (A_F, LW^{-1}, C_F, W^{-1}), \quad (15)$$

$$\begin{cases} \hat{x}(k+1) = A_L\hat{x}(k) + B_K \begin{bmatrix} u(k) \\ y(k) \end{bmatrix} \\ r_u(k) = V^{-1}F\hat{x}(k) + [V^{-1} \ 0] \begin{bmatrix} u(k) \\ y(k) \end{bmatrix}, \end{cases} \quad (16)$$

$$r_u(z) = [X(z) \ Y(z)] \begin{bmatrix} u(z) \\ y(z) \end{bmatrix}, \quad (17)$$

$$X = (A_L, -B_L, V^{-1}F, V^{-1}), Y = (A_L, -L, V^{-1}F, 0). \quad (18)$$

Here, F, L are selected such that A_F and A_L are Schur matrices, and W and V are invertible matrices [1], [44].

Remark 1. For the sake of simplicity but without loss of generality, it is often assumed in our subsequent work that $W = I, V = I$.

Notice that (14) and (17) imply

$$\begin{aligned} u(z) &= -\hat{Y}(z)r_y(z) = -\hat{Y}(z)\hat{X}^{-1}(z)y(z), \\ X(z)u(z) + Y(z)y(z) &= r_u(z) = 0 \\ \implies u(z) &= -X^{-1}(z)Y(z)y(z). \end{aligned}$$

That is, the control law $K(z)$ in (1) is given by

$$K(z) = -\hat{Y}(z)\hat{X}^{-1}(z) = -X^{-1}(z)Y(z) \quad (19)$$

with $(\hat{X}(z), \hat{Y}(z))$ and $(X(z), Y(z))$ as its RCF and LCF. In other words, the feedback controller in (19) is equivalent to an observer-based state feedback controller or an input residual generator

$$r_u(z) = u(z) - F\hat{x}(z) = X(z)u(z) + Y(z)y(z). \quad (20)$$

It is of remarkable interest to notice that both residual generators, (11) and (17), share the same state observer.

We now introduce a special type of LCF and RCF of the plant dynamic. They are called normalized coprime factorisations, denoted by (\hat{M}_0, \hat{N}_0) and (M_0, N_0) , respectively, and satisfy

$$[\hat{N}_0(z) \quad \hat{M}_0(z)] \begin{bmatrix} \hat{N}_0^*(z) \\ \hat{M}_0^*(z) \end{bmatrix} = I, \quad (21)$$

$$[M_0^*(z) \quad N_0^*(z)] \begin{bmatrix} M_0(z) \\ N_0(z) \end{bmatrix} = I. \quad (22)$$

The state space realizations of (\hat{M}_0, \hat{N}_0) and (M_0, N_0) are summarized in the following lemma [45].

Lemma 1. Given the system model (3), (\hat{M}_0, \hat{N}_0) and (M_0, N_0) are LCP and RCP with $L = L_0, W = W_0, F = F_0$ and $V = V_0$, as given below:

$$L_0 = (BD^T + APC^T)(I + DD^T + CPC^T)^{-1}, \quad (23)$$

$$W_0 = (I + DD^T + CPC^T)^{-1/2}, \quad (24)$$

$$F_0 = -(I + D^T D + B^T S B)^{-1}(D^T C + B^T S A), \quad (25)$$

$$V_0 = (I + D^T D + B^T S B)^{-1/2}. \quad (26)$$

Here, $P > 0, S > 0$ solve the following Riccati equations respectively,

$$P = APA^T + BB^T - L_0(I + DD^T + CPC^T)L_0^T, \quad (27)$$

$$S = A^T S A + C^T C - F_0^T(I + D^T D + B^T S B)F_0. \quad (28)$$

The normalized SIR and SKR can be interpreted as a linear quadratic (LQ) controller and a least squares (LS) estimator, respectively [43], and will serve as a useful tool in our subsequent study.

Remark 2. Hereafter, we may drop the domain variable z or k when there is no risk of confusion.

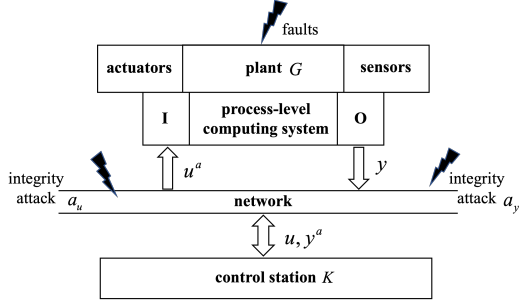


Fig. 1. The CPCS under consideration

C. Youla parameterization and its observer-based realization

Youla parameterization is a well-established method that, for given the LCFs and RCFs of the plant G and controller K , parametrizes all stabilizing controllers as

$$K = -(\hat{Y} - MQ)(\hat{X} + NQ)^{-1} = -(X + Q\hat{N})^{-1}(Y - Q\hat{M}) \quad (29)$$

where $Q \in \mathcal{RH}_\infty$ is the parameter system [43], [44]. For our investigation purpose, the observer-based realization of (29) is presented [1],

$$\begin{cases} \hat{x}(k+1) = A_F\hat{x}(k) + Br_Q(k) + LW^{-1}r_y(k) \\ u(k) = F\hat{x}(k) + r_Q(k), \end{cases} \quad (30)$$

$$r_Q = Qr_y = Q(\hat{M}y - \hat{N}u),$$

which is equivalent to

$$\begin{bmatrix} u \\ y \end{bmatrix} = \begin{bmatrix} -\hat{Y} + MQ \\ \hat{X} + NQ \end{bmatrix} r_y$$

with r_y acting as the latent variable. Now, let the observer (30) be equivalently written into the observer form (16). It turns out

$$u - F\hat{x} = Xu + Yy = Qr_y, \quad (31)$$

which is the input residual realization of the Youla parameterization (29).

D. Problem formulation

As schematically sketched in Fig. 1, the feedback control system (1) is implemented in a CPCS configuration, where the plant G is connected to the control station K by a communication network. The control station calculates u and transmits it to the plant. The plant receives control signal u^a and sends the measurement output y to the control station. Specifically, the CPCS model is described by

$$\begin{cases} y(z) = G(z)u^a(z) + f_0(z) + r_{y,0}(z) \\ u(z) = K(z)y^a(z) + r_{u,0}(z), \end{cases} \quad (32)$$

where K is the feedback control law subject to (19), $r_{u,0} = \bar{v}$ is the reference signal, f_0 denotes the influence of faults on the system dynamic that will be specified in the sequel, and

$$u^a = u + a_u, y^a = y + a_y \quad (33)$$

represent the input and output signals transmitted over the network and corrupted by the injected attack signals (a_u, a_y) . On the assumption that the attacker is able to access the input

and output (transmission) channels and inject signals into the channels, it is supposed that the cyber-attacks (a_u, a_y) are modelled by

$$\begin{bmatrix} a_u(z) \\ a_y(z) \end{bmatrix} = \Pi^a(z) \begin{bmatrix} u(z) \\ y(z) \end{bmatrix} + \begin{bmatrix} E_u \eta_u(z) \\ E_y \eta_y(z) \end{bmatrix} \quad (34)$$

where Π^a is a stable dynamic system with (u, y) as the input variables, (E_u, E_y) are structure matrices indicating which channels of the input u and output y are attacked, and (η_u, η_y) are ℓ_2 -bounded, unknown and independent of (u, y) . In this regard, $(E_u \eta_u, E_y \eta_y)$ and $\Pi^a [u^T \ y^T]^T$ are called additive and multiplicative attacks, respectively.

Remark 3. The term *multiplicative attacks* is rarely used in the literature on secure CPCSSs research. We adopt it to emphasize the fact that such attacks are driven by the process data. Differing from additive attacks, they affect system eigen-dynamics. For instance, a replay attack defined by

$$y^a(k) = y(k-T), \quad k > T(>0),$$

is a multiplicative attack [40], that is,

$$a_y(z) = -y(z) + z^{-T} y(z) \implies y^a = z^{-T} y, \\ \Pi^a = \begin{bmatrix} \Pi_u^a \\ \Pi_y^a \end{bmatrix}, \quad \Pi_y^a = [0 \ z^{-T} - I]$$

with Π_u^a arbitrarily designed by attackers. DoS attacks are random multiplicative attacks as well. In fact, multiplicative attacks are often implicitly adopted for attack design [46], [47].

For the sake of simplicity, the uncertainty $r_{y,0}$ is assumed to be the output of an LTI system driven by additive disturbances. Corresponding to the state space realization of G , (2), the dynamic of $r_{y,0}$ is modelled by

$$r_{y,0} = G_d d, \quad G_d = C(zI - A)^{-1} E_d + F_d, \quad (35)$$

where two types of the unknown input $d \in \mathbb{R}^{k_d}$ are under consideration,

$$\begin{bmatrix} E_d \\ F_d \end{bmatrix} d = \begin{cases} \begin{bmatrix} w \\ v \end{bmatrix}, & \text{process and measurement noises} \\ \begin{bmatrix} \bar{E}_d d_P \\ \bar{F}_d d_S \end{bmatrix}, & \|\bar{d}\|_2 = \sqrt{\|\bar{d}_P\|_2^2 + \|\bar{d}_S\|_2^2} \leq \delta_d. \end{cases} \quad (36)$$

$w \sim \mathcal{N}(0, \Sigma_w)$, $\nu \sim \mathcal{N}(0, \Sigma_\nu)$ are white noise series, δ_d is the known upper-bound and \bar{E}_d, \bar{F}_d are known matrices. The vector f_0 represents the influence of faults on the plant dynamic, which is modelled by

$$f_0(z) = \Pi_0^f(z) \begin{bmatrix} u(z) \\ y(z) \end{bmatrix} + \bar{f}_0(z). \quad (37)$$

The fault model (37) is a general form of multiplicative faults. Here, Π_0^f is assumed to be a stable unknown dynamic system and the additive fault \bar{f}_0 is ℓ_2 -bounded.

Remark 4. The additive fault affects the system dynamic in a way like the unknown disturbances modelled by (35). In fact, in the context of fault diagnosis and fault-tolerant control, multiplicative faults are considerably critical, because

they might impair the system eigen-dynamic and even cause instability.

Along the lines of the three-step explorations procedure towards the objective of this paper, the following problems will be addressed. At first, the core ideas, basic methods, and analysis and design schemes are examined aiming at exploring those, which are particularly appropriate for studying CPCSSs under faults and attacks modelled by (32)-(37). This work will be complemented by reviewing well-established attack detection and resilient control methods. In particular, it is of importance to re-formulate these methods in the unified framework of control and detection, and to examine how far they might be generalized and improved. The main part of our work is the endeavour to establish a control-theoretic paradigm, which enables, in a unified manner,

- analyzing (i) CPCS's structural and information properties, (ii) system behavior under faults and attacks, (iii) existence conditions of stealthy attacks, expressed in terms of the system dynamic and information model and independent of applied detection schemes, and (iii) specified system vulnerability;
- developing schemes of simultaneous detection of faults and attacks;
- exploring fault-tolerant and attack-resilient feedback control systems with an analysis of the achievable control performance and stability conditions, and finally
- addressing system privacy issues in the unified framework of control and detection.

III. THE UNIFIED FRAMEWORK OF CONTROL AND DETECTION, AND APPLICATIONS TO SECURE CPCSS

The unified framework is proposed to deal with control and detection issues uniformly. In this framework, the control and detection problems are handled in the space of the system input and output data (u, y) . Its groundwork is both the output and input residual signals. Instead of the loop model (32), the so-called kernel-based system model is introduced, based on which the system image and residual subspaces are defined. Thereby, the input and output residual pair (r_u, r_y) serves as latent variables that comprise information of the system dynamic, including the nominal system behavior and uncertainties. Consequently, the overall system dynamic, during nominal operation and under faults and attacks, is fully characterized by the residual pair (r_u, r_y) and the associated subspaces. In this context, detection of faults and cyber-attacks, and fault-tolerant and attack-resilient control can be addressed uniformly. In fact, both the controllers and detectors are residual-driven, whose core is a (single) observer. In the framework, the Bezout identity serves as the core mathematical tool. On its basis, the coprime factorizations of the plant and controller can be parameterized by a dynamic system triple $(R(z), Q(z), T(z))$. On the other hand, the system image and residual subspaces are invariant with respect to the dynamic system triple. This property is particularly useful to design and construct secure CPCSSs.

In this section, we firstly introduce the alternative loop model form, the kernel-based model, and the concepts of system image

and residual subspaces. They build the basis of our subsequent work. We will then parameterize the coprime factorizations of the plant and controller, and highlight their relations to the system image and residual subspaces. Finally, we will leverage the aforementioned results, serving as a control-theoretic and mathematical tool, to propose alternative methods to some established schemes in the research of secure CPCSSs.

A. Alternative loop model forms and signal subspaces

Consider the control system model (32) with K subject to (19). On the assumption that the system is operating attack-free, let us rewrite the model into

$$\begin{cases} r_y = \hat{M}y - \hat{N}u = \hat{M}(r_{y,0} + f_0) \\ r_u = Xu + Yy = Xr_{u,0} =: v, \end{cases} \quad (38)$$

whose state space representation is given by

$$\begin{aligned} \hat{x}(k+1) &= A_L \hat{x}(k) + B_K \begin{bmatrix} u(k) \\ y(k) \end{bmatrix}, \\ \begin{bmatrix} r_u(k) \\ r_y(k) \end{bmatrix} &= \begin{bmatrix} V^{-1}F \\ C_K \end{bmatrix} \hat{x}(k) + \begin{bmatrix} V^{-1} & 0 \\ WD & W \end{bmatrix} \begin{bmatrix} u(k) \\ y(k) \end{bmatrix}. \end{aligned} \quad (39)$$

The model (38) is called kernel-based model. Note that the model (38) is equivalent to

$$\begin{cases} W^{-1}r_y = y - \hat{y} \\ Vr_u = u - \hat{u} \end{cases} \Leftrightarrow \begin{cases} y = \hat{y} + W^{-1}r_y \\ u = \hat{u} + Vr_u, \end{cases}$$

$$\begin{bmatrix} \hat{u}(k) \\ \hat{y}(k) \end{bmatrix} = \begin{bmatrix} F \\ C \end{bmatrix} \hat{x}(k) + \begin{bmatrix} 0 \\ D \end{bmatrix} u(k).$$

That means, the kernel model is equivalent to the original loop model (32). The kernel-based model (38) is characterized by modelling any uncertainties in the control loop in term of the residual signals that are online computed. It is capable of fully describing the system dynamic online and under all possible (incl. under faults and attacks) operating conditions. Moreover, its core consists of a single observer, i.e. the state observer (39). Accordingly, the needed computation is moderate.

Attributed to the Bezout identity (6), the model (38) is recast into

$$\begin{bmatrix} u \\ y \end{bmatrix} = \begin{bmatrix} M \\ N \end{bmatrix} v + \begin{bmatrix} -\hat{Y} \\ \hat{X} \end{bmatrix} r_y. \quad (40)$$

The models (38) and (40) are two dual representation forms of the closed-loop (32) during attack-free operations. Observe that the output residual r_y ,

$$\begin{aligned} r_y &= \hat{M}(r_{y,0} + f_0) = \hat{N}_d d + f, \\ \hat{N}_d &= \hat{M}G_d = (A - LC, E_d - LF_d, C, F_d), \\ f &= \Pi^f \begin{bmatrix} u \\ y \end{bmatrix} + \bar{f}, \Pi^f = \hat{M}\Pi_0^f, \bar{f} = \hat{M}\bar{f}_0, \end{aligned} \quad (41)$$

includes exclusively uncertain and faulty dynamics in the plant. In contrast, the first term in (40) describes the nominal system dynamic. In other words, the model (40) highlights a notable fact that the uncertainties (including faults) and the reference signal v act on two different subspaces in the system input-output data space (u, y) . In this context, we introduce the following definitions.

Definition 1. Given the RCP and LCP (M, N) and (\hat{M}, \hat{N}) of the plant G , the \mathcal{H}_2 subspaces \mathcal{I}_G and \mathcal{K}_G ,

$$\mathcal{I}_G = \left\{ \begin{bmatrix} u \\ y \end{bmatrix} : \begin{bmatrix} u \\ y \end{bmatrix} = \begin{bmatrix} M \\ N \end{bmatrix} v, v \in \mathcal{H}_2^p \right\}, \quad (42)$$

$$\mathcal{K}_G = \left\{ \begin{bmatrix} u \\ y \end{bmatrix} : \begin{bmatrix} -\hat{N} & \hat{M} \end{bmatrix} \begin{bmatrix} u \\ y \end{bmatrix} = 0, \begin{bmatrix} u \\ y \end{bmatrix} \in \mathcal{H}_2^{m+p} \right\}, \quad (43)$$

are called (plant) image and kernel subspaces, respectively.

It is a well-known result that $\mathcal{I}_G = \mathcal{K}_G$ [48]. The complementary subspace of \mathcal{I}_G , \mathcal{I}_G^\perp , is of considerable importance in our subsequent work. It is apparent from the relation $\hat{N}\hat{M} - \hat{M}\hat{N} = 0$ that \mathcal{I}_G^\perp is characterized by

$$\forall \begin{bmatrix} u \\ y \end{bmatrix} \in \mathcal{I}_G^\perp, r_y = \begin{bmatrix} -\hat{N} & \hat{M} \end{bmatrix} \begin{bmatrix} u \\ y \end{bmatrix} \neq 0.$$

On the basis of the Bezout identity (6) and considering that r_y reflects the uncertain and faulty dynamics in the plant, we introduce the concept of residual subspace as the complementary subspace of \mathcal{I}_G .

Definition 2. Given the RCP (\hat{X}, \hat{Y}) of K , the \mathcal{H}_2 subspace

$$\mathcal{R}_G = \left\{ \begin{bmatrix} u \\ y \end{bmatrix} : \begin{bmatrix} u \\ y \end{bmatrix} = \begin{bmatrix} -\hat{Y} \\ \hat{X} \end{bmatrix} r, r \in \mathcal{H}_2^m \right\}, \quad (44)$$

is called canonical residual subspace.

Remark 5. In the above definition, we've abused the expression canonical residual subspace to distinguish it from the general form of residual subspace to be introduced in the next subsection.

It is noteworthy that the canonical residual subspace is the image subspace of the controller as well, i.e.

$$\mathcal{I}_K = \left\{ \begin{bmatrix} u \\ y \end{bmatrix} : \begin{bmatrix} u \\ y \end{bmatrix} = \begin{bmatrix} -\hat{Y} \\ \hat{X} \end{bmatrix} r, r \in \mathcal{H}_2^m \right\}.$$

Apparently, the residual subspace \mathcal{R}_G is the complement of \mathcal{I}_G , and

$$\mathcal{H}_2^{p+m} = \mathcal{I}_G \oplus \mathcal{R}_G = \mathcal{I}_G \oplus \mathcal{I}_K. \quad (45)$$

The system response (40) is indeed the consequence of (45) and it is sufficient to use the observer-based residual generator (11) to detect faults, which pinpoints the data in the residual subspace.

It is known that \mathcal{I}_G and \mathcal{R}_G are closed subspaces in \mathcal{H}_2 space [48]. Hence, by means of the orthogonal projection method and the concept gap metric [48] we are able to measure the similarity of two subspaces. The orthogonal projection method and gap metric are a mathematical tool that plays an essential role in the unified framework of control and detection [42], [49], [50]. Below, we summarize some basic definitions, concepts and computations of the orthogonal projection method, which will be applied in our subsequent work. For details, the reader is referred to [48], [51], [52]. Let (M_0, N_0) be the normalized RCP of G . The operator $\mathcal{P}_{\mathcal{I}_G}$,

$$\mathcal{P}_{\mathcal{I}_G} := \begin{bmatrix} M_0 \\ N_0 \end{bmatrix} \mathcal{P}_{\mathcal{H}_2} \begin{bmatrix} M_0 \\ N_0 \end{bmatrix}^*: \mathcal{H}_2 \rightarrow \mathcal{H}_2,$$

defines an orthogonal projection onto the system image subspace \mathcal{I}_G , where $\mathcal{P}_{\mathcal{H}_2}$ is the operator of the orthogonal projection onto \mathcal{H}_2 [51]. Given system data (u, y) , the distance from (u, y) to \mathcal{I}_G is defined as

$$\begin{aligned} \text{dist} \left(\begin{bmatrix} u \\ y \end{bmatrix}, \mathcal{I}_G \right) &= \inf_{\begin{bmatrix} u_{\mathcal{I}_G} \\ y_{\mathcal{I}_G} \end{bmatrix} \in \mathcal{I}_G} \left\| \begin{bmatrix} u \\ y \end{bmatrix} - \begin{bmatrix} u_{\mathcal{I}_G} \\ y_{\mathcal{I}_G} \end{bmatrix} \right\|_2 \\ &= \left\| (\mathcal{I} - \mathcal{P}_{\mathcal{I}_G}) \begin{bmatrix} u \\ y \end{bmatrix} \right\|_2. \end{aligned}$$

It holds (Pythagorean equation)

$$\left\| \begin{bmatrix} u \\ y \end{bmatrix} \right\|_2^2 = \left\| \mathcal{P}_{\mathcal{I}_G} \begin{bmatrix} u \\ y \end{bmatrix} \right\|_2^2 + \left\| (\mathcal{I} - \mathcal{P}_{\mathcal{I}_G}) \begin{bmatrix} u \\ y \end{bmatrix} \right\|_2^2. \quad (46)$$

For two systems G_1 and G_2 , the gap metric between $\mathcal{I}_{G_1}, \mathcal{I}_{G_2} \in \mathcal{H}_2^{m+p}$ is defined by

$$\begin{aligned} \delta(\mathcal{I}_{G_1}, \mathcal{I}_{G_2}) &= \max \left\{ \vec{\delta}(\mathcal{I}_{G_1}, \mathcal{I}_{G_2}), \vec{\delta}(\mathcal{I}_{G_2}, \mathcal{I}_{G_1}) \right\} \\ &= \left\| \mathcal{P}_{\mathcal{I}_{G_1}} - \mathcal{P}_{\mathcal{I}_{G_2}} \right\|, \end{aligned}$$

where $\vec{\delta}(\cdot, \cdot)$ is called directed gap, $\mathcal{P}_{\mathcal{I}_{G_1}} : \mathcal{H}_2 \rightarrow \mathcal{H}_2, \mathcal{P}_{\mathcal{I}_{G_2}} : \mathcal{H}_2 \rightarrow \mathcal{H}_2$, are orthogonal projection operators, respectively, and $\left\| \mathcal{P}_{\mathcal{I}_{G_1}} - \mathcal{P}_{\mathcal{I}_{G_2}} \right\|$ is the operator norm [48], [51], [52]. The gap metric $\delta(\mathcal{I}_{G_1}, \mathcal{I}_{G_2})$ is of the properties

$$\delta(\mathcal{I}_{G_1}, \mathcal{I}_{G_2}) \in [0, 1], \delta(\mathcal{I}_{G_1}, \mathcal{I}_{G_2}) = 1 \implies \mathcal{I}_{G_1} \perp \mathcal{I}_{G_2}, \quad (47)$$

$$\delta(\mathcal{I}_{G_1}, \mathcal{I}_{G_2}) = 0 \implies \mathcal{I}_{G_1} = \mathcal{I}_{G_2}, \quad (48)$$

and for $\delta(\mathcal{I}_{G_1}, \mathcal{I}_{G_2}) \in (0, 1)$,

$$\delta(\mathcal{I}_{G_1}, \mathcal{I}_{G_2}) = \vec{\delta}(\mathcal{I}_{G_1}, \mathcal{I}_{G_2}) = \vec{\delta}(\mathcal{I}_{G_2}, \mathcal{I}_{G_1}).$$

B. Parameterization of the coprime factorizations and Bezout identity

Notice that the RCFs and LCFs of G and K are parameterized by four matrices (F, L, V, W) . The following theorem describes the corresponding variations in the RCFs and LCFs caused by varying these four parameter matrices.

Theorem 1. Given $(M_i, N_i), (\hat{M}_i, \hat{N}_i), (\hat{X}_i, \hat{Y}_i), (X_i, Y_i)$ satisfying (9), (12), (15) and (18), respectively, $i = 1, 2$, it holds

$$\begin{bmatrix} \hat{M}_2 & \hat{N}_2 \end{bmatrix} = R_{21} \begin{bmatrix} \hat{M}_1 & \hat{N}_1 \end{bmatrix}, \quad (49)$$

$$\begin{bmatrix} M_2 \\ N_2 \end{bmatrix} = \begin{bmatrix} M_1 \\ N_1 \end{bmatrix} T_{21}, \quad (50)$$

$$\begin{bmatrix} X_1 & Y_1 \end{bmatrix} = T_{21} \begin{bmatrix} X_2 & Y_2 \end{bmatrix} + \bar{T}_{21} \begin{bmatrix} -\hat{N}_2 & \hat{M}_2 \end{bmatrix}, \quad (51)$$

$$\begin{bmatrix} -\hat{Y}_1 \\ \hat{X}_1 \end{bmatrix} = \begin{bmatrix} -\hat{Y}_2 \\ \hat{X}_2 \end{bmatrix} R_{21} + \begin{bmatrix} M_2 \\ N_2 \end{bmatrix} \bar{R}_{21}, \quad (52)$$

where $R_{21} = R_{12}^{-1}$ and $T_{21} = T_{12}^{-1}$ are invertible over \mathcal{RH}_∞ ,

$$R_{21} = W_2 \left(I - C(zI - A_{L_2})^{-1} (L_2 - L_1) \right) W_1^{-1} \in \mathcal{RH}_\infty,$$

$$T_{21} = V_1^{-1} \left(I + (F_2 - F_1)(zI - A_{F_2})^{-1} B \right) V_2 \in \mathcal{RH}_\infty,$$

$$\bar{T}_{21} = V_1^{-1} \left((F_2 - F_1)(zI - A_{F_2})^{-1} L_2 - \right) \in \mathcal{RH}_\infty,$$

$$\bar{R}_{21} = \begin{pmatrix} (F_1 - F_2)(zI - A_{F_1})^{-1} L_1 - \\ F_2(zI - A_{L_2})^{-1} (L_2 - L_1) \end{pmatrix} W_1^{-1} \in \mathcal{RH}_\infty.$$

While (49)-(50) are known result, the proof of (51)-(52) can be found in [40], [42].

An immediate result of Theorem 1 is that the closed-loop dynamic (40) is subject to

$$\begin{aligned} \begin{bmatrix} u \\ y \end{bmatrix} &= \begin{bmatrix} M_1 \\ N_1 \end{bmatrix} v + \begin{bmatrix} -\hat{Y}_1 \\ \hat{X}_1 \end{bmatrix} r_y \\ &= \begin{bmatrix} M_2 \\ N_2 \end{bmatrix} T_{12} v + \left(\begin{bmatrix} -\hat{Y}_2 \\ \hat{X}_2 \end{bmatrix} R_{21} + \begin{bmatrix} M_2 \\ N_2 \end{bmatrix} \bar{R}_{21} \right) r_y \\ &= \begin{bmatrix} M_2 \\ N_2 \end{bmatrix} v_2 + \left(\begin{bmatrix} -\hat{Y}_2 \\ \hat{X}_2 \end{bmatrix} + \begin{bmatrix} M_2 \\ N_2 \end{bmatrix} Q_2 \right) r_{y,2}, \quad (53) \\ v_2 &= T_{12} v, r_{y,2} = R_{21} \begin{bmatrix} -\hat{N}_1 & \hat{M}_1 \end{bmatrix} \begin{bmatrix} u \\ y \end{bmatrix}, Q_2 = \bar{R}_{21} R_{21}^{-1}. \end{aligned}$$

We are interested in a special case that is useful for our subsequent study.

Corollary 1. Given $(\hat{M}, \hat{N}), (M, N), (X, Y)$ and (\hat{X}, \hat{Y}) , with parameter matrices (F, L, V, W) , and their normalized realizations, $(\hat{M}_0, \hat{N}_0), (M_0, N_0), (X_0, Y_0)$, and associated with them, (\hat{X}_0, \hat{Y}_0) , it holds

$$\begin{aligned} \begin{bmatrix} u \\ y \end{bmatrix} &= \begin{bmatrix} M \\ N \end{bmatrix} v + \begin{bmatrix} -\hat{Y} \\ \hat{X} \end{bmatrix} r_y \\ &= \begin{bmatrix} M_0 \\ N_0 \end{bmatrix} v_0 + \left(\begin{bmatrix} -\hat{Y}_0 \\ \hat{X}_0 \end{bmatrix} + \begin{bmatrix} M_0 \\ N_0 \end{bmatrix} Q \right) r_0, \quad (54) \end{aligned}$$

$$\begin{bmatrix} v \\ r_y \end{bmatrix} = \begin{bmatrix} X & Y \\ -\hat{N} & \hat{M} \end{bmatrix} \begin{bmatrix} u \\ y \end{bmatrix} \iff \begin{bmatrix} v_0 - Rr_0 \\ r_0 \end{bmatrix} = \begin{bmatrix} X_0 - R\hat{N}_0 & Y_0 + R\hat{M}_0 \\ -\hat{N}_0 & \hat{M}_0 \end{bmatrix} \begin{bmatrix} u \\ y \end{bmatrix}, \quad (55)$$

$$v_0 = [X_0 \ Y_0] \begin{bmatrix} u \\ y \end{bmatrix}, r_0 = [-\hat{N}_0 \ \hat{M}_0] \begin{bmatrix} u \\ y \end{bmatrix},$$

$$Q = \bar{R}_0 R_0^{-1}, R = T_0^{-1} \bar{T}_0,$$

$$R_0 = W_0 \left(I - C(zI - A_{L_0})^{-1} (L_0 - L) \right) W^{-1},$$

$$\bar{R}_0 = \begin{pmatrix} (F - F_0)(zI - A_F)^{-1} L - \\ F_0(zI - A_{L_0})^{-1} (L_0 - L) \end{pmatrix} W^{-1},$$

$$T_0 = V^{-1} \left(I + (F_0 - F)(zI - A_{F_0})^{-1} B \right) V_0,$$

$$\bar{T}_0 = V^{-1} \left(\begin{array}{c} (F_0 - F)(zI - A_{F_0})^{-1} L_0 - \\ F(zI - A_L)^{-1} (L - L_0) \end{array} \right).$$

Proof. The proof follows from Theorem 1 and (53). \square

Observe that the second term of (53) is a special case of the observer-based Youla parameterization (30). In fact, on account of the general form of the Bezout identity [44],

$$\begin{bmatrix} X + Q\hat{N} & Y - Q\hat{M} \\ -\hat{N} & \hat{M} \end{bmatrix} \begin{bmatrix} M & -\hat{Y} + MQ \\ N & \hat{X} + NQ \end{bmatrix} = I \quad (56)$$

for $Q \in \mathcal{RH}_\infty$, the loop model (1), the models (38) and (40) are given by

$$\begin{cases} y = Gu + r_{y,0} \\ u = Ky + r_{u,0}, r_{u,0} = (X + Q\hat{N})^{-1} v, \end{cases} \quad (57)$$

$$\begin{cases} \hat{M}y - \hat{N}u = r_y \\ Xu + Yy = r_u, r_u = v + Qr_y, \end{cases} \quad (58)$$

$$\begin{bmatrix} u \\ y \end{bmatrix} = \begin{bmatrix} M \\ N \end{bmatrix} v + \left(\begin{bmatrix} -\hat{Y} \\ \hat{X} \end{bmatrix} + \begin{bmatrix} M \\ N \end{bmatrix} Q \right) r_y. \quad (59)$$

Here, the feedback control law K is described by (29). It should be emphasized that the controller (57) can be realized in the observer-based form (30), which plays a special role in our subsequent work.

On account of the Bezout identity (56) and loop dynamic (59), the canonical residual subspace introduced in Definition 2 is extended to the following general form.

Definition 3. Given the RCPs (M, N) and (\hat{X}, \hat{Y}) of G and K , respectively, the \mathcal{H}_2 subspace \mathcal{R}_G ,

$$\mathcal{R}_G = \left\{ \begin{bmatrix} u \\ y \end{bmatrix} : \begin{bmatrix} u \\ y \end{bmatrix} = \left(\begin{bmatrix} -\hat{Y} \\ \hat{X} \end{bmatrix} + \begin{bmatrix} M \\ N \end{bmatrix} Q \right) r \right\}, \quad (60)$$

is called residual subspace.

Corollary 2 is an immediate result of Theorem 1.

Corollary 2. Given the RCPs (M, N) and (\hat{X}, \hat{Y}) of G and K , the image subspace (42) and residual subspace (60) are invariant with respect to (F, L, V, W) .

The proof follows directly from (50) and (52) in Theorem 1 as well as Definitions 2 and 3. Thus, it is omitted.

C. Applications to secure CPCS study

In the literature on secure CPCSs, several active defence schemes have emerged to detect cyber-attacks, in particular those stealthy attacks [13]. Among others, Moving Target Defense (MTD) [53], dynamic watermarking [24], and auxiliary subsystem [54], [55] methods are well-established. In this subsection, the aforementioned results are leveraged to the MTD and watermark methods, while the auxiliary subsystem scheme will be addressed in Subsection V-A. We will also exemplify the concept of output-nulling invariant subspace [56], which builds the control-theoretic basis for designing zero-dynamics attacks, a well-studied class of stealthy attacks [34], in the unified framework of control and detection. To begin with, the unified framework is exploited aiming at secure CPCS configurations.

1) *Secure CPCS configurations:* In their survey paper [13], Segovia-Ferreira et al. pointed out that modifying the system architecture, e.g. using different hardware, software, firmware, or protocols, is capable of improving the resilience of the system to absorb or survive the attack impact. To author's best knowledge, there are rarely reported efforts on modifying control system configurations for the attack-resilient purpose. We notice that the observer-based realization of a Youla parameterized controller (30) enables two-site control architectures. On this basis, it is possible to implement a controller in two separate units running on the plant and the control station, respectively. Such architectures naturally obscure the overall loop dynamic behavior from an attacker.

Specifically, the observer-based realization (30) offers two possible variations,

- Variation I: on the plant side, the observer-based system

$$\begin{cases} \hat{x}(k+1) = A_L \hat{x}(k) + B_K \begin{bmatrix} u(k) \\ y(k) \end{bmatrix} \\ u(k) = F \hat{x}(k) + r_Q(k) + v(k) \\ r_y(k) = C_K \hat{x}(k) + D_K \begin{bmatrix} u(k) \\ y(k) \end{bmatrix}, \end{cases}$$

is implemented and the residual r_y is transmitted to the control station, and on the control station, $Qr_y + v$ is calculated and transmitted to the plant;

- Variation II: on the control station side, the system

$$\begin{cases} \hat{x}_0(k+1) = A_L \hat{x}_0(k) + B_K \begin{bmatrix} u_0(k) \\ y(k) \end{bmatrix} \\ u_0(k) = F \hat{x}_0(k) + v(k) \end{cases} \quad (61)$$

is realized and u_0 is transmitted to the plant, where the system

$$\begin{cases} \hat{x}(k+1) = A_L \hat{x}(k) + B_K \begin{bmatrix} u(k) \\ y(k) \end{bmatrix} \\ r_y(k) = W(y(k) - C \hat{x}(k) - Du(k)) \\ u(k) = u_0(k) + r_Q(k) \end{cases}$$

and Qr_y are implemented, and the output y is sent to the control station.

Variation I is of the advantages that (i) higher security, since the essential system performance like the system stability is guaranteed also in case of communication failure, (ii) system privacy preserving, where the residual signal r_y instead of y is transmitted over the communication network. A potential and significant application is the cloud computing-based fault-tolerant control of CPCSs [57], where the fault-tolerant control system Qr_y is online computed in the cloud computing system. With the aid of Variation II, the degree of design freedom can be remarkably increased so that capable attack and fault detection, tolerant and resilient control systems are designed, as exemplified in the subsequent sections. Note that the controller (61) implemented on the control station can be alternatively an output feedback controller $u_0 = K_0 y + \bar{v}$. It is noteworthy that the above two system configurations are often adopted in the context of plug-and-play (PnP) control systems. In engineering practice, control systems are often equipped with a default controller whose configuration and parameters are fixed. In order to meet the control performance requirements, the PnP configuration and control strategy are often employed to recover the system performance when the system is suffered from faults and disturbances [57]–[59]. The following theorem is an alternative form of the Youla parameterization that serves as a theoretic basis of a PnP controller.

Theorem 2. Given the feedback control system (1) equipped with a default (stabilizing) controller $u_0 = K_0 y$, then

$$u = u_0 + Qr_y, r_y = \hat{M}y - \hat{N}u, \quad (62)$$

$Q \in \mathcal{RH}_\infty$, gives a parameterization form of all stabilizing controllers, where (\hat{M}, \hat{N}) is an LCP of G .

Proof. In [59], a proof based on the observer-based implementation form is given. Below, an alternative proof is delineated using the kernel model (38). As stabilizing controller, K_0 can be written as $K_0 = -(X + Q_0 \hat{N})^{-1}(Y - Q_0 \hat{M})$. Let the Youla parameterization form of K be written into

$$K = -(X + Q_0 \hat{N} + \bar{Q} \hat{N})^{-1}(Y - Q_0 \hat{M} - \bar{Q} \hat{M}), \bar{Q} \in \mathcal{RH}_\infty.$$

It turns out

$$\begin{aligned} (X + Q_0 \hat{N} + \bar{Q} \hat{N})u &= -(Y - Q_0 \hat{M} - \bar{Q} \hat{M})y \implies \\ u &= -(X + Q_0 \hat{N})^{-1} \left((Y - Q_0 \hat{M})y + \bar{Q} r_y \right). \end{aligned}$$

Imposing $\bar{Q} = -(X + Q_0 \hat{N})Q, Q \in \mathcal{RH}_\infty$, finally results in the parameterization form (62). \square

The parameterization (62) will be adopted in our subsequent work on fault-tolerant and attack-resilient control.

2) *An application to MTD technique:* Roughly speaking, the MTD technique introduces time-varying or deliberately switched system configurations to obscure system information over time [53], [60]. [13] describes the MTD technique as a strategy of increasing the complexity and cost of attack design and limiting the exposure of the system vulnerabilities. Below, we briefly highlight the advantageous application of the unified framework to the design of MTD schemes.

Consider the closed-loop dynamic (59) with the stabilizing controller (29). According to Corollary 2, the process data (u, y) are invariant with respect to the variations of the four parameters (F, L, V, W) . Specifically, it follows from Theorem 1 that the variations of (F, L, V, W) can be represented by a pre-filter $T(z)$, a post-filter $R(z)$ and a parameterization matrix $Q(z)$. Since

$$\begin{aligned} G &= \left(R \hat{M} \right)^{-1} R \hat{N} = NT(MT)^{-1}, \\ K &= \left(-\hat{Y} R^{-1} + MQ \right) \left(\hat{X} R^{-1} + NQ \right)^{-1} \\ &= \left(T^{-1} X - Q \hat{N} \right)^{-1} \left(T^{-1} Y + Q \hat{M} \right), \end{aligned}$$

with $(R, T) \in \mathcal{RH}_\infty$ being invertible over \mathcal{RH}_∞ , the closed-loop dynamic (59) is generally parameterized by a triple of \mathcal{RH}_∞ -systems (Q, R, T) with (R, T) invertible over \mathcal{RH}_∞ . This result can be further extended to linear time-varying (LTV) systems. To be specific, it is a known result that the general form of the Bezout identity (56) exists for LTV systems as well with \mathcal{Q} as the parameterization matrix, and the coprime factorizations presented in Subsection II-B can be well extended to the case with LTV post- and pre-filters, \mathcal{R} and \mathcal{T} [52], [61], where $(\mathcal{Q}, \mathcal{R}, \mathcal{T})$ are the operators representing stable LTV systems with the state space representations

$$\begin{aligned} \mathcal{Q} : & \begin{cases} x_Q(k+1) = A_Q(k)x_Q(k) + B_Q(k)r_y(k) \\ r_Q(k) = C_Q(k)x_Q(k) + D_Q(k)r_y(k), \end{cases} \\ \mathcal{R} : & \begin{cases} x_R(k+1) = A_R(k)x_R(k) + B_R(k)r_y(k) \\ r_R(k) = C_R(k)x_R(k) + D_R(k)r_y(k), \end{cases} \\ \mathcal{T} : & \begin{cases} x_T(k+1) = A_T(k)x_T(k) + B_T(k)v(k) \\ \bar{v}(k) = C_T(k)x_T(k) + D_T(k)v(k), \end{cases} \end{aligned}$$

and $(\mathcal{R}, \mathcal{T})$ invertible. With the aid of the above results, we are able to design more capable MTD systems. For instance,

the LTV post- and pre-filters $(\mathcal{R}, \mathcal{T})$ generalize time-varying input/output transformations $(R(k), T(k))$, a state of the art MTD scheme applied in the research of secure CPCSs [13]. In this case, the controller and observer invert $(\mathcal{R}, \mathcal{T})$ dynamically, while the attacker sees a time-varying system. The use of LTV parameter system \mathcal{Q} injects unpredictability in the closed-loop dynamic so that it is hard for attackers to identify the plant model, the controller and observer. Mathematically, $(\mathcal{Q}, \mathcal{R}, \mathcal{T})$ build an admissible set in the Banach space of bounded causal linear operators, which is vastly larger than the set formed by time-varying input/output transformations $(R(k), T(k))$.

3) *An application to watermark technique:* The basic idea of watermarking consists in injecting an excitation signal as a watermark, often a stochastic series, into the control inputs. The injected watermark causes measurable correlations that expose malicious tampering when the outputs fail to reflect the watermark [24]. The watermark technique is a popular method of detecting cyber-attacks, in particular dealing with the so-called replay attacks. Below, we propose a watermark-based detection scheme in the unified framework.

Suppose that the CPCS with noises modelled by (36) is described by its kernel model

$$\begin{cases} r_y = \hat{M}_n y - \hat{N}_n u = r_{y,n} \\ r_u = Xu + Yy = X_n u + Y_n y + Q_n r_{y,n}, \end{cases}$$

where $(\hat{M}_n, \hat{N}_n), (X_n, Y_n)$ are the LCPs of the plant and the controller with Kalman-filter gain $L = L_K, r_{y,n} \sim \mathcal{N}(0, \Sigma_{r_{y,n}})$ is the generated innovation series, and r_u is given by

$$\begin{aligned} u &= Ky = -X^{-1}Yy \implies \\ r_u &= Xu + Yy = X_n u + Y_n y + Q_n r_{y,n}. \end{aligned}$$

Here, the last equation is attributed to Theorem 1 with

$$Q_n = -F(zI - A_L)^{-1}(L - L_K),$$

and (F, L) denoting the setting of (X, Y) . The system dynamic is described by

$$\begin{aligned} \begin{bmatrix} u \\ y \end{bmatrix} &= \begin{bmatrix} M \\ N \end{bmatrix} r_{u_0} + \begin{bmatrix} -\hat{Y}_n + MQ_n \\ \hat{X}_n + NQ_n \end{bmatrix} r_{y,n}, \\ \implies y(k) &\sim \mathcal{N}(r_{u_0}(k), \Sigma_{y_r}(k)), r_{u_0} = X_n u + Y_n y \end{aligned} \quad (63)$$

with Σ_{y_r} as the covariance matrix of y_r ,

$$y_r = (\hat{X}_n + NQ_n) r_{y,n}. \quad (64)$$

On the assumption that the CPCS is working in the steady state, a replay attack is modelled by (refer to Remark 3)

$$y^a(k) = y(k) + a_y(k), a_y(k) = -y(k) + y(k-T). \quad (65)$$

We now configure the CPCS as follows. Suppose that the control station receives y^a from the plant and generates the residual and control signals,

$$r_Q = Q \begin{bmatrix} -\hat{N}_n & \hat{M}_n \end{bmatrix} \begin{bmatrix} u \\ y^a \end{bmatrix}, u = Ky^a,$$

and send the signal u_Q ,

$$u_Q = u + r_Q,$$

to the plant, where r_Q serves as a watermark signal with $Q \in \mathcal{RH}_\infty$. On the plant side, the input signal u is recovered by

$$u = u_Q^a - Qr_y,$$

$$r_y = \begin{bmatrix} -\hat{N}_n & \hat{M}_n \end{bmatrix} \begin{bmatrix} u_Q^a - Qr_y \\ y \end{bmatrix}.$$

To detect replay attacks, a detector,

$$r_u = \begin{bmatrix} X_n & Y_n \end{bmatrix} \begin{bmatrix} u_Q^a - Qr_y \\ y \end{bmatrix} - Q_n r_y, \quad (66)$$

is implemented on the plant side. It is apparent that in case of attack-free, $r_u = 0$. Against it, under replay attacks it turns out

$$r_u = \begin{bmatrix} X_n & Y_n \end{bmatrix} \begin{bmatrix} Ky^a + r_Q + a_u - Qr_y \\ y \end{bmatrix} - Q_n r_y \quad (67)$$

$$= X_n a_u - Y_n a_y + (Q - Q_n) (\hat{N}_n a_u + \hat{M}_n a_y)$$

$$= \begin{bmatrix} X_n - \bar{Q} \hat{N}_n & Y_n + \bar{Q} \hat{M}_n \end{bmatrix} \begin{bmatrix} a_u \\ z^{-T} y \end{bmatrix}, \bar{Q} = Q - Q_n. \quad (68)$$

It is of interest to notice that the closed-loop dynamic under the attacks is governed by

$$\begin{bmatrix} u \\ y \end{bmatrix} = \begin{bmatrix} M \\ N \end{bmatrix} r_u + \begin{bmatrix} -\hat{Y}_n + MQ_n \\ \hat{X}_n + NQ_n \end{bmatrix} r_{y,n},$$

which yields, recalling (63)-(65),

$$r_u(k) \sim \mathcal{N}(r_{a_u}(k), \Sigma_{r_{a_y}}(k)),$$

$$r_{a_u} = (X_n - \bar{Q} \hat{N}_n) a_u, r_{a_y} = (Y_n + \bar{Q} \hat{M}_n) r_{y,a},$$

$$r_{y,a} \sim \mathcal{N}(0, 2\Sigma_{r_{y,n}}),$$

where $\Sigma_{r_{a_y}}$ is the covariance matrix of r_{a_y} . Note that the above relations are attributed to the facts that

$$a_y(k) = -y(k) + y(k-T) = r_{y,a}(k) \sim \mathcal{N}(0, 2\Sigma_{r_{y,n}}),$$

$$\mathcal{E}y(k) = \mathcal{E}y(k-T) = r_{u_0},$$

and a_u is a deterministic signal. As a result, the detection logic is defined as

$$r_u = \begin{cases} 0, & \text{attack-free} \\ \sim \mathcal{N}(r_{a_u}(k), \Sigma_{r_{a_y}}(k)) \neq 0, & \text{alarm.} \end{cases}$$

We would like to call the reader's attention to a useful by-product of the detection scheme. Selecting \bar{Q} such that

$$\| \begin{bmatrix} X_n & Y_n \end{bmatrix} - \bar{Q} \begin{bmatrix} -\hat{N}_n & \hat{M}_n \end{bmatrix} \|_\infty \rightarrow \min$$

enhances the attack resilience of the system.

4) *Zero-dynamics*: Zero-dynamics attacks are a type of stealthy attacks that have been intensively researched in the literature, dedicated to attack detection and design [7], [34], [62]. Generally speaking, this type of attacks exploits the plant's inherent zero dynamics to remain perfectly stealthy against (output) residual-based detectors. As well delineated in [34], the control-theoretic basis for constructing zero-dynamics attacks is the output-nulling invariant subspace [56]. This motivates us to examine the relation between the output-nulling invariant subspace and the RCF/LCF of G as well as the associated

image/kernel subspaces. To this end, consider the output-nulling invariant subspace \mathcal{V} in the sense of [56], for some $u, v \in \mathcal{V}$

$$Av + Bu \subset \mathcal{V}, Cv + Du = 0,$$

which is equivalent to

$$(A + BF) \mathcal{V} \subset \mathcal{V}, (C + DF) \mathcal{V} = 0, \quad (69)$$

for some F . Subsequently, associated to each $x \in \mathcal{V}$, we have an input-output pair (u, y) so that $y = 0$. According to (69), this can be expressed in terms of the RCF of G as

$$u = Mv, Nv = 0 \implies y = NM^{-1}u = 0.$$

Thus, the set of the input and output pairs associated with the output-nulling invariant subspace corresponds to a subspace in the image subspace \mathcal{I}_G

$$\left\{ \begin{bmatrix} u \\ y \end{bmatrix} : \begin{bmatrix} u \\ y \end{bmatrix} = \begin{bmatrix} M \\ N \end{bmatrix} v, \begin{array}{l} Nv = 0, v \neq 0 \end{array} \right\} \subset \mathcal{I}_G.$$

The dual form is the input-nulling invariant subspace. The associated input-output pair (u, y) satisfies, for some u ,

$$\hat{N}u = 0, \hat{M}y = \hat{N}u = 0 \implies y = 0.$$

It is apparent that the set of all associated input-output pairs builds a subspace in the kernel subspace \mathcal{K}_G ,

$$\left\{ \begin{bmatrix} u \\ y \end{bmatrix} : \begin{bmatrix} -\hat{N} & \hat{M} \end{bmatrix} \begin{bmatrix} u \\ y \end{bmatrix} = 0, \begin{array}{l} \hat{N}u = 0, u \neq 0 \end{array} \right\} \subset \mathcal{K}_G.$$

Motivated by the recent endeavours to study local stealthy attacks [7], [34], [63], we now extend the aforementioned results to the case, when only partial input and output channels are under consideration. Specifically, let

$$B = [B_1 \ B_2], C = \begin{bmatrix} C_1 \\ C_2 \end{bmatrix}, D = \begin{bmatrix} D_{11} & D_{12} \\ D_{21} & D_{22} \end{bmatrix} \quad (70)$$

where the input channels modelled by B_1 are of interest, e.g. representing the control inputs that are attacked, and $(C_1, [D_{11} \ D_{12}])$ represents the output channels that should not be affected by the inputs acted on the input channels B_1 like attacks. Below, we examine the existence conditions expressed in terms of RCF/LCF and image/kernel subspaces schematically and without rigorous mathematical details. For our purpose, corresponding to (70) (u, y) are written into

$$u = \begin{bmatrix} u_1 \\ u_2 \end{bmatrix} = \begin{bmatrix} F_1 x + v_1 \\ 0 \end{bmatrix}, y = \begin{bmatrix} y_1 \\ y_2 \end{bmatrix},$$

which yields an SIR of G ,

$$\begin{aligned} \begin{bmatrix} u \\ y \end{bmatrix} &= \begin{bmatrix} M \\ N \end{bmatrix} v = \begin{bmatrix} M_1 \\ N_1 \\ N_2 \end{bmatrix} v_1, \\ M_1 &= \begin{bmatrix} F_1 (zI - A - B_1 F_1)^{-1} B_1 + I \\ 0 \end{bmatrix}, \\ \begin{bmatrix} N_1 \\ N_2 \end{bmatrix} &= \begin{bmatrix} (C_1 + D_{11} F_1) (zI - A - B_1 F_1)^{-1} B_1 + D_{11} \\ (C_2 + D_{21} F_1) (zI - A - B_1 F_1)^{-1} B_1 + D_{21} \end{bmatrix}. \end{aligned}$$

As a result, $y_1 = 0$, if and only if, for some $v_1 \neq 0$, $N_1 v_1 = 0$. It is obvious that

$$\left\{ \begin{array}{l} \left[\begin{array}{c} u \\ y \end{array} \right] : \left[\begin{array}{c} u \\ y \end{array} \right] = \left[\begin{array}{c} M \\ N \end{array} \right] v = \left[\begin{array}{c} u_1 \\ 0 \\ 0 \\ y_2 \end{array} \right], \\ N_1 v_1 = 0, v_1 \neq 0 \end{array} \right\} \subset \mathcal{I}_G.$$

The dual results are summarized as follows. For some $u_1 \neq 0, u_2 = 0$,

$$\begin{aligned} \hat{N}u &= \left[\begin{array}{c} \hat{N}_1 u_1 \\ \hat{N}_2 u_1 \end{array} \right] = \left[\begin{array}{c} 0 \\ \hat{N}_2 u_1 \end{array} \right], \\ \hat{M}y &= \left[\begin{array}{cc} \hat{M}_1 & \hat{M}_2 \end{array} \right] \left[\begin{array}{c} y_1 \\ y_2 \end{array} \right] = \left[\begin{array}{cc} \hat{M}_{11} & \hat{M}_{12} \\ \hat{M}_{21} & \hat{M}_{22} \end{array} \right] \left[\begin{array}{c} y_1 \\ y_2 \end{array} \right], \\ \hat{N}_1 &= C_1 (zI - A + L_1 C_1)^{-1} (B_1 - L_1 D_{11}) + D_{11}, \\ \hat{N}_2 &= C_2 (zI - A + L_1 C_1)^{-1} (B_1 - L_1 D_{21}) + D_{21}, \\ \hat{M}_1 &= \left[\begin{array}{c} I \\ 0 \end{array} \right] - C (zI - A + L_1 C_1)^{-1} L_1, \hat{M}_2 = \left[\begin{array}{c} 0 \\ I \end{array} \right], \end{aligned}$$

which finally results in

$$\begin{aligned} \hat{N}u = \hat{M}y &= \left[\begin{array}{c} 0 \\ y_2 \end{array} \right] \implies y_1 = 0, y_2 = \hat{N}_2 u_1 \\ \left\{ \begin{array}{l} \left[\begin{array}{c} u \\ y \end{array} \right] : \left[\begin{array}{cc} -\hat{N} & \hat{M} \end{array} \right] \left[\begin{array}{c} u \\ y \end{array} \right] = 0 \Leftrightarrow \\ \left[\begin{array}{cc} -\hat{N}_2 & I \end{array} \right] \left[\begin{array}{c} u_1 \\ y_2 \end{array} \right] = 0, \hat{N}_1 u_1 = 0, u_1 \neq 0 \end{array} \right\} &\subset \mathcal{K}_G. \end{aligned}$$

The above results are achieved on the assumption that merely system model knowledge (A, B_1, C_1, D_{11}) is used. In Subsection IV-C, application of the above results to constructing zero-dynamics attacks will be addressed.

IV. ANALYSIS OF SYSTEM DYNAMICS UNDER CYBER-ATTACKS AND FAULTS

In this section, dynamics of the system (32) and their impairment under cyber-attacks and faults are firstly analyzed. On this basis, the issues of stealthy attacks like definitions, detection conditions and their construction are closely examined.

A. Analysis of faulty dynamics

We begin with an analysis of the closed-loop dynamic under faults modelled by (37).

Theorem 3. *Given the kernel-based loop model (38) with the fault modelled by (37), then the closed-loop system is stable if*

$$\Phi^f = \left(I - \Pi^f \left[\begin{array}{c} -\hat{Y} \\ \hat{X} \end{array} \right] \right)^{-1} \in \mathcal{RH}_\infty. \quad (71)$$

Moreover, the closed-loop dynamic is governed by

$$\begin{aligned} \left[\begin{array}{c} u \\ y \end{array} \right] &= \left[\begin{array}{c} M \\ N \end{array} \right] v + \left[\begin{array}{c} -\hat{Y} \\ \hat{X} \end{array} \right] \left(\Phi^f \hat{N}dd + \Phi^f \bar{f} + \Psi^f v \right), \quad (72) \\ \Psi^f &= \Phi^f \Pi^f \left[\begin{array}{c} M \\ N \end{array} \right]. \end{aligned}$$

Proof. It follows from (40) that

$$\left[\begin{array}{c} u \\ y \end{array} \right] = \left[\begin{array}{c} M \\ N \end{array} \right] v + \left[\begin{array}{c} -\hat{Y} \\ \hat{X} \end{array} \right] r_y.$$

During faulty operations,

$$r_y = \hat{M} (r_{y,0} + f_0) = \hat{N}dd + \Pi^f \left[\begin{array}{c} u \\ y \end{array} \right] + \bar{f} \implies$$

$$\begin{aligned} \left[\begin{array}{c} u \\ y \end{array} \right] &= \left[\begin{array}{c} M \\ N \end{array} \right] v + \left[\begin{array}{c} -\hat{Y} \\ \hat{X} \end{array} \right] \left(\hat{N}dd + \bar{f} + \Pi^f \left[\begin{array}{c} u \\ y \end{array} \right] \right) \implies \\ \left[\begin{array}{c} u \\ y \end{array} \right] &= \left(I - \left[\begin{array}{c} -\hat{Y} \\ \hat{X} \end{array} \right] \Pi^f \right)^{-1} \left(\begin{array}{c} \left[\begin{array}{c} M \\ N \end{array} \right] v \\ + \left[\begin{array}{c} -\hat{Y} \\ \hat{X} \end{array} \right] \left(\hat{N}dd + \bar{f} \right) \end{array} \right), \end{aligned}$$

leading to (72). It is clear that the closed-loop is stable if (71) is true. \square

As expected, equation (72) showcases that the uncertain dynamics caused by the unknown input d and fault f act on the system residual subspace. Their influence on the closed-loop dynamic is decoupled from the nominal system response

$$\left[\begin{array}{c} u_n \\ y_n \end{array} \right] := \left[\begin{array}{c} M \\ N \end{array} \right] v.$$

Consequently, it is sufficient to detect the fault using the output residual r_y , that is

$$r_y = \Phi^f \hat{N}dd + \Phi^f \bar{f} + \Psi^f v. \quad (73)$$

Note that r_y acts as the latent variable building the residual subspace \mathcal{R}_G defined in Definition 2.

Next, an alternative form of the closed-loop dynamic is derived, which underlines the influence of the faults on the system dynamic and is useful for our subsequent study on secure CPCSs.

Theorem 4. *The kernel-based loop model (38) with the fault modelled by (37) can be equivalently expressed by*

$$\begin{cases} y(z) = G_\Delta(z)u(z) + r_{y,f}(z) \\ u(z) = K(z)y(z) + r_{u,0}(z), \end{cases} \quad (74)$$

$$\begin{aligned} G_\Delta &= \left(\hat{M} + \Delta_{\hat{M}} \right)^{-1} \left(\hat{N} + \Delta_{\hat{N}} \right) \\ &= (N + \Delta_N)(M + \Delta_M)^{-1}, \end{aligned} \quad (75)$$

$$\left[\begin{array}{c} \Delta_M \\ \Delta_N \end{array} \right] = \left[\begin{array}{c} -\hat{Y} \Psi^f \\ \hat{X} \Psi^f \end{array} \right], \left[\begin{array}{cc} \Delta_{\hat{N}} & -\Delta_{\hat{M}} \end{array} \right] = \Pi^f, \quad (76)$$

$$r_{y,f} = \left(\hat{M} + \Delta_{\hat{M}} \right)^{-1} \left(\hat{N}dd + \bar{f} \right).$$

Proof. It follows from (38) that

$$\begin{aligned} r_y &= \left[\begin{array}{cc} -\hat{N} & \hat{M} \end{array} \right] \left[\begin{array}{c} u \\ y \end{array} \right] = \hat{N}dd + \Pi^f \left[\begin{array}{c} u \\ y \end{array} \right] + \bar{f} \\ &\implies \left(\left[\begin{array}{cc} -\hat{N} & \hat{M} \end{array} \right] - \Pi^f \right) \left[\begin{array}{c} u \\ y \end{array} \right] = \hat{N}dd + \bar{f}, \\ &\quad Xu + Yy = r_u = v, \end{aligned}$$

from which (74) with

$$y = G_\Delta u + r_{y,f}(z), G_\Delta = \left(\hat{M} + \Delta_{\hat{M}} \right)^{-1} \left(\hat{N} + \Delta_{\hat{N}} \right)$$

is proven. We now examine (75), which is equivalent to

$$[-\hat{N} - \Delta_{\hat{N}} \hat{M} + \Delta_{\hat{M}}] \left(\begin{bmatrix} M \\ N \end{bmatrix} + \begin{bmatrix} \Delta_M \\ \Delta_N \end{bmatrix} \right) = 0.$$

Notice that

$$\begin{aligned} [-\Delta_{\hat{N}} \Delta_{\hat{M}}] \begin{bmatrix} M \\ N \end{bmatrix} &= -\Pi^f \begin{bmatrix} M \\ N \end{bmatrix}, \\ [-\Delta_{\hat{N}} \Delta_{\hat{M}}] \begin{bmatrix} \Delta_M \\ \Delta_N \end{bmatrix} &= -\Pi^f \begin{bmatrix} -\hat{Y} \\ \hat{X} \end{bmatrix} \Psi^f, \\ [-\hat{N} \hat{M}] \begin{bmatrix} \Delta_M \\ \Delta_N \end{bmatrix} &= \Psi^f \implies \\ [-\hat{N} - \Delta_{\hat{N}} \hat{M} + \Delta_{\hat{M}}] \left(\begin{bmatrix} M \\ N \end{bmatrix} + \begin{bmatrix} \Delta_M \\ \Delta_N \end{bmatrix} \right) \\ &= \left(I - \Pi^f \begin{bmatrix} -\hat{Y} \\ \hat{X} \end{bmatrix} \right) \Psi^f - \Pi^f \begin{bmatrix} M \\ N \end{bmatrix} = 0. \end{aligned}$$

Hence, (75) is proven. \square

Theorem 4 implies that the variation caused by the fault (37) can be equivalently modelled by the coprime factor uncertainty of the plant [48]. In robust control theory, $(\Delta_{\hat{M}}, \Delta_{\hat{N}})$ and (Δ_M, Δ_N) are called coprime factor uncertainty of the plant [48], i.e.

$$\begin{aligned} I_G &= \begin{bmatrix} M \\ N \end{bmatrix} + \Delta I_G, \Delta I_G = \begin{bmatrix} \Delta_M \\ \Delta_N \end{bmatrix}, \\ K_G &= [-\hat{N} \hat{M}] + \Delta K_G, \Delta K_G = [-\Delta_{\hat{N}} \Delta_{\hat{M}}]. \end{aligned}$$

B. Analysis of system dynamics under cyber-attacks

In this section, we consider the CPCSSs (32) with K subject to (19) and attack model (34). It is supposed that the system is operating under fault-free conditions.

1) *The information patterns and essential models:* The available data on the plant and control station sides are different. While the accessible input-output data on the plant side are (u^a, y) , the control station has the input-output data (u, y^a) available. This information mismatching results in attack information potential

$$IP_a := \begin{bmatrix} u^a \\ y \end{bmatrix} - \begin{bmatrix} u \\ y^a \end{bmatrix} = \begin{bmatrix} a_u \\ -a_y \end{bmatrix} \quad (77)$$

that indicates the existence of cyber-attacks. In order to avoid nomenclatural inconsistency due to the information mismatching, we define the residual (r_u, r_y) in the sequel by means of the kernel-based model according to the information pattern on the plant side,

$$\begin{cases} \hat{M}y - \hat{N}u^a = r_y, \\ Xu^a + Yy = r_u \end{cases}, r_y = \hat{M}r_{y,0} = \hat{N}r_{u,0}, r_u = v. \quad (78)$$

The loop dynamic expressed in terms of (u^a, y) is governed, considering the information pattern on the control station and information potential (77), by

$$\begin{aligned} \begin{bmatrix} X & Y \\ -\hat{N} & \hat{M} \end{bmatrix} \begin{bmatrix} u^a \\ y \end{bmatrix} &= \begin{bmatrix} Xa_u - Ya_y + v \\ r_y \end{bmatrix} \implies \\ \begin{bmatrix} u^a \\ y \end{bmatrix} &= \begin{bmatrix} M \\ N \end{bmatrix} (Xa_u - Ya_y + v) + \begin{bmatrix} -\hat{Y} \\ \hat{X} \end{bmatrix} r_y. \end{aligned} \quad (79)$$

Attributed to the Bezout identity (6), the attacks can be expressed by

$$\begin{bmatrix} a_u \\ -a_y \end{bmatrix} = \begin{bmatrix} M \\ N \end{bmatrix} a_{r_u} + \begin{bmatrix} -\hat{Y} \\ \hat{X} \end{bmatrix} a_{r_y}, \quad (80)$$

$$a_{r_u} = [X \ Y] \begin{bmatrix} a_u \\ -a_y \end{bmatrix}, a_{r_y} = [-\hat{N} \ \hat{M}] \begin{bmatrix} a_u \\ -a_y \end{bmatrix}, \quad (81)$$

which models the influence of (a_u, a_y) on the image and residual subspaces \mathcal{I}_G and \mathcal{R}_G , respectively. Relations (77)-(80) are essential for our subsequent work. Note that, attribute to (80), the attack information potential can be expressed by

$$IP_a = \begin{bmatrix} M \\ N \end{bmatrix} a_{r_u} + \begin{bmatrix} -\hat{Y} \\ \hat{X} \end{bmatrix} a_{r_y}. \quad (82)$$

2) *System dynamics under cyber-attacks:* We now examine the loop dynamic under cyber-attacks modelled by (34).

Theorem 5. *Given the loop model (78) and the attack model (34), the plant dynamics under additive and multiplicative attacks,*

$$\begin{bmatrix} a_u \\ a_y \end{bmatrix} = \begin{bmatrix} E_u \eta_u \\ E_y \eta_y \end{bmatrix}, \begin{bmatrix} a_u \\ a_y \end{bmatrix} = \Pi^a \begin{bmatrix} u \\ y \end{bmatrix}, \quad (83)$$

are respectively governed by

$$\begin{bmatrix} u^a \\ y \end{bmatrix} = \begin{bmatrix} M \\ N \end{bmatrix} (v + \bar{a}_{r_u}) + \begin{bmatrix} -\hat{Y} \\ \hat{X} \end{bmatrix} r_y, \quad (84)$$

$$\bar{a}_{r_u} = [X \ Y] \begin{bmatrix} E_u \eta_u(z) \\ -E_y \eta_y(z) \end{bmatrix},$$

$$\begin{bmatrix} u^a \\ y \end{bmatrix} = \begin{bmatrix} M \\ N \end{bmatrix} (v_\Delta + \Psi^a r_y) + \begin{bmatrix} -\hat{Y} \\ \hat{X} \end{bmatrix} r_y, \quad (85)$$

$$v_\Delta = \left(I - [X \ Y] \Phi^a \begin{bmatrix} M \\ N \end{bmatrix} \right)^{-1} v,$$

$$\Psi^a = \left(I - [X \ Y] \Phi^a \begin{bmatrix} M \\ N \end{bmatrix} \right)^{-1} [X \ Y] \Phi^a \begin{bmatrix} -\hat{Y} \\ \hat{X} \end{bmatrix},$$

$$\Phi^a = \begin{bmatrix} I & 0 \\ 0 & -I \end{bmatrix} \Pi^a \left(I + \begin{bmatrix} I & 0 \\ 0 & 0 \end{bmatrix} \Pi^a \right)^{-1}.$$

Proof. The dynamic under additive attacks (84) follows immediately from (79). We prove (85), the system response to the multiplicative attacks. Observe that

$$\begin{bmatrix} a_u \\ -a_y \end{bmatrix} = \begin{bmatrix} I & 0 \\ 0 & -I \end{bmatrix} \Pi^a \begin{bmatrix} u^a - a_u \\ y \end{bmatrix}.$$

By some routine computations, it turns out

$$\begin{bmatrix} a_u \\ -a_y \end{bmatrix} = \Phi^a \begin{bmatrix} u^a \\ y \end{bmatrix}. \quad (86)$$

Substituting it into (79) yields

$$\begin{bmatrix} u^a \\ y \end{bmatrix} = \begin{bmatrix} M \\ N \end{bmatrix} \left([X \ Y] \Phi^a \begin{bmatrix} u^a \\ y \end{bmatrix} + v \right) + \begin{bmatrix} -\hat{Y} \\ \hat{X} \end{bmatrix} r_y,$$

from which (85) follows. \square

The system responses (84) and (85) demonstrate that the cyber-attacks act on the system image subspace, and their influence is decoupled from the residual behavior

$$\begin{bmatrix} u_r^a \\ y_r \end{bmatrix} = \begin{bmatrix} -\hat{Y} \\ \hat{X} \end{bmatrix} r_y.$$

On this account, it is impossible to detect cyber-attacks on the plant side by means of the output residual generator. Instead, the input residual

$$r_u = Xu^a + Yy$$

is a capable detector of the cyber-attacks.

Considering that attack detection is generally performed on the control station, we now examine the system dynamic in the information pattern (u, y^a) , i.e. from the viewpoint of the control station. It follows from the information potential (77) and (79)-(80) that

$$\begin{bmatrix} u \\ y^a \end{bmatrix} = \begin{bmatrix} M \\ N \end{bmatrix} v + \begin{bmatrix} -\hat{Y} \\ \hat{X} \end{bmatrix} (r_y - a_{r_y}). \quad (87)$$

According to (86),

$$\begin{aligned} \begin{bmatrix} a_u \\ -a_y \end{bmatrix} &= \Phi^a \left(\begin{bmatrix} u \\ y^a \end{bmatrix} + \begin{bmatrix} a_u \\ -a_y \end{bmatrix} \right) + \begin{bmatrix} \bar{\eta}_u \\ \bar{\eta}_y \end{bmatrix} \quad (88) \\ \implies \begin{bmatrix} a_u \\ -a_y \end{bmatrix} &= (I - \Phi^a)^{-1} \left(\Phi^a \begin{bmatrix} u \\ y^a \end{bmatrix} + \begin{bmatrix} \bar{\eta}_u \\ \bar{\eta}_y \end{bmatrix} \right), \\ \begin{bmatrix} \bar{\eta}_u \\ \bar{\eta}_y \end{bmatrix} &= \begin{bmatrix} I & 0 \\ 0 & -I \end{bmatrix} \left(I + \Pi^a \begin{bmatrix} I & 0 \\ 0 & 0 \end{bmatrix} \right)^{-1} \begin{bmatrix} E_u \eta_u \\ E_y \eta_y \end{bmatrix}. \end{aligned}$$

Substituting it into a_{r_y} in (87) yields

$$\begin{bmatrix} u \\ y^a \end{bmatrix} = \Gamma^{-1} \left(\begin{bmatrix} M \\ N \end{bmatrix} v + \begin{bmatrix} -\hat{Y} \\ \hat{X} \end{bmatrix} \left(r_y - \Theta \begin{bmatrix} \bar{\eta}_u \\ \bar{\eta}_y \end{bmatrix} \right) \right), \quad (89)$$

$$\Gamma = I + \begin{bmatrix} -\hat{Y} \\ \hat{X} \end{bmatrix} \begin{bmatrix} -\hat{N} & \hat{M} \end{bmatrix} (I - \Phi^a)^{-1} \Phi^a, \quad (90)$$

$$\Theta = \begin{bmatrix} -\hat{N} & \hat{M} \end{bmatrix} (I - \Phi^a)^{-1},$$

from which we have the following theorem.

Theorem 6. *Given the loop model (78) and the attack model (34), then it holds*

$$\begin{bmatrix} u \\ y^a \end{bmatrix} = \begin{bmatrix} M \\ N \end{bmatrix} v + \begin{bmatrix} -\hat{Y} \\ \hat{X} \end{bmatrix} (v_\Delta^a + \Gamma^a r_y + \bar{a}_\Delta), \quad (91)$$

$$v_\Delta^a = -\Gamma^{-1} \begin{bmatrix} -\hat{Y} \\ \hat{X} \end{bmatrix} \begin{bmatrix} -\hat{N} & \hat{M} \end{bmatrix} (I - \Phi^a)^{-1} \Phi^a \begin{bmatrix} M \\ N \end{bmatrix} v,$$

$$\Gamma^a = \left(I + \begin{bmatrix} -\hat{N} & \hat{M} \end{bmatrix} (I - \Phi^a)^{-1} \Phi^a \begin{bmatrix} -\hat{Y} \\ \hat{X} \end{bmatrix} \right)^{-1},$$

$$\bar{a}_\Delta = -\Gamma^a \Theta \begin{bmatrix} \bar{\eta}_u \\ \bar{\eta}_y \end{bmatrix}.$$

Proof. The equation (91) follows from (89) by some routine computations. \square

The result (91) showcases that, due to the information potential (77), the cyber-attacks, faults and unknown input act exclusively on the residual subspace of (u, y^a) , which is the information pattern on the control station side, and are decoupled from the image subspace.

3) *Duality between system dynamics under faults and attacks:* Theorems 4-5 build the basis for our endeavours to leverage the unified framework to address simultaneous detection, fault-tolerant and resilient control of faults and attacks. Before that, we firstly reveal the duality between system dynamics under faults and attacks, which is helpful for the subsequent work.

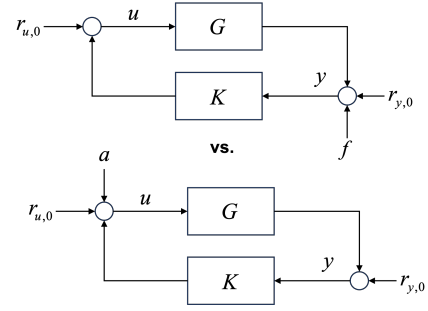


Fig. 2. The duality of the equivalent system configurations under the additive faults and cyber-attacks

Theorem 7. *The closed-loop model (32) under cyber-attackers modelled by (34) is equivalent to*

$$\begin{cases} y = Gu^a + r_{y,0} \\ u^a = K_\Delta y + r_{u,a}, \end{cases} \quad (92)$$

$$r_{u,a} = (X + \Delta_X)^{-1} (v + a_\eta), \quad a_\eta = \begin{bmatrix} X & Y \end{bmatrix} \begin{bmatrix} \bar{\eta}_u \\ -\bar{\eta}_y \end{bmatrix}, \quad (93)$$

$$K_\Delta = -(X + \Delta_X)^{-1} (Y + \Delta_Y), \quad (94)$$

$$\begin{bmatrix} \Delta_X & \Delta_Y \end{bmatrix} = -\begin{bmatrix} X & Y \end{bmatrix} \Phi^a. \quad (95)$$

Proof. On account of (88), the attack model (34) is recast into

$$\begin{bmatrix} a_u \\ -a_y \end{bmatrix} = \Phi^a \begin{bmatrix} u^a \\ y \end{bmatrix} + \begin{bmatrix} \bar{\eta}_u \\ \bar{\eta}_y \end{bmatrix}. \quad (96)$$

Similar to the proof of Theorem 5, consider

$$\begin{aligned} \begin{bmatrix} u^a \\ y \end{bmatrix} &= \begin{bmatrix} M \\ N \end{bmatrix} \left(\begin{bmatrix} X & Y \end{bmatrix} \Phi^a \begin{bmatrix} u^a \\ y \end{bmatrix} + a_\eta + v \right) \\ &+ \begin{bmatrix} -\hat{Y} \\ \hat{X} \end{bmatrix} r_y, \quad a_\eta = \begin{bmatrix} X & Y \end{bmatrix} \begin{bmatrix} \bar{\eta}_u \\ -\bar{\eta}_y \end{bmatrix}, \end{aligned}$$

and write it into

$$(\begin{bmatrix} X & Y \end{bmatrix} - \begin{bmatrix} X & Y \end{bmatrix} \Phi^a) \begin{bmatrix} u^a \\ y \end{bmatrix} = a_\eta + v.$$

Defining $r_{u,a}$, $\begin{bmatrix} \Delta_X & \Delta_Y \end{bmatrix}$ according to (93)-(95) yields

$$u^a = -(X + \Delta_X)^{-1} (Y + \Delta_Y) y + r_{u,a}.$$

The theorem is proven. \square

Comparing with the result in Theorem 4 makes it painfully clear that the faults and cyber-attacks impair the closed-loop dynamic in a dual manner. Fig. 2 and Fig. 3 sketch the duality of the equivalent system configurations under additive and multiplicative faults and cyber-attacks, respectively. This important property insightfully reveals the structural relations between the faults and cyber-attacks. It inspires us to design detection and control systems towards simultaneous detection, tolerant and resilient control of the faults and cyber-attacks in a dual manner, which builds the control-theoretic foundation for establishing a novel framework of designing fault-tolerant and attack-resilient control systems in a unified way.

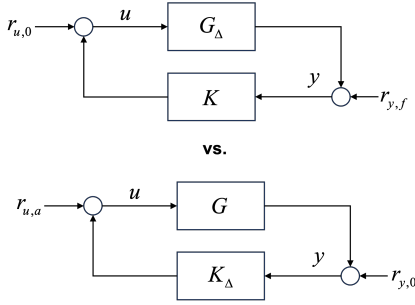


Fig. 3. The duality of the equivalent system configurations under the multiplicative faults and cyber-attacks

C. Detectability and actuability of attacks, and vulnerability analysis

Issues associated with the concept stealthy attacks have continually attracted remarkable research attention since the publication of several real cases of cyber-attacks on industrial infrastructures [8]–[11]. These are, among others, detection and design of stealthy attacks, vulnerability of CPCSSs. In this subsection, the analysis results presented in the previous sections are leveraged to reveal new aspects of stealthy cyber-attacks, viewed in the unified framework of control and detection. The focus is on alternative definitions, existence conditions of stealthy attacks and vulnerability analysis.

1) *Definitions and existence conditions of detectability and actuability of attacks:* In the literature, stealthy attacks, for instance, replay [24], zero dynamics [7] and covert [64] attacks, are usually defined with respect to a certain type of detector [8]–[11], [13]. As detectors, observers or Kalman-filters serve as residual generators. It is assumed, often implicitly, that the detection is performed in the information pattern (u, y^a) , i.e. on the control station side. In our recent work, the concept of kernel attacks was introduced [40], which can be equivalently expressed as the so-called image attacks [65], thanks to the equivalence between the kernel and image subspaces, $\mathcal{I}_G = \mathcal{K}_G$, as described in Subsection III-A. The concept of kernel/image attacks not only gives a uniform form of stealthy attacks like covert, zero dynamics and replay attacks, but also, and more importantly, characterizes stealthy attacks independent of the used detection schemes. Instead, kernel/image attacks are defined in terms of plant model knowledge, G or (A, B, C, D) , and on the assumption of the information pattern (u, y^a) . Below, the concept of detectability of attacks is introduced. It is not only an alternative to stealthy attacks, but also more general and independent of the type of detectors. In other words, any stealthy attack should be an undetectable attack, but a stealthy attack under the use of an observer-based detector may be detected using other types of detectors.

We would like to call the reader's attention to (79) and Theorem 5. It can be observed that a certain class of attacks is effectless. Although they act on the system, they do not cause any change in the system dynamic. In the literature, this fact is obviously overlooked. This motivates us to introduce the concept of actuability of attacks, a dual form to the undetectability of attacks. For our purpose, we consider the

system model (1) under cyber-attacks with the attack model (34),

$$\begin{cases} y = Gu^a + r_{y,0}, G = (A, B, C, D) \\ u = Ky^a + r_{u,0}, K = -\hat{Y}\hat{X}^{-1} = X^{-1}Y. \end{cases} \quad (97)$$

Definition 4. Given the control system (97), the attack pair (a_u, a_y) is called undetectable, if

$$\begin{bmatrix} u^I \\ y^I \end{bmatrix} \equiv \begin{bmatrix} u_0 \\ y_0 \end{bmatrix}, \quad (98)$$

where (u_0, y_0) represent the system dynamic under attack-free operation conditions, and (u^I, y^I) denote the accessible input-output data (u, y) with respect to the information pattern,

$$(u^I, y^I) = \begin{cases} (u, y^a), & \text{detection on the control station side} \\ (u^a, y), & \text{detection on the plant side.} \end{cases}$$

Equation (98) means, the attack does not cause any changes comparing with the attack-free dynamic,

$$\begin{bmatrix} u_0 \\ y_0 \end{bmatrix} = \begin{bmatrix} M \\ N \end{bmatrix} v + \begin{bmatrix} -\hat{Y} \\ \hat{X} \end{bmatrix} r_y.$$

Definition 5. Given the control system (97), the attack pair (a_u, a_y) is called actuatable, if

$$\begin{bmatrix} u^a \\ y \end{bmatrix} \not\equiv \begin{bmatrix} u_0 \\ y_0 \end{bmatrix}. \quad (99)$$

It is apparent that the undetectability and actuability given in the above definitions are exclusively expressed in terms of the system behavior. Now, we are in a good position to address the existence conditions of undetectable attacks and actuatable attacks. For the former, it is assumed that attackers possess model knowledge (A, B, C, D) of the plant.

Theorem 8. Given the control system (78) and the attack model (34), the attacks (a_u, a_y) are undetectable under the information pattern (u, y^a) if and only if

$$\begin{bmatrix} a_u \\ -a_y \end{bmatrix} = \begin{bmatrix} M \\ N \end{bmatrix} \xi, \quad (100)$$

where ξ is an arbitrary \mathcal{L}_2 bounded signal.

Proof. Since $\forall \xi$

$$[-\hat{N} \quad \hat{M}] \begin{bmatrix} M \\ N \end{bmatrix} \xi = 0,$$

according (87), it is apparent that (100) is a sufficient condition. To prove the necessity, we examine the existence condition for

$$[-\hat{N} \quad \hat{M}] \begin{bmatrix} a_u \\ -a_y \end{bmatrix} = 0 \quad (101)$$

following Definition 4 and (87). Let (a_u, a_y) be \mathcal{L}_2 bounded, which can be written as

$$\begin{bmatrix} a_u \\ -a_y \end{bmatrix} = \begin{bmatrix} M & -\hat{Y} \\ N & \hat{X} \end{bmatrix} \begin{bmatrix} \xi_1 \\ \xi_2 \end{bmatrix} \quad (102)$$

for some \mathcal{L}_2 bounded (ξ_1, ξ_2) . Consequently,

$$[-\hat{N} \quad \hat{M}] \begin{bmatrix} a_u \\ -a_y \end{bmatrix} = \xi_2,$$

from which it can be immediately concluded that (101) is true only if $\xi_2 = 0$, which implies

$$\begin{bmatrix} a_u \\ -a_y \end{bmatrix} = \begin{bmatrix} M \\ N \end{bmatrix} \xi_1 =: \begin{bmatrix} M \\ N \end{bmatrix} \xi.$$

□

Remark 6. Since the stability of the closed-loop is assured, the signal ξ can be a function of (u, y) as well. That is, the result (100) holds for both additive and multiplication attacks.

Note that (100) implies that the attack pair (a_u, a_y) is undetectable, when

$$\begin{bmatrix} a_u \\ -a_y \end{bmatrix} \in \mathcal{I}_G. \quad (103)$$

Hence, we call undetectable attacks image attacks as well to emphasize the fact that they lie in the system image subspace \mathcal{I}_G [40], [65]. Recall that the system image subspace is invariant with respect to the gain matrix F . Thus, it is sufficient for attackers to construct the image subspace using model knowledge (A, B, C, D) . In fact, [40] firstly proposed the concept kernel attacks for the undetectable (stealthy) attacks, as it was proven that (a_u, a_y) should belong to the kernel subspace \mathcal{K}_G , i.e. satisfy (101), and then introduced the concept of image attacks using the equivalence $\mathcal{K}_G = \mathcal{I}_G$. It was proven that the covert, zero dynamics and replay attacks are kernel attackers [40]. It is noteworthy that the aforementioned results are true for any class of cyber-attacks, including those that attack a part of the input and output channels. Specifically, let the input and output channels (B, C, D) be split into two groups as described by (70) with the attacked channels (B_1, D_{21}, C_2) and unattacked channels $(B_2, D_{22},)$ and $(C_1, [D_{11} \ D_{12}])$. Correspondingly, write

$$a_u = \begin{bmatrix} a_{u_1} \\ 0 \end{bmatrix}, \quad a_y = \begin{bmatrix} 0 \\ a_{y_1} \end{bmatrix},$$

and the existence conditions for the kernel and image attacks are respectively,

$$\begin{bmatrix} -\hat{N} & \hat{M} \end{bmatrix} \begin{bmatrix} a_{u_1} \\ 0 \\ 0 \\ a_{y_1} \end{bmatrix} = 0 \iff \begin{bmatrix} a_{u_1} \\ 0 \\ 0 \\ a_{y_1} \end{bmatrix} \in \mathcal{K}_G,$$

for some ξ ,

$$\begin{bmatrix} a_{u_1} \\ 0 \\ 0 \\ a_{y_1} \end{bmatrix} = \begin{bmatrix} M \\ N \end{bmatrix} \xi \in \mathcal{I}_G.$$

As described in Subsection III-C4, zero dynamics attacks studied in [7], [34], [62] are a special case of the above result.

We now attend to the attack actuability.

Theorem 9. Given the control system (78) and the attack model (34), the attacks (a_u, a_y) are unactuable if and only if

$$\begin{bmatrix} a_u \\ -a_y \end{bmatrix} = \begin{bmatrix} -\hat{Y} \\ \hat{X} \end{bmatrix} r, \quad (104)$$

where $r \neq 0$ is an arbitrary \mathcal{L}_2 bounded signal.

Proof. Since $\forall r$

$$\begin{bmatrix} X & Y \end{bmatrix} \begin{bmatrix} -\hat{Y} \\ \hat{X} \end{bmatrix} r = 0,$$

it follows from (79) that (104) is a sufficient condition. To prove the necessity, let (a_u, a_y) be

$$\begin{bmatrix} a_u \\ -a_y \end{bmatrix} = \begin{bmatrix} M & -\hat{Y} \\ N & \hat{X} \end{bmatrix} \begin{bmatrix} r_1 \\ r_2 \end{bmatrix}$$

for some \mathcal{L}_2 bounded (r_1, r_2) . Consequently,

$$\begin{bmatrix} X & Y \end{bmatrix} \begin{bmatrix} a_u \\ -a_y \end{bmatrix} = r_1.$$

As a result, according to (79), the attacks are unactuable only if $r_1 = 0$, which implies

$$\begin{bmatrix} a_u \\ -a_y \end{bmatrix} = \begin{bmatrix} -\hat{Y} \\ \hat{X} \end{bmatrix} r_2.$$

The theorem is thus proven. □

Remember that $(\hat{X}, -\hat{Y})$ spans the image subspace of the controller \mathcal{I}_K . Hence, the condition (104) is equivalent to

$$\begin{bmatrix} a_u \\ -a_y \end{bmatrix} \in \mathcal{I}_K,$$

which implies, on the other hand, if

$$\begin{bmatrix} X & Y \end{bmatrix} \begin{bmatrix} a_u \\ -a_y \end{bmatrix} \neq 0,$$

then (a_u, a_y) are actuatable.

It is interesting to notice the following two claims as the immediate results of Theorems 8-9.

Corollary 3. Given the control system (78) and the attack model (34), (i) any actuatable attacks (a_u, a_y) are detectable in the information pattern (u^a, y) , (ii) the closed-loop dynamic (u^a, y) under any image attack,

$$\begin{bmatrix} a_u \\ -a_y \end{bmatrix} = \begin{bmatrix} M \\ N \end{bmatrix} \xi,$$

is governed by

$$\begin{bmatrix} u^a \\ y \end{bmatrix} = \begin{bmatrix} M \\ N \end{bmatrix} (\xi + v) + \begin{bmatrix} -\hat{Y} \\ \hat{X} \end{bmatrix} r_y. \quad (105)$$

Proof. The claim (i) follows immediately from (79), Theorem 9, and Definition 4. The claim (ii) with relation (105) is the result of Theorem 8 and the relation

$$\begin{bmatrix} X & Y \end{bmatrix} \begin{bmatrix} M \\ N \end{bmatrix} = I.$$

□

The claim (i) is useful for detecting (stealthy) attacks, as will be addressed in Subsection V-A, while the claim (ii) is essential for dealing with attack design issues. In fact, the condition (101) for kernel attacks builds the control-theoretic basis for attack detection, and its dual (and equivalent) form, the condition (100) for the image attacks, is a capable model for designing cyber-attacks. We would like to call the reader's

attention to the fact that ANY (actuable) attacks (a_u, a_y) act on the system dynamic (u^a, y) via the signal r_{a_u} , namely

$$\begin{bmatrix} u^a \\ y \end{bmatrix} = \begin{bmatrix} M \\ N \end{bmatrix} (r_{a_u} + v) + \begin{bmatrix} -\hat{Y} \\ \hat{X} \end{bmatrix} r_y, \quad (106)$$

Moreover, write (a_u, a_y) as

$$\begin{bmatrix} a_u \\ -a_y \end{bmatrix} = \begin{bmatrix} M & -\hat{Y} \\ N & \hat{X} \end{bmatrix} \begin{bmatrix} \xi_1 \\ \xi_2 \end{bmatrix},$$

the closed-loop dynamic is governed by

$$\begin{bmatrix} u^a \\ y \end{bmatrix} = \begin{bmatrix} M \\ N \end{bmatrix} (\xi_1 + v) + \begin{bmatrix} -\hat{Y} \\ \hat{X} \end{bmatrix} r_y, \quad (107)$$

independent of ξ_2 . In other words, **it is sufficient to construct image (stealthy) attacks exclusively.**

Remark 7. In our aforementioned discussion, the attack detectability and actuability have been defined and analyzed in the context that cyber-attacks are dedicated to degrade system control performance. Notice that in industrial practice, system monitoring and fault diagnosis are often implemented on the side of control station and in the information pattern (u, y^a) . According to Theorem 6,

$$\begin{aligned} \begin{bmatrix} u \\ y^a \end{bmatrix} &= \begin{bmatrix} M \\ N \end{bmatrix} v + \begin{bmatrix} -\hat{Y} \\ \hat{X} \end{bmatrix} (r_y - a_{r_y}) \Rightarrow \\ r_{y,cs} &= [-\hat{N} \quad \hat{M}] \begin{bmatrix} u \\ y^a \end{bmatrix} = r_y - a_{r_y}. \end{aligned}$$

Consequently, a fault diagnosis based on the residual $r_{y,cs}$ generated at the control station can be significantly disturbed by the attack signal a_{r_y} . Suppose that cyber-attacks are directed at the fault diagnosis system rather than the control performance. Attackers may design the attack pair (a_u, a_y) in such a way that

$$r_{a_u} = Xa_u - Ya_y = 0, a_{r_y} = -\hat{M}a_y + \hat{N}a_u \neq 0,$$

i.e. (a_u, a_y) is undetectable by means of the residual r_u , and actuatable via the residual $r_{y,cs}$. This can remarkably increase false alarm rate, and even result in alarm flooding [66]. The consequence is strongly reduced production rate and, when fault-tolerant control action is triggered, degradation of control performance as well. This engineering practical aspect is totally overlooked in the research on secure CPCSSs.

2) *Vulnerability analysis and image attack design:* In the literature, in the context of vulnerability analysis, major attention has been mainly paid to degrade the tracking performance, enlarge the state estimation error, and increase linear quadratic Gaussian (LQG) control performance [23], [36], [67], [68], while limit research efforts have been made on deteriorating the feedback control performance [19]. Furthermore, most of the existing attack design schemes are implemented based on some strict assumptions, which limits the applications.

In this subsection, we analyze system vulnerability and delineate a scheme of designing image attacks. Apart from the above-mentioned sufficiency of constructing image attacks, further two advantages of this design scheme are (i) the design is performed in the context of a constraint-free optimization

problem with respect to the system vulnerability, (ii) instead of $(a_u, a_y) \in \mathbb{R}^{p+m}$, the latent variable $\xi \in \mathbb{R}^p$ serves as the optimization variable, which may considerably reduce optimization computations.

Remark 8. In the literature, optimal design of stealthy attacks is typically formulated as an optimization problem with the stealthiness as a constraint. It can be proven that such constraint conditions can be reformulated as the kernel condition (101) for strictly stealthy attacks or

$$\left\| \begin{bmatrix} -\hat{N} & \hat{M} \end{bmatrix} \begin{bmatrix} a_u \\ -a_y \end{bmatrix} \right\| \leq \varepsilon$$

for stealthy attacks, where $\|\cdot\|$ denotes some norm or index, and ε is a small constant.

Vulnerability analysis is receiving increasing attention in the research area of secure CPCSSs and attack design [19], [34], [69], [70]. Informally speaking, vulnerability describes attacker's ability to induce significant degradation of a control performance like optimal control and estimation objective, while remaining within the system's admissible operating range. Below, we firstly introduce the concept of attack stability margin and, on this basis, define the system vulnerability. In this context, image attack design is addressed. To this end, we consider the control system (78) and the attack model (34), and assume that attackers possess the process knowledge (A, B, C, D) and are able to access the system data (u, y) .

Theorem 7 reveals that the impact of cyber-attacks on the CPCSS dynamic is equivalent to variations in controller. Specifically, the altered control gain is subject to

$$K_\Delta = - (X + \Delta_X)^{-1} (Y + \Delta_Y),$$

with (Δ_X, Δ_Y) denoting the variation caused by attacks. One critical endangerment of such variations is the system stability. In robust control theory, stability margin is a well-established concept of quantifying the impact of model uncertainty on the closed-loop stability [44], [71]. According to Theorems 5 and 7, attacks exclusively act on the system image subspace, the stability margin of the system dynamic under attacks is to be defined in terms of (M, N) . Specifically, dual to the stability margin with respect to the model uncertainty defined by [44], [71]

$$\left\| \begin{bmatrix} K \\ I \end{bmatrix} (I - GK)^{-1} \hat{M}^{-1} \right\|_\infty^{-1} = \left\| \begin{bmatrix} -\hat{Y} \\ \hat{X} \end{bmatrix} \right\|_\infty^{-1},$$

the loop dynamic

$$\begin{aligned} & \begin{bmatrix} I \\ G \end{bmatrix} (I - K_\Delta G)^{-1} (X + \Delta_X)^{-1} \\ &= \begin{bmatrix} M \\ N \end{bmatrix} ((X + \Delta_X) M + (Y + \Delta_Y) N)^{-1} \\ &= \begin{bmatrix} M \\ N \end{bmatrix} \left(I + [\Delta_X \quad \Delta_Y] \begin{bmatrix} M \\ N \end{bmatrix} \right)^{-1} \end{aligned} \quad (108)$$

is conceded, from which it can be concluded that the loop dynamic is stable when

$$\left\| [\Delta_X \quad \Delta_Y] \begin{bmatrix} M \\ N \end{bmatrix} \right\|_\infty < 1 \implies$$

$$\|[\Delta_X \ \Delta_Y]\|_{\infty} \left\| \begin{bmatrix} M \\ N \end{bmatrix} \right\|_{\infty} < 1.$$

In this context, we introduce the definition of attack stability margin.

Definition 6. Given the attacked CPCS model,

$$\begin{cases} y = Gu^a + r_{y,0} \\ u^a = K_{\Delta}y + r_{u,a}, \end{cases} \quad (109)$$

where K_{Δ} and $r_{u,a}$ are described in Theorem 7, the value b_a ,

$$b_a = \left\| \begin{bmatrix} M \\ N \end{bmatrix} \right\|_{\infty}^{-1}, \quad (110)$$

is called attack stability margin.

It is apparent that the loop dynamic may become unstable, when $\|[\Delta_X \ \Delta_Y]\|_{\infty} \geq b_a$. In other words, the value

$$\left\| \begin{bmatrix} M \\ N \end{bmatrix} \right\|_{\infty} = b_a^{-1}$$

reflects the degree of vulnerability. We now delineate a design scheme of image attacks and the vulnerability in the context of system stability.

Let an image attack be described by

$$\begin{bmatrix} a_u \\ a_y \end{bmatrix} = \Pi^a \begin{bmatrix} u \\ y \end{bmatrix}, \quad \Pi^a := \begin{bmatrix} M_a \\ N_a \end{bmatrix} \Pi_u^a,$$

where (M_a, N_a) represents an SIR of the plant constructed by the attackers with parameters (F_a, V_a) , and Π_u^a is to be determined. The attack model (86) is then further written into

$$\begin{aligned} \begin{bmatrix} a_u \\ a_y \end{bmatrix} &= \Pi^a \left(I + \begin{bmatrix} I & 0 \\ 0 & 0 \end{bmatrix} \Pi^a \right)^{-1} \begin{bmatrix} u^a \\ y \end{bmatrix} \\ &= \begin{bmatrix} M_a \\ N_a \end{bmatrix} \Pi_u^a \left(I + \begin{bmatrix} M_a \\ 0 \end{bmatrix} \Pi_u^a \right)^{-1} \begin{bmatrix} u^a \\ y \end{bmatrix}. \end{aligned}$$

Attributed to Theorem 1, (M, N) and (X, Y) are subject to

$$\begin{aligned} \begin{bmatrix} M \\ N \end{bmatrix} &= \begin{bmatrix} M_a \\ N_a \end{bmatrix} T_a, \quad T_a \in \mathcal{RH}_{\infty}, \\ [X \ Y] \begin{bmatrix} M_a \\ N_a \end{bmatrix} &= T_a^{-1}, \quad T_a^{-1} \in \mathcal{RH}_{\infty}, \end{aligned}$$

for some T_a . It follows from Theorem 7

$$\begin{aligned} \left(I + [\Delta_X \ \Delta_Y] \begin{bmatrix} M \\ N \end{bmatrix} \right)^{-1} &= \left(I - [X \ Y] \Phi^a \begin{bmatrix} M \\ N \end{bmatrix} \right)^{-1} \\ &= \left(I - T_a^{-1} \Pi_u^a \left(I + \begin{bmatrix} M_a \\ 0 \end{bmatrix} \Pi_u^a \right)^{-1} \begin{bmatrix} M_a \\ N_a \end{bmatrix} T_a \right)^{-1} \\ &= T_a^{-1} \left(I - \Pi_u^a \left(I + \begin{bmatrix} M_a \\ 0 \end{bmatrix} \Pi_u^a \right)^{-1} \begin{bmatrix} M_a \\ N_a \end{bmatrix} \right)^{-1} T_a. \quad (111) \end{aligned}$$

Consequently, it is sufficient to consider

$$\left(I - \Pi_u^a \left(I + \begin{bmatrix} M_a \\ 0 \end{bmatrix} \Pi_u^a \right)^{-1} \begin{bmatrix} M_a \\ N_a \end{bmatrix} \right)^{-1} \quad (112)$$

for examining the system stability. Note that the expression (112) exclusively comprises the transfer functions designed by the attackers. Now, impose

$$\Pi_u^a \left(I + \begin{bmatrix} M_a \\ 0 \end{bmatrix} \Pi_u^a \right)^{-1} = \begin{bmatrix} \Pi_1^a & \Pi_2^a \end{bmatrix} \begin{bmatrix} X_a & Y_a \\ -\hat{N}_a & \hat{M}_a \end{bmatrix},$$

$(\Pi_1^a, \Pi_2^a) \in \mathcal{RH}_{\infty}$, leading to

$$\begin{aligned} \Pi_u^a &= \left(I - \begin{bmatrix} \Pi_1^a & \Pi_2^a \end{bmatrix} \begin{bmatrix} X_a \\ -\hat{N}_a \end{bmatrix} M_a \right)^{-1} \cdot \\ &\quad \begin{bmatrix} \Pi_1^a & \Pi_2^a \end{bmatrix} \begin{bmatrix} X_a & Y_a \\ -\hat{N}_a & \hat{M}_a \end{bmatrix}. \end{aligned}$$

Hereby, (X_a, Y_a) and (\hat{M}_a, \hat{N}_a) are the LCPs of the controller and plant set by the attackers, and (Π_1^a, Π_2^a) are selected so that

$$\left(I - \begin{bmatrix} \Pi_1^a & \Pi_2^a \end{bmatrix} \begin{bmatrix} X_a \\ -\hat{N}_a \end{bmatrix} M_a \right)^{-1} \in \mathcal{RH}_{\infty}. \quad (113)$$

Consequently,

$$I - \Pi_u^a \left(I + \begin{bmatrix} M_a \\ 0 \end{bmatrix} \Pi_u^a \right)^{-1} \begin{bmatrix} M_a \\ N_a \end{bmatrix} = I - \Pi_1^a. \quad (114)$$

We summarize the above results in the following theorem and definition.

Theorem 10. Given the attacked CPCS modelled by (109) in Definition 6, if there exists LCPs and RCPs of the plant and controller, (\hat{M}_a, \hat{N}_a) , (X_a, Y_a) , (M_a, N_a) , and $(\Pi_1^a, \Pi_2^a) \in \mathcal{RH}_{\infty}$ so that (i) the condition (113) holds, and (ii) the system $I - \Pi_1^a$ has a zero in the closed right half-plane (an unstable zero), the loop dynamic (108) is unstable.

Proof. The proof follows from (111)-(112) and (114). \square

Definition 7. Given the attacked CPCS model (109) and suppose that the condition (113) is satisfied, the system $(I - \Pi_1^a)^{-1}$ is called vulnerability model.

It is worth emphasizing that all relevant transfer functions in (113)-(114) can be arbitrarily designed by the attackers. They pose no strict conditions, as demonstrated by the following example.

Example 1. Consider a stable plant system $G \in \mathcal{RH}_{\infty}^{m \times p}$, $m \geq p$. It is apparent that for $F_a = 0, V_a = I$,

$$(X_a, Y_a) = (I, 0), \quad (M_a, N_a) = (I, G).$$

Accordingly,

$$I - \begin{bmatrix} \Pi_1^a & \Pi_2^a \end{bmatrix} \begin{bmatrix} X_a \\ -\hat{N}_a \end{bmatrix} M_a = I - \Pi_1^a + \Pi_2^a \hat{N}_a.$$

We now select $\Pi_2^a \in \mathcal{RH}_{\infty}$ so that $\Pi_2^a \hat{N}_a$ is subject to

$$\Pi_2^a \hat{N}_a = \frac{Z_0}{P_0} I, \quad \frac{Z_0}{P_0} = \frac{\beta_{\vartheta} z^{\vartheta} + \dots + \beta_0}{\gamma_{\eta} z^{\eta} + \dots + \gamma_0}, \quad (115)$$

where Z_0 contains all zeros of \hat{N}_a in the closed right half-plane, $\eta - \vartheta \geq 0$ (depending on the relative degree of \hat{N}_a), which ensures the existence of (115), and $\gamma_i, i = 0, \dots, \eta$, are

arbitrarily selectable, so far the stability of $\Pi_2^a \hat{N}_a$ is guaranteed. Next, set

$$\begin{aligned}\Pi_1^a &= \frac{\alpha_\eta z^\eta + \cdots + \alpha_0}{P_0} I \in \mathcal{RH}_\infty \implies \\ I - \Pi_1^a + \Pi_2^a \hat{N}_a &= \frac{\Xi_0}{P_0} I, I - \Pi_1^a = \frac{\Pi_0}{P_0} I, \\ \Xi_0 &= (\gamma_\eta - \alpha_\eta) z^\eta + \cdots + (\gamma_{\vartheta+1} - \alpha_{\vartheta+1}) z^{\vartheta+1} + \\ &(\gamma_\vartheta + \beta_\vartheta - \alpha_\vartheta) z^\vartheta + \cdots + \gamma_0 + \beta_0 - \alpha_0, \\ \Pi_0 &= (\gamma_\eta - \alpha_\eta) z^\eta + \cdots + \gamma_0 - \alpha_0,\end{aligned}$$

and determine $\alpha_i, \gamma_i, i = 0, \dots, \eta$, such that the zeros of polynomial Ξ_0 are in the left half-plane, and Π_0 contains zeros in the closed right half-plane. As a result,

$$\left(I - \begin{bmatrix} \Pi_1^a & \Pi_2^a \end{bmatrix} \begin{bmatrix} X_a \\ -\hat{N}_a \end{bmatrix} M_a \right)^{-1} = \frac{P_0}{\Xi_0} I \in \mathcal{RH}_\infty,$$

and $(I - \Pi_1^a)^{-1} = \frac{P_0}{\Xi_0} I$ is unstable.

V. DETECTION, CONTROL, AND SYSTEM PRIVACY

We now attend to the simultaneous detection of the faults and cyber-attacks, their tolerant and resilient control. At the end of this section, we will address system privacy issues as well. For our purpose, the fault model (37) and attack model (34) are under consideration.

A. Simultaneous detection of faults and cyber-attacks

In industrial CPCSSs, faults and attacks may occur concurrently, and their effects on system operations are often similar and can be mutually masking. Consequently, conventional diagnosis methods that detect faults and cyber-attacks separately may lead to misdiagnosis, false alarms, and even overlook threats. Congruously, simultaneous detection of faults and cyber-attacks attracts considerable attention in industrial applications [72]–[75]. On the other hand, it can be observed that endeavours to research simultaneous detection of faults and attacks, in comparison with the current enthusiasm for attack detection, and in particular attack design, are remarkably limited [76]–[79]. In the previous sections, it is revealed that (i) there exists an attack information potential IP_a on the plant and control station sides, (ii) there is no fault information difference for the two information patterns, since the output residual r_y identically affects (u, y^a) and (u^a, y) . In particular, Theorem 6 clearly showcases that a simultaneous detection of faults and attacks in the information pattern (u, y^a) , i.e. detection on the control station, is challenging due to the strong coupling of faults and attacks in the closed-loop data (u, y^a) . These results motivate us to leverage the unified framework to achieve the simultaneous detection in different information patterns.

1) *Simultaneous detection scheme A*: It follows from Theorems 3, 5 and (79) that the closed-loop dynamic under simultaneous existence of the faults and attacks is governed by

$$\begin{bmatrix} u^a \\ y \end{bmatrix} = \begin{bmatrix} M \\ N \end{bmatrix} (v + a_{r_u}) + \begin{bmatrix} -\hat{Y} \\ \hat{X} \end{bmatrix} \begin{pmatrix} \Phi^f (\hat{N}_d d + \bar{f}) \\ + \Psi^f (v + a_{r_u}) \end{pmatrix}. \quad (116)$$

That means, in the information pattern (u^a, y) , (i) the faults exclusively act on the residual subspace, (ii) the cyber-attacks act on the image and residual subspaces, whereby the influence on the residual subspace is coupled with the (multiplicative) fault Ψ^f . These distinguishing features allow us to detect the faults and attacks simultaneously on the plant side. To be specific, on the assumption that the reference signal v is known or equal to zero, an assumption mostly adopted in the literature, detecting the injected cyber-attack a_{r_u} by means of the residual r_u ,

$$r_u = Xu^a + Yy = v + a_{r_u}, \quad (117)$$

is straightforward, namely $a_{r_u} = r_u - v$. Considering that, during fault-free operations, the dynamic of the residual generator is subject to

$$r_y = \hat{M}y - \hat{N}u^a = \hat{N}_d d, \quad (118)$$

where the unknown input vector d is either a stochastic process or an ℓ_2 -bounded signal and modelled by (36), an optimal fault detection is achieved by adding an post-filter R to the residual r_y ,

$$r = Rr_y = R\hat{N}_d d,$$

whose design and the corresponding threshold setting are summarized in Algorithm 1.

Algorithm 1: Detection scheme A

1) Do a co-inner-outer factorization of \hat{N}_d ,

$$\hat{N}_d = \hat{N}_d^{co} \hat{N}_d^{in}; \quad (119)$$

2) set R as

$$R = \left(\hat{N}_d^{co} \right)^{-1}; \quad (120)$$

3) corresponding to the residual evaluation function,

$$J = \begin{cases} r^T(k) \Sigma_r^{-1} r(k), d = \begin{bmatrix} w \\ v \end{bmatrix} \\ \|r\|_2, d = \begin{bmatrix} d_P \\ d_S \end{bmatrix}, \end{cases}$$

set the threshold J_{th} as

$$J_{th} = \begin{cases} \chi_\alpha^2(m), d = \begin{bmatrix} w \\ v \end{bmatrix} \\ \delta_d, d = \begin{bmatrix} d_P \\ d_S \end{bmatrix} \end{cases}$$

where $\alpha \in (0, 1)$ is pre-defined false alarm rate.

The control-theoretic background of the above algorithm is the application of a co-inner-outer factorization of a transfer function matrix to optimize an observer-based fault detection system with white noises or an ℓ_2 -bounded unknown input vector. The reader is referred to [1], [5] for details. As delineated in [1], the residual generation system satisfies

$$\begin{cases} r \sim \mathcal{N}(0, \Sigma_r), \text{ and white, } d = \begin{bmatrix} w \\ v \end{bmatrix} \\ R\hat{N}_d \text{ is co-inner, } d = \begin{bmatrix} d_P \\ d_S \end{bmatrix}. \end{cases}$$

As a result,

$$\begin{cases} r^T(k)\Sigma_r^{-1}r(k) \sim \chi^2(m), d = \begin{bmatrix} w \\ v \end{bmatrix} \\ \|r\|_2 \leq d, d = \begin{bmatrix} d_P \\ d_S \end{bmatrix}. \end{cases}$$

Remark 9. In the literature, the χ^2 test statistic with the threshold setting χ_{α}^2 is widely applied for attack detection, even though the corresponding residual signal is a color noise series. It leads to higher false alarm rate and lower detectability. The co-inner-outer factorization described in Algorithm 1 ensures the whiteness of the residual signal. Correspondingly, the χ^2 test statistic delivers the maximal detectability [1].

It is worth emphasizing that the generation of the residual pair (r_u, r_y) is realized by means of a single observer, as described in Subsection II-B,

$$\begin{cases} \hat{x}(k+1) = (A - LC)\hat{x}(k) - (B - LD)u^a(k) - Ly(k) \\ \begin{bmatrix} r_u(k) \\ r_y(k) \end{bmatrix} = \begin{bmatrix} F \\ C \end{bmatrix}\hat{x}(k) + \begin{bmatrix} I \\ -D \end{bmatrix}u^a(k) + \begin{bmatrix} 0 \\ I \end{bmatrix}y(k). \end{cases}$$

and implemented on the plant side. So far, the associated online computations are moderate.

2) *Simultaneous detection scheme B, an improved auxiliary system-based detection method* : Roughly speaking, the basic idea of the auxiliary subsystem based detection methods is to augment the plant with an auxiliary/monitoring subsystem whose dynamics are unknown to the attacker, but similar to the one of the system. The auxiliary subsystem is so constructed that deviations induced by an attack become observable in auxiliary residuals [54], [55], [60]. The auxiliary system-based detection methods are mainly applied for detecting stealthy attacks. In this regard, it can be plainly seen from the system dynamic (116) and Theorem 5 that the input residual generator,

$$r_u = Xu + Yy = v + \begin{bmatrix} X & Y \end{bmatrix} \begin{bmatrix} a_u \\ a_y \end{bmatrix}, \quad (121)$$

is an ideal auxiliary subsystem for the detection purpose. Recall that on the control station side,

$$\begin{bmatrix} u \\ y^a \end{bmatrix} = \begin{bmatrix} M \\ N \end{bmatrix}v + \begin{bmatrix} -\hat{Y} \\ \hat{X} \end{bmatrix}(r_y - a_{r_y}).$$

Hence, in case of an undetectable faults (stealthy attacks), $a_{r_y} = 0$, leading to

$$\begin{bmatrix} u \\ y^a \end{bmatrix} = \begin{bmatrix} M \\ N \end{bmatrix}v + \begin{bmatrix} -\hat{Y} \\ \hat{X} \end{bmatrix}r_y.$$

Subsequently, simultaneous detection of faults and (stealthy) attacks can be realized by (i) attack detection on the plant side using the detection system (121), (ii) the detection information is transmitted to the control station via a well-encrypted channel, and (iii) fault detection by means of the output residual system r_y and Algorithm 1 running on the control station.

3) *Simultaneous detection scheme C*: We now address the situation that attack detection is to be realized on the control station side. For instance, the latent variable v as a control reference signal is calculated real-time. In this case, the detection scheme A cannot be realized. In this regard, Theorem 5 plainly depicts that the attacks exclusively act on

the residual subspace and are tightly coupled with the faults. The consequence is that an attack detection based on the residual

$$\hat{M}y^a - \hat{N}u = r_y + \hat{M}a_y + \hat{N}a_u$$

raises two problems, (i) attackers may easily construct stealthy attacks when they possess system knowledge (A, B, C, D) , (ii) the strong coupling between the residual r_y and the attack function $\hat{M}a_y + \hat{N}a_u$ make it impossible to distinguish the faults from the attacks. The following detection scheme is proposed to manage these two issues. Let

$$u^a = u_0 + Q_u r_u + a_{u_0}, Q_u \in \mathcal{RH}_{\infty},$$

where $u_0 = Ky^a + r_{u,0}$ is the input signal computed at the control station and sent to the plant, a_{u_0} is the attack injected into the control channel,

$$r_u = Xu^a + Yy$$

is computed on the plant side with Q_u to be specified subsequently. Note that $Q_u r_u$ is constructed and computed on the plant side and not transmitted over the network. Moreover, concerning the system nominal control performance, $Q_u r_u$ solely changes the system response to the reference signal v , which can be fully recovered by re-setting the reference (refer to (125)-(126)). We now examine the kernel-based model from the viewpoint of the control station,

$$\begin{cases} Xu_0 + Yy^a = Xr_{u,0} = v \\ \hat{M}y^a - \hat{N}u_0 = r_y + \hat{M}a_y + \hat{N}a_{u_0} + \hat{N}Q_u r_u. \end{cases} \quad (122)$$

Subsequently, the information pattern at the control station is

$$\begin{bmatrix} u \\ y^a \end{bmatrix} = \begin{bmatrix} M \\ N \end{bmatrix}v + \begin{bmatrix} -\hat{Y} \\ \hat{X} \end{bmatrix}(r_y + \hat{M}a_y + \hat{N}a_{u_0} + \hat{N}Q_u r_u),$$

and the system dynamic is governed by

$$\begin{aligned} \begin{bmatrix} u^a \\ y \end{bmatrix} &= \begin{bmatrix} u_0 \\ y^a \end{bmatrix} + \begin{bmatrix} Q_u r_u \\ 0 \end{bmatrix} + \begin{bmatrix} a_{u_0} \\ -a_y \end{bmatrix} \\ &= \begin{bmatrix} M \\ N \end{bmatrix}(v + XQ_u r_u + Xa_{u_0} - Ya_y) + \begin{bmatrix} -\hat{Y} \\ \hat{X} \end{bmatrix}r_y. \end{aligned}$$

The last equation is attributed to (80)-(81). Observe that

$$r_u = Xu + Yy^a + Xa_{u_0} - Ya_y + XQ_u r_u.$$

Suppose that Q_u is so selected that $(I - XQ_u)^{-1} \in \mathcal{RH}_{\infty}$. It turns out

$$r_u = (I - XQ_u)^{-1}(Xa_{u_0} - Ya_y + v). \quad (123)$$

As a result,

$$\begin{aligned} \begin{bmatrix} u_0 \\ y^a \end{bmatrix} &= \left(\begin{bmatrix} M \\ N \end{bmatrix} + \begin{bmatrix} -\hat{Y} \\ \hat{X} \end{bmatrix}Q \right)v \\ &+ \begin{bmatrix} -\hat{Y} \\ \hat{X} \end{bmatrix}(r_y + \hat{M}a_y + \hat{N}a_{u_0} + Q(Xa_{u_0} - Ya_y)), \end{aligned} \quad (124)$$

$$\begin{aligned} \begin{bmatrix} u^a \\ y \end{bmatrix} &= \begin{bmatrix} M \\ N \end{bmatrix}\bar{v} + \begin{bmatrix} -\hat{Y} \\ \hat{X} \end{bmatrix}r_y \\ &+ \begin{bmatrix} M \\ N \end{bmatrix}(I - XQ_u)^{-1}(Xa_{u_0} - Ya_y), \end{aligned} \quad (125)$$

$$Q = \hat{N}Q_u(I - XQ_u)^{-1}, v = (I - XQ_u)\bar{v}. \quad (126)$$

Equation (125) describes the loop dynamic. It is clear that adding $Q_u r_u$ in the control signal results in no change in the system nominal (attack-free) dynamic, when \bar{v} is set according to (126) on the control station side. Subsequently,

$$r_y = \hat{M}y - \hat{N}u^a = \Phi^f \left(\hat{N}_d d + \bar{f} \right) + \Psi^f v, \quad (127)$$

attributed to Theorem 3. Thus, detecting the faults can be realized by running Algorithm 1 on the plant side, and it is decoupled from the cyber-attacks. If a fault is detected, an alarm is released and the corresponding message is sent to the control station.

To detect the cyber-attacks on the control station side, the residual signal $r_{u,ad}$ is built,

$$\begin{aligned} r_{u,ad} &= \begin{bmatrix} -\hat{N} & \hat{M} \end{bmatrix} \left(\begin{bmatrix} u_0 \\ y^a \end{bmatrix} - \left(\begin{bmatrix} M \\ N \end{bmatrix} + \begin{bmatrix} -\hat{Y} \\ \hat{X} \end{bmatrix} Q \right) v \right) \\ &= \hat{M}y^a - \hat{N}u_0 - Qv \end{aligned} \quad (128)$$

which, according to (124), yields

$$r_{u,ad} = r_y + \hat{M}a_y + \hat{N}a_{u_0} + Q(Xa_{u_0} - Ya_y). \quad (129)$$

Concerning stealthy attacks, consider

$$\begin{aligned} a_{u,y} &:= \hat{M}a_y + \hat{N}a_{u_0} + Q(Xa_{u_0} - Ya_y) \\ &= [Q \ I] \begin{bmatrix} X & Y \\ -\hat{N} & \hat{M} \end{bmatrix} \begin{bmatrix} a_{u_0} \\ -a_y \end{bmatrix}. \end{aligned}$$

Although attackers possess system knowledge of (A, B, C, D) , they are limited to access the process data (u_0, y) rather than (u, y) . Consequently, it is hard for attackers to identify Q_u and thus Q . In other words, the missing information about Q poses a hard existence condition, i.e.

$$a_{u,y} = \hat{M}a_y + \hat{N}a_{u_0} + Q(Xa_{u_0} - Ya_y) = 0,$$

for realizing stealthy attacks.

As far as no alarm for a fault is released, the attacks can be detected based on the residual signal (129),

$$r_{u,ad} = \hat{N}_d d + a_{u,y}, a_{u,y} \neq 0, \quad (130)$$

using Algorithm 1. It is apparent that in the case of a detected fault, it holds

$$r_{u,ad} = \Phi^f \left(\hat{N}_d d + \bar{f} \right) + \Psi^f v + r_{u,ad}. \quad (131)$$

Thus, it is unrealistic and, from the engineering viewpoint, also unnecessary to detect the attacks. The implementation of the detection scheme C is summarized in Algorithm 2.

Algorithm 2: Detection scheme C

- 1) Implementation of $Q_u r_u$ and $u = u_0^a + Q_u r_u$ on the plant side;
- 2) Implementation of $r_y = \hat{M}y - \hat{N}u^a$ and Algorithm 1 for fault detection, transmission of the fault information once the faults are detected;
- 3) Implementation of the residual generator (128) and Algorithm 1 for attack detection.

It is emphasized again that the core of generating the residual pair $(r_{u,ad}, r_y)$ is two observer-based residual generators driven

by (u^a, y) and (u_0, y^a) and realized on the plant and control station sides, respectively, as described in Subsection II-B.

At the end of this subsection, we would like to remark that (i) in engineering applications, it is possible to enhance the detection reliability by a combined use of the proposed detections schemes, (ii) thanks to the advantage of the use of the identical observer-based residual generators, the demanded online computation is less costly, (iii) aiming at fault detection, the (output) residual generated on the plant side is reliable and capable, in particular, when cyber-attacks are dedicated to the fault detection system running at the control station (refer to Remark 7), and (iv) there exists no change of the nominal system control performance.

B. Fault-tolerant and attack resilient feedback control

As described in the section of *Problem Formulation*, there are few publications dedicated to simultaneous fault-tolerant and attack resilient feedback control. In this subsection, we leverage the unified framework and robust control methods to propose an integrated fault-tolerant and attack resilient control scheme aiming at mitigating the control performance degradation caused by the faults and attacks. The basic idea behind this scheme is to configure the CPCS in the structure form of Variation II described in Subsection III-C1, which enables us to optimally make use of (i) the attack information potential IP_a , (ii) the additional degree of design freedom, and (iii) the duality between faulty and attack dynamics, to obviate performance degradation.

1) *The control scheme*: Consider the attack information potential IP_a (82), the loop dynamics on the plant side (79) and on the control station side (87). It becomes obvious that the impact of a_{r_u} on the information pattern (u^a, y) and a_{r_y} on the information pattern (u, y^a) results in the attack information potential. In order to reduce IP_a and the influence of a_{r_u} on the system dynamic (u^a, y) , compensating a_{r_u} by feeding back a_{r_y} is a potential solution. This is the basic idea behind the control scheme described below. The controller comprises two sub-controllers, respectively located on the both sides of the CPCS,

$$u_1 = Ky^a + r_{u,0}, \quad (132)$$

$$\begin{aligned} K &= - \left(X + Q_1 \hat{N} \right)^{-1} \left(Y - Q_1 \hat{M} \right), \\ u_2 &= Q_2 \left(\hat{M}y - \hat{N}u^a \right), Q_1, Q_2 \in \mathcal{RH}_\infty. \end{aligned} \quad (133)$$

The sub-controller u_1 is implemented on the control station side, while u_2 is embedded in the plant side. The overall controller u acting on the plant is

$$u^a = u_1 + u_2 + a_{u_1}. \quad (134)$$

Notice that the controller (134) is a stabilizing controller and PnP-configured (refer to Theorem 2). During attack-free operations, it is equivalent to

$$\begin{aligned} u &= Ky + r_{u,0}, \\ K &= - \left(X + Q \hat{N} \right)^{-1} \left(Y - Q \hat{M} \right), \\ Q &= Q_1 + \left(X + Q_1 \hat{N} \right) Q_2, \end{aligned}$$

whose observer-based realization is given by

$$u = F\hat{x} + (Q_1 + Q_2) (\hat{M}y - \hat{N}u).$$

It is of considerable importance to emphasize that two output residuals are embedded in the controller and they serve for different control purposes. While the residual $\hat{M}y^a - \hat{N}u$ is generated on the control station side and used for resilient control of cyber-attacks, the residual $r_y = \hat{M}y - \hat{N}u^a$, added to the controller on the plant side, is applied to enhance the fault-tolerance. To highlight this core idea, we now examine the closed-loop dynamic.

Consider the kernel-based model of the closed-loop,

$$\begin{aligned} & \hat{M}y - \hat{N}u^a = r_y, \\ & (X + Q_1\hat{N})u^a + (Y - Q_1\hat{M})y \\ &= [X + Q_1\hat{N} \quad Y - Q_1\hat{M}] \begin{pmatrix} u \\ y^a \end{pmatrix} + \begin{pmatrix} a_{u_1} \\ a_y \end{pmatrix} \\ &= v + \bar{Q}_2r_y + (X + Q_1\hat{N})a_{u_1} - (Y - Q_1\hat{M})a_y, \\ & v = (X + Q_1\hat{N})r_{u,0}, \bar{Q}_2 = (X + Q_1\hat{N})Q_2. \end{aligned}$$

It follows from (56) that

$$\begin{pmatrix} u^a \\ y \end{pmatrix} = \begin{bmatrix} M \\ N \end{bmatrix} v + \left(\begin{bmatrix} -\hat{Y} \\ \hat{X} \end{bmatrix} + \begin{bmatrix} M \\ N \end{bmatrix} Q \right) r_y + \begin{bmatrix} M \\ N \end{bmatrix} ([X \quad Y] - Q_1[-\hat{N} \quad \hat{M}]) \begin{pmatrix} a_{u_1} \\ -a_y \end{pmatrix}. \quad (135)$$

It is apparent that solving the MMP

$$J_1 = \inf_{Q_1 \in \mathcal{RH}_\infty} \| [X \quad Y] - Q_1 [-\hat{N} \quad \hat{M}] \|_\infty \quad (136)$$

leads to the optimal resilience to the attacks, while the fault-tolerance is enhanced by solving the following MMP

$$\inf_{Q_2 \in \mathcal{RH}_\infty} \left\| \begin{bmatrix} -\hat{Y} \\ \hat{X} \end{bmatrix} + \begin{bmatrix} M \\ N \end{bmatrix} (Q_1 + (X + Q_1\hat{N})Q_2) \right\|_\infty \quad (137)$$

for given Q_1 . It is of considerable interest to study the case

$$(X + Q_1\hat{N})^{-1} \in \mathcal{RH}_\infty, \quad (138)$$

that is, the controller K is stable. Subsequently, for $\bar{Q}_1 = (X + Q_1\hat{N})^{-1}(\bar{Q}_1 - Q_1)$, the MMP (137) is equivalent to

$$\bar{J}_1 = \inf_{\bar{Q}_1 \in \mathcal{RH}_\infty} \left\| \begin{bmatrix} -\hat{Y} \\ \hat{X} \end{bmatrix} + \begin{bmatrix} M \\ N \end{bmatrix} \bar{Q}_1 \right\|_\infty. \quad (139)$$

The fault-tolerant and attack resilient controller (134) is triggered when faults or/and attacks are detected. The system operation modes and the corresponding controllers are summarized below.

2) *On controller design:* Recall that (\hat{M}, \hat{N}) and (M, N) are the dual coprime factorization pairs of the plant, while (X, Y) and (\hat{X}, \hat{Y}) are the dual pairs of the equivalent "controller", and they are subject to the Bezout identity (6). In this context, the MMPs (136) and (139) are presented in a dual form. In other words, the proposed control scheme enables us to solve the fault-tolerant control and attack resilient

System operation modes and the corresponding controllers

- 1) Fault- and attack-free operation: $u = Ky + r_{u,0}$, running on the control station side with K subject to (19);
- 2) Faulty and attack-free operation: $u = Ky + r_{u,0} + Q_2r_y$, K is subject to (19), and $u_2 = Q_2r_y$ is added on the plant side;
- 3) Operation under attacks but fault-free: $u = Ky + r_{u,0}$, running on the control station side with K subject to (132);
- 4) Operation under attacks and faults: $u = Ky + r_{u,0} + Q_2r_y$, K is subject to (132), and $u_2 = Q_2r_y$ is added on the plant side.

control as two dual and independent MMPs. This fact motivates us to have a close look at these two dual MMPs. To begin with, a special case with the normalized LCF and RCF of G , (\hat{M}_0, \hat{N}_0) and (M_0, N_0) , is considered. The corresponding LCF and RCF of the controller are denoted by (X_0, Y_0) and (\hat{X}_0, \hat{Y}_0) , respectively. Observe that

$$\begin{aligned} & \| [X_0 \quad Y_0] - Q_1 [-\hat{N}_0 \quad \hat{M}_0] \|_\infty \\ &= \| ([X_0 \quad Y_0] - Q_1 [-\hat{N}_0 \quad \hat{M}_0]) \begin{bmatrix} -\hat{N}_0^* & M_0 \\ \hat{M}_0^* & N_0 \end{bmatrix} \|_\infty \\ &= \| [Y_0\hat{M}_0^* - X_0\hat{N}_0^* - Q_1 \quad I] \|_\infty, \\ & \quad \| \begin{bmatrix} -\hat{Y} \\ \hat{X} \end{bmatrix} + \begin{bmatrix} M_0 \\ N_0 \end{bmatrix} \bar{Q}_1 \|_\infty \\ &= \| \begin{bmatrix} M_0^* & N_0^* \\ -\hat{N}_0 & \hat{M}_0 \end{bmatrix} \left(\begin{bmatrix} -\hat{Y}_0 \\ \hat{X}_0 \end{bmatrix} + \begin{bmatrix} M_0 \\ N_0 \end{bmatrix} \right) \bar{Q}_1 \|_\infty \\ &= \| \begin{bmatrix} N_0^*\hat{X}_0 - M_0^*\hat{Y}_0 + \bar{Q}_1 \\ I \end{bmatrix} \|_\infty. \end{aligned}$$

Hence, it holds

$$\begin{aligned} J_1 &= (J_0^2 + 1)^{1/2}, J_0 = \inf_{Q_1 \in \mathcal{RH}_\infty} \| Y_0\hat{M}_0^* - X_0\hat{N}_0^* - Q_1 \|_\infty, \\ \bar{J}_1 &= (\bar{J}_0^2 + 1)^{1/2}, \bar{J}_0 = \inf_{\bar{Q}_1 \in \mathcal{RH}_\infty} \| N_0^*\hat{X}_0 - M_0^*\hat{Y}_0 + \bar{Q}_1 \|_\infty. \end{aligned}$$

Next, we repeat the above procedure to examine the general case. It follows from Corollary 1 that

$$\begin{aligned} & ([X \quad Y] - Q_1 [-\hat{N} \quad \hat{M}]) \begin{bmatrix} -\hat{N}_0^* & M_0 \\ \hat{M}_0^* & N_0 \end{bmatrix} \\ &= ([X_0 \quad Y_0] - Q_0 [-\hat{N}_0 \quad \hat{M}_0]) \begin{bmatrix} -\hat{N}_0^* & M_0 \\ \hat{M}_0^* & N_0 \end{bmatrix} \\ &= [Y_0\hat{M}_0^* - X_0\hat{N}_0^* - Q_0 \quad I], Q_0 = Q_1R_0^{-1} + T_0^{-1}\bar{T}_0, \end{aligned} \quad (140)$$

$$\begin{aligned} & \begin{bmatrix} M_0^* & N_0^* \\ -\hat{N}_0 & \hat{M}_0 \end{bmatrix} \left(\begin{bmatrix} -\hat{Y} \\ \hat{X} \end{bmatrix} + \begin{bmatrix} M \\ N \end{bmatrix} \bar{Q}_1 \right) \\ &= \begin{bmatrix} M_0^* & N_0^* \\ -\hat{N}_0 & \hat{M}_0 \end{bmatrix} \left(\begin{bmatrix} -\hat{Y}_0 \\ \hat{X}_0 \end{bmatrix} + \begin{bmatrix} M_0 \\ N_0 \end{bmatrix} \bar{Q}_0 \right) \\ &= \begin{bmatrix} N_0^*\hat{X}_0 - M_0^*\hat{Y}_0 + \bar{Q}_0 \\ I \end{bmatrix}, \bar{Q}_0 = \bar{R}_0R_0^{-1} + T_0^{-1}\bar{Q}_1, \end{aligned} \quad (141)$$

where $R_0^{-1}, \bar{R}_0, T_0, \bar{T}_0$ are defined in Corollary 1. Accordingly, the closed-loop dynamic (135) is equivalent to

$$\begin{bmatrix} u^a \\ y \end{bmatrix} = \begin{bmatrix} M_0 \\ N_0 \end{bmatrix} v_0 + \left(\begin{bmatrix} -\hat{Y}_0 \\ \hat{X}_0 \end{bmatrix} + \begin{bmatrix} M_0 \\ N_0 \end{bmatrix} \bar{Q}_0 \right) r_0 + \begin{bmatrix} M_0 \\ N_0 \end{bmatrix} \left(\begin{bmatrix} X_0 & Y_0 \end{bmatrix} - Q_0 \begin{bmatrix} -\hat{N}_0 & \hat{M}_0 \end{bmatrix} \right) \begin{bmatrix} a_{u^a} \\ -a_y \end{bmatrix}, \quad (142)$$

$$v_0 = \begin{bmatrix} X_0 & Y_0 \end{bmatrix} \begin{bmatrix} u^a \\ y \end{bmatrix}, \quad r_0 = \begin{bmatrix} -\hat{N}_0 & \hat{M}_0 \end{bmatrix} \begin{bmatrix} u^a \\ y \end{bmatrix}.$$

Since the reference signal and the residual signal can be constructed by the designer, the dynamic (142) is identical with (135). The above results are summarized as in the form of a theorem.

Theorem 11. *Given the control system model (32) with the controller u (134), the optimal controller design problems (136) and (139) are equivalent to*

$$J_1 = (J_0^2 + 1)^{1/2}, \quad J_0 = \inf_{Q_0 \in \mathcal{RH}_\infty} \left\| Y_0 \hat{M}_0^* - X_0 \hat{N}_0^* + Q_0 \right\|_\infty, \quad (143)$$

$$\bar{J}_1 = (\bar{J}_0^2 + 1)^{1/2}, \quad \bar{J}_0 = \inf_{\bar{Q}_0 \in \mathcal{RH}_\infty} \left\| N_0^* \hat{X}_0 - M_0^* \hat{Y}_0 + \bar{Q}_0 \right\|_\infty. \quad (144)$$

Proof. The proof follows from (142) and (140)-(141). \square

3) *System performance:* We analyze the system performance under two aspects, control difference and stability. For the simplicity and without loss of application generality, it is supposed that the condition (138), i.e. a stable controller, holds, and the optimal fault-tolerant and attack-resilient controller is applied, namely, Q_0 and \bar{Q}_0 are the solutions of the optimization problems (143) and (144). We begin with systems under additive faults and cyber-attacks. It follows from (142), the fault and attack models (34) and (37) that the control difference is given by

$$\begin{bmatrix} e_u \\ e_y \end{bmatrix} = \begin{bmatrix} u^a \\ y \end{bmatrix} - \begin{bmatrix} M_0 \\ N_0 \end{bmatrix} v_0 =$$

$$\begin{bmatrix} -\hat{Y}_0, \bar{Q}_0 \\ \hat{X}_0, \bar{Q}_0 \end{bmatrix} \left(\hat{N}_{d,0} d + f \right) + \begin{bmatrix} M_0 \\ N_0 \end{bmatrix} \begin{bmatrix} X_{0,Q_0} & Y_{0,Q_0} \end{bmatrix} \begin{bmatrix} \eta_u \\ -\eta_y \end{bmatrix} \quad (145)$$

$$\begin{bmatrix} -\hat{Y}_0, \bar{Q}_0 \\ \hat{X}_0, \bar{Q}_0 \end{bmatrix} = \begin{bmatrix} -\hat{Y}_0 \\ \hat{X}_0 \end{bmatrix} + \begin{bmatrix} M_0 \\ N_0 \end{bmatrix} \bar{Q}_0,$$

$$\begin{bmatrix} X_{0,Q_0} & Y_{0,Q_0} \end{bmatrix} = \begin{bmatrix} X_0 & Y_0 \end{bmatrix} - Q_0 \begin{bmatrix} -\hat{N}_0 & \hat{M}_0 \end{bmatrix},$$

$$\hat{N}_{d,0} = \hat{M}_0 G_d = (A - L_0 C, E_d - F_d L_0, W_0 C, W_0 F_d).$$

Theorem 12. *Given the system model (32) with the normalized LCR (\hat{M}_0, \hat{N}_0) , RCF (M_0, N_0) of the plant, the corresponding LCP, RCP $(X_0, Y_0), (\hat{X}_0, \hat{Y}_0)$, and the controller (134), then the control difference (145) satisfies*

$$\left\| \begin{bmatrix} e_u \\ e_y \end{bmatrix} \right\|_2^2 = \left\| \begin{bmatrix} e_{u,f} \\ e_{y,f} \end{bmatrix} \right\|_2^2 + \left\| \begin{bmatrix} e_{u,a} \\ e_{y,a} \end{bmatrix} \right\|_2^2 \quad (146)$$

$$\leq (J_0^2 + 1) \left\| \begin{bmatrix} \eta_u \\ -\eta_y \end{bmatrix} \right\|_2^2 + (\bar{J}_0^2 + 1) \left\| \hat{N}_{d,0} d + f \right\|_2^2, \quad (147)$$

$$\begin{bmatrix} e_{u,f} \\ e_{y,f} \end{bmatrix} = \begin{bmatrix} -\hat{Y}_{0,\bar{Q}_0} \\ \hat{X}_{0,\bar{Q}_0} \end{bmatrix} \left(\hat{N}_{d,0} d + f \right),$$

$$\begin{bmatrix} e_{u,a} \\ e_{y,a} \end{bmatrix} = \begin{bmatrix} M_0 \\ N_0 \end{bmatrix} \begin{bmatrix} X_{0,Q_0} & Y_{0,Q_0} \end{bmatrix} \begin{bmatrix} \eta_u \\ -\eta_y \end{bmatrix}.$$

Proof. We firstly prove that

$$\begin{bmatrix} -\hat{Y}_0 \\ \hat{X}_0 \end{bmatrix} + \begin{bmatrix} M_0 \\ N_0 \end{bmatrix} \bar{Q}_0^* \text{ and } \begin{bmatrix} M_0 \\ N_0 \end{bmatrix},$$

$$\bar{Q}_0^* = \arg \inf_{Q_0 \in \mathcal{RH}_\infty} \left\| Y_0 \hat{M}_0^* - X_0 \hat{N}_0^* + Q_0 \right\|_\infty$$

build two orthogonal subspaces. As described in Subsection III-A, let

$$\mathcal{P}_{\mathcal{I}_G} := \begin{bmatrix} M_0 \\ N_0 \end{bmatrix} \mathcal{P}_{\mathcal{H}_2} \begin{bmatrix} M_0 \\ N_0 \end{bmatrix}^* : \mathcal{H}_2 \rightarrow \mathcal{H}_2,$$

be the operator of an orthogonal projection onto the system image subspace \mathcal{I}_G . Examining

$$\begin{bmatrix} M_0 \\ N_0 \end{bmatrix} \mathcal{P}_{\mathcal{H}_2} \begin{bmatrix} M_0 \\ N_0 \end{bmatrix}^* \left(\begin{bmatrix} -\hat{Y}_0 \\ \hat{X}_0 \end{bmatrix} + \begin{bmatrix} M_0 \\ N_0 \end{bmatrix} \bar{Q}_0 \right)$$

$$= \begin{bmatrix} M_0 \\ N_0 \end{bmatrix} \left(\mathcal{P}_{\mathcal{H}_2} (N_0^* \hat{X}_0 - M_0^* \hat{Y}_0) + \bar{Q}_0 \right) = 0$$

verifies the claim. Here, the last equation is attributed to the optimal solution of (144),

$$\bar{Q}_0^* = -\mathcal{P}_{\mathcal{H}_2} (N_0^* \hat{X}_0 - M_0^* \hat{Y}_0).$$

As a result of the orthogonality, the Pythagorean equation (112), and (143)-(144), we have (146). The inequality (147) follows from Theorem 11. \square

Theorem 12 gives the minimum \mathcal{L}_2 -norm of the control difference (e_u, e_y) achieved by the optimal controller. It is obvious that the additive faults and attacks do not affect the system stability.

Next, the system performance under the multiplicative faults and attacks is closely examined. At first, the fault-free systems under the attacks are considered. Analogous to the analysis and computations in Theorem 5 and Corollary 1, some routine computations yield

$$\begin{bmatrix} u^a \\ y \end{bmatrix} = \begin{bmatrix} M_0 \\ N_0 \end{bmatrix} v_0 + \begin{bmatrix} -\hat{Y}_{0,\bar{Q}_0} \\ \hat{X}_{0,\bar{Q}_0} \end{bmatrix} r_{y,0}$$

$$+ \begin{bmatrix} M_0 \\ N_0 \end{bmatrix} \begin{bmatrix} X_{0,Q_0} & Y_{0,Q_0} \end{bmatrix} \left(\Phi^a \begin{bmatrix} u^a \\ y \end{bmatrix} + \begin{bmatrix} \bar{\eta}_u \\ -\bar{\eta}_y \end{bmatrix} \right) \Rightarrow$$

$$\begin{bmatrix} u^a \\ y \end{bmatrix} = \begin{bmatrix} M_0 \\ N_0 \end{bmatrix} \Lambda_{Q_0}^a v_0 + \bar{\Lambda}_{Q_0}^a \begin{bmatrix} -\hat{Y}_{0,\bar{Q}_0} \\ \hat{X}_{0,\bar{Q}_0} \end{bmatrix} r_{y,0}$$

$$+ \begin{bmatrix} M_0 \\ N_0 \end{bmatrix} \Psi_{Q_0}^a \begin{bmatrix} \bar{\eta}_u \\ -\bar{\eta}_y \end{bmatrix}, \quad (148)$$

$$\bar{\Lambda}_{Q_0}^a = \left(I - \begin{bmatrix} M_0 \\ N_0 \end{bmatrix} \begin{bmatrix} X_{0,Q_0} & Y_{0,Q_0} \end{bmatrix} \Phi^a \right)^{-1},$$

$$\Lambda_{Q_0}^a = \left(I - \begin{bmatrix} X_{0,Q_0} & Y_{0,Q_0} \end{bmatrix} \Phi^a \begin{bmatrix} M_0 \\ N_0 \end{bmatrix} \right)^{-1},$$

$$\Psi_{Q_0}^a = \Lambda_{Q_0}^a \begin{bmatrix} X_{0,Q_0} & Y_{0,Q_0} \end{bmatrix}.$$

It turns out

$$\begin{bmatrix} e_u \\ e_y \end{bmatrix} = \begin{bmatrix} M_0 \\ N_0 \end{bmatrix} \left(v_{0,\Delta} + r_{y,0,\Delta} + \Psi_{Q_0}^a \begin{bmatrix} \bar{\eta}_u \\ -\bar{\eta}_y \end{bmatrix} \right)$$

$$+ \begin{bmatrix} -\hat{Y}_{0,\bar{Q}_0} \\ \hat{X}_{0,\bar{Q}_0} \end{bmatrix} r_{y,0} \quad (149)$$

$$v_{0,\Delta} = \Psi_{Q_0}^a \Phi^a \begin{bmatrix} M_0 \\ N_0 \end{bmatrix} v_0, r_{y,0,\Delta} = \Psi_{Q_0}^a \Phi^a \begin{bmatrix} -\hat{Y}_{0,\bar{Q}_0} \\ \hat{X}_{0,\bar{Q}_0} \end{bmatrix} r_{y,0}.$$

Theorem 13. Given the system as described in Theorem 12, then the closed-loop dynamic under the multiplicative attacks (34) is stable, if

$$\|\Phi^a\|_\infty = \left\| \Pi^a \left(I + \begin{bmatrix} I & 0 \\ 0 & 0 \end{bmatrix} \Pi^a \right)^{-1} \right\|_\infty < (J_0^2 + 1)^{-1/2}. \quad (150)$$

Moreover,

$$\begin{aligned} \left\| \begin{bmatrix} e_u \\ e_y \end{bmatrix} \right\|_2^2 &\leq (\bar{J}_0^2 + 1) \|r_{y,0}\|_2^2 + \\ &\left(\|\Psi_{Q_0}^a \Phi^a\|_\infty \left((\bar{J}_0^2 + 1)^{1/2} \|r_{y,0}\|_2 + \|v_0\|_2 \right) + \right)^2 \\ &\quad \|\Psi_{Q_0}^a\|_\infty \left\| \begin{bmatrix} \bar{\eta}_u \\ -\bar{\eta}_y \end{bmatrix} \right\|_2 \end{aligned} \quad (151)$$

Proof. According to Small Gain Theorem (SGT), the closed-loop system (148) is stable, if

$$\begin{aligned} \left\| \begin{bmatrix} M_0 \\ N_0 \end{bmatrix} \begin{bmatrix} X_{0,Q_0} & Y_{0,Q_0} \end{bmatrix} \Phi^a \right\|_\infty &= \left\| \begin{bmatrix} X_{0,Q_0} & Y_{0,Q_0} \end{bmatrix} \Phi^a \right\|_\infty \\ &\leq \left\| \begin{bmatrix} X_{0,Q_0} & Y_{0,Q_0} \end{bmatrix} \right\|_\infty \|\Phi^a\|_\infty < 1. \end{aligned}$$

It follows from (143) that

$$\begin{aligned} \left\| \begin{bmatrix} X_{0,Q_0} & Y_{0,Q_0} \end{bmatrix} \right\|_\infty \|\Phi^a\|_\infty &= (J_0^2 + 1)^{1/2} \|\Phi^a\|_\infty \\ \implies \left\| \begin{bmatrix} X_{0,Q_0} & Y_{0,Q_0} \end{bmatrix} \right\|_\infty \|\Phi^a\|_\infty &< 1 \\ \iff \|\Phi^a\|_\infty &< (J_0^2 + 1)^{-1/2}. \end{aligned}$$

Concerning inequality (151), it is a straightforward result of (146) on account of (143)-(144). \square

Now, we analyze the system dynamic simultaneously under the faults and attacks. For our purpose, the dynamic of the residual $r_{y,0}$ with respect to the faults is firstly analyzed. It turns out,

$$r_{y,0} = \begin{bmatrix} -\hat{N}_0 & \hat{M}_0 \end{bmatrix} \begin{bmatrix} u^a \\ y \end{bmatrix} = \Pi^f \begin{bmatrix} u^a \\ y \end{bmatrix} + \bar{f}.$$

It leads to

$$\begin{aligned} \begin{bmatrix} u^a \\ y \end{bmatrix} &= \begin{bmatrix} M_0 \\ N_0 \end{bmatrix} v_0 + \begin{bmatrix} M_0 & -\hat{Y}_{0,\bar{Q}_0} \\ N_0 & \hat{X}_{0,\bar{Q}_0} \end{bmatrix} \begin{bmatrix} \bar{\eta} \\ \bar{f} \end{bmatrix} \\ &\quad + \begin{bmatrix} M_0 & -\hat{Y}_{0,\bar{Q}_0} \\ N_0 & \hat{X}_{0,\bar{Q}_0} \end{bmatrix} \begin{bmatrix} \bar{\Phi}^a \\ \Pi^f \end{bmatrix} \begin{bmatrix} u^a \\ y \end{bmatrix} \implies \\ \begin{bmatrix} u^a \\ y \end{bmatrix} &= \left(I - \begin{bmatrix} M_0 & -\hat{Y}_{0,\bar{Q}_0} \\ N_0 & \hat{X}_{0,\bar{Q}_0} \end{bmatrix} \begin{bmatrix} \bar{\Phi}^a \\ \Pi^f \end{bmatrix} \right)^{-1} \begin{bmatrix} M_0 \\ N_0 \end{bmatrix} v_0 + \\ &\quad \left(I - \begin{bmatrix} M_0 & -\hat{Y}_{0,\bar{Q}_0} \\ N_0 & \hat{X}_{0,\bar{Q}_0} \end{bmatrix} \begin{bmatrix} \bar{\Phi}^a \\ \Pi^f \end{bmatrix} \right)^{-1} \begin{bmatrix} M_0 & -\hat{Y}_{0,\bar{Q}_0} \\ N_0 & \hat{X}_{0,\bar{Q}_0} \end{bmatrix} \begin{bmatrix} \bar{\eta} \\ \bar{f} \end{bmatrix} \end{aligned} \quad (152)$$

$$\Phi^a = \begin{bmatrix} X_{0,Q_0} & Y_{0,Q_0} \end{bmatrix} \Phi^a,$$

$$\bar{\eta} = \begin{bmatrix} X_{0,Q_0} & Y_{0,Q_0} \end{bmatrix} \begin{bmatrix} \bar{\eta}_u \\ -\bar{\eta}_y \end{bmatrix}.$$

Theorem 14. Given the system as described in Theorem 12, then the closed-loop dynamic under the faults (37) and attacks (34) is stable, if

$$b := \left((J_0^2 + 1) \|\Phi^a\|_\infty^2 + (\bar{J}_0^2 + 1) \|\Pi^f\|_\infty^2 \right)^{1/2} < 1. \quad (153)$$

Moreover,

$$\begin{aligned} \left\| \begin{bmatrix} e_u \\ e_y \end{bmatrix} \right\|_2 &\leq \frac{b}{1-b} \|v_0\|_2 + \\ \frac{1}{1-b} \left((J_0^2 + 1) \left\| \begin{bmatrix} \bar{\eta}_u \\ -\bar{\eta}_y \end{bmatrix} \right\|_2^2 + (\bar{J}_0^2 + 1) \|\bar{f}\|_2^2 \right)^{1/2}. \end{aligned} \quad (154)$$

Proof. The proof of (153) follows from (152) using SGT, that is, the closed-loop system (152) is stable, if

$$\begin{aligned} &\left\| \begin{bmatrix} M_0 & -\hat{Y}_{0,\bar{Q}_0} \\ N_0 & \hat{X}_{0,\bar{Q}_0} \end{bmatrix} \begin{bmatrix} \bar{\Phi}^a \\ \Pi^f \end{bmatrix} \right\|_\infty \\ &= \left(\left\| \begin{bmatrix} M_0 \\ N_0 \end{bmatrix} \bar{\Phi}^a \right\|_\infty^2 + \left\| \begin{bmatrix} -\hat{Y}_{0,\bar{Q}_0} \\ \hat{X}_{0,\bar{Q}_0} \end{bmatrix} \Pi^f \right\|_\infty^2 \right)^{1/2} \\ &= \left((J_0^2 + 1) \|\Phi^a\|_\infty^2 + (\bar{J}_0^2 + 1) \|\Pi^f\|_\infty^2 \right)^{1/2} < 1. \end{aligned}$$

Notice that under the condition (153),

$$\begin{aligned} &\left\| \left(I - \begin{bmatrix} M_0 & -\hat{Y}_{0,\bar{Q}_0} \\ N_0 & \hat{X}_{0,\bar{Q}_0} \end{bmatrix} \begin{bmatrix} \bar{\Phi}^a \\ \Pi^f \end{bmatrix} \right)^{-1} - I \right\|_\infty \\ &\leq \frac{\left\| \begin{bmatrix} M_0 & -\hat{Y}_{0,\bar{Q}_0} \\ N_0 & \hat{X}_{0,\bar{Q}_0} \end{bmatrix} \begin{bmatrix} \bar{\Phi}^a \\ \Pi^f \end{bmatrix} \right\|_\infty}{1 - \left\| \begin{bmatrix} M_0 & -\hat{Y}_{0,\bar{Q}_0} \\ N_0 & \hat{X}_{0,\bar{Q}_0} \end{bmatrix} \begin{bmatrix} \bar{\Phi}^a \\ \Pi^f \end{bmatrix} \right\|_\infty} \leq \frac{b}{1-b}, \\ &\left\| \left(I - \begin{bmatrix} M_0 & -\hat{Y}_{0,\bar{Q}_0} \\ N_0 & \hat{X}_{0,\bar{Q}_0} \end{bmatrix} \begin{bmatrix} \bar{\Phi}^a \\ \Pi^f \end{bmatrix} \right)^{-1} \right\|_\infty \leq \frac{1}{1-b}. \end{aligned}$$

It yields

$$\begin{aligned} \left\| \begin{bmatrix} e_u \\ e_y \end{bmatrix} \right\|_2 &\leq \frac{1}{1-b} \left(b \left\| \begin{bmatrix} M_0 \\ N_0 \end{bmatrix} v_0 \right\|_2 + \left\| \begin{bmatrix} M_0 & -\hat{Y}_{0,\bar{Q}_0} \\ N_0 & \hat{X}_{0,\bar{Q}_0} \end{bmatrix} \begin{bmatrix} \bar{\eta} \\ \bar{f} \end{bmatrix} \right\|_2 \right) \\ &\leq \frac{1}{1-b} \left(b \|v_0\|_2 + \sqrt{\left\| \begin{bmatrix} M_0 \\ N_0 \end{bmatrix} \bar{\eta} \right\|_2^2 + \left\| \begin{bmatrix} -\hat{Y}_{0,\bar{Q}_0} \\ \hat{X}_{0,\bar{Q}_0} \end{bmatrix} \bar{f} \right\|_2^2} \right). \end{aligned}$$

Observe that

$$\left\| \begin{bmatrix} M_0 \\ N_0 \end{bmatrix} \bar{\eta} \right\|_2 = \left\| \begin{bmatrix} X_{0,Q_0} & Y_{0,Q_0} \end{bmatrix} \begin{bmatrix} \bar{\eta}_u \\ -\bar{\eta}_y \end{bmatrix} \right\|_2.$$

Hence, following Theorem 11 we finally obtain (154). \square

Theorem 14 provides us with a sufficient condition of the closed-loop stability under the worst case operation condition, the system simultaneously under attacks and faults. Notice that, in the condition (153), J_0 and \bar{J}_0 are the only two values designed by the designer, which reach the minimum, when the optimal feedback gains Q_0 and \bar{Q}_0 are adopted. In this case, a tighter upper-bound of the \mathcal{L}_2 -norm of the control difference (e_u, e_y) is reached as well.

C. A subspace-based privacy-preserving scheme

The last few years have seen a sharp rise in interest in privacy-preserving control, driven by the growing use of networked, cloud-based, and data-driven control architectures. These settings expose internal states, system parameters, and user data to potential leakage, making system-level privacy a core concern. Congruously, new research directions have emerged that integrate differential privacy, encryption, and privacy-aware controller design into classical control theory. This has produced a rapidly expanding body of work aiming to ensure reliable control while protecting sensitive system information [13], [37]–[39]. For instance, recent advances in privacy-performance trade-off characterizations [80] and co-design of controllers with privacy mechanisms [39].

In this subsection, we present a subspace-based privacy-preserving scheme in the unified framework of control and detection. To protect sensitive system information, the system transfer function G and its state space representation (A, B, C, D) , we introduce a privacy filter, which generates an auxiliary signal added to the system output. The modified output defines an augmented image subspace whose deviation from the original subspace quantifies privacy via the gap metric. This approach yields a system-theoretic privacy layer that geometrically characterizes possible information leakage and, importantly, fully preserves the control performance.

1) *Auxiliary signal and privacy filter:* We now consider the system modelled by (1) whose kernel-based closed-loop model is subject to

$$\begin{cases} r_y(z) = \hat{M}(z)y(z) - \hat{N}(z)u(z) = \hat{M}(z)r_{y,0}(z) \\ r_u(z) = X(z)u(z) + Y(z)y(z) = X(z)r_{u,0}(z). \end{cases} \quad (155)$$

For our purpose, an auxiliary signal p generated by the privacy filter implemented on the plant side,

$$p = \Pi \begin{bmatrix} u \\ y \end{bmatrix}, \Pi \in \mathcal{RH}_\infty, \quad (156)$$

is added to the plant output y , yielding the signal y^p ,

$$y^p := y + p = y + \Pi \begin{bmatrix} u \\ y \end{bmatrix}.$$

y^p (instead of y) is transmitted to the control station over the communication network. It follows from Theorem 4 that

$$y^p = G_\Delta u + \bar{r}_y \quad (157)$$

$$G_\Delta = (N + \Delta_N)(M + \Delta_M)^{-1} \quad (158)$$

$$= (\hat{M} + \Delta_{\hat{M}})^{-1} (\hat{N} + \Delta_{\hat{N}}), \quad (159)$$

$$(\Delta_M, \Delta_N) = (-\hat{Y}\Psi, \hat{X}\Psi), [\Delta_{\hat{N}} - \Delta_{\hat{M}}] = \Pi,$$

$$\Psi = \left(I - \Pi \begin{bmatrix} -\hat{Y} \\ \hat{X} \end{bmatrix} \right)^{-1} \Pi \begin{bmatrix} M \\ N \end{bmatrix},$$

$$\bar{r}_y = (\hat{M} + \Delta_{\hat{M}})^{-1} \hat{N}_d d.$$

To ensure the system stability, Π is to be selected so that

$$\left(I - \Pi \begin{bmatrix} -\hat{Y} \\ \hat{X} \end{bmatrix} \right)^{-1} \in \mathcal{RH}_\infty.$$

It is natural that the injected signal p will cause degradation of the system performance, which is now specified. Let's recast the closed-loop dynamic under the injected signal p ,

$$\begin{cases} \hat{M}y = \hat{N}u + r_y \\ Xu + Yy^p = v, \end{cases} \quad (160)$$

into the form

$$\begin{bmatrix} X & Y \\ -\hat{N} & \hat{M} \end{bmatrix} \begin{bmatrix} u \\ y \end{bmatrix} = \begin{bmatrix} v - Y\Pi \begin{bmatrix} u \\ y \end{bmatrix} \\ r_y \end{bmatrix}.$$

It turns out

$$\begin{aligned} \begin{bmatrix} u \\ y \end{bmatrix} &= \begin{bmatrix} M \\ N \end{bmatrix} \left(v - Y\Pi \begin{bmatrix} u \\ y \end{bmatrix} \right) + \begin{bmatrix} -\hat{Y} \\ \hat{X} \end{bmatrix} r_y \Rightarrow \\ \begin{bmatrix} u \\ y \end{bmatrix} &= \begin{bmatrix} M \\ N \end{bmatrix} \Phi v + \left(I + \begin{bmatrix} M \\ N \end{bmatrix} Y\Pi \right)^{-1} \begin{bmatrix} -\hat{Y} \\ \hat{X} \end{bmatrix} r_y, \\ \Phi &= \left(I + Y\Pi \begin{bmatrix} M \\ N \end{bmatrix} \right)^{-1}. \end{aligned}$$

Thus, the control difference,

$$\begin{aligned} \begin{bmatrix} e_u \\ e_y \end{bmatrix} &= \begin{bmatrix} u \\ y \end{bmatrix} - \begin{bmatrix} M \\ N \end{bmatrix} v - \begin{bmatrix} -\hat{Y} \\ \hat{X} \end{bmatrix} r_y \\ &= -\begin{bmatrix} M \\ N \end{bmatrix} \Phi Y\Pi \begin{bmatrix} M \\ N \end{bmatrix} v \\ &\quad - \left(I + \begin{bmatrix} M \\ N \end{bmatrix} Y\Pi \right)^{-1} \begin{bmatrix} M \\ N \end{bmatrix} Y\Pi \begin{bmatrix} -\hat{Y} \\ \hat{X} \end{bmatrix} r_y, \end{aligned}$$

models the control performance degradation.

2) *Performance-preserving controller:* In order to fully recover the system performance, the controller (on the plant side) is extended by adding a feedback of the residual signal r_y^p as

$$\begin{aligned} Xu &= -Yy^p + v + Qr_y^p \quad (161) \\ &= (Q\hat{M} - Y)y^p - Q\hat{N}u + v, Q \in \mathcal{RH}_\infty, \end{aligned}$$

$$r_y^p = \hat{M}y^p - \hat{N}u = r_y + \hat{M}\Pi \begin{bmatrix} u \\ y \end{bmatrix}.$$

It yields

$$\begin{aligned} \begin{bmatrix} u \\ y \end{bmatrix} &= \begin{bmatrix} M \\ N \end{bmatrix} \left(v + (Q\hat{M} - Y)\Pi \begin{bmatrix} u \\ y \end{bmatrix} \right) \\ &\quad + \left(\begin{bmatrix} -\hat{Y} \\ \hat{X} \end{bmatrix} + \begin{bmatrix} M \\ N \end{bmatrix} Q \right) r_y \\ \Rightarrow \begin{bmatrix} u \\ y \end{bmatrix} &= \begin{bmatrix} M \\ N \end{bmatrix} \left(I - (Q\hat{M} - Y)\Pi \begin{bmatrix} M \\ N \end{bmatrix} \right)^{-1} v \\ &\quad + \left(I - \begin{bmatrix} M \\ N \end{bmatrix} (Q\hat{M} - Y)\Pi \right)^{-1} \left(\begin{bmatrix} M \\ N \end{bmatrix} Q + \begin{bmatrix} -\hat{Y} \\ \hat{X} \end{bmatrix} \right) r_y. \end{aligned}$$

Some routine computations lead to

$$\begin{aligned} \begin{bmatrix} u \\ y \end{bmatrix} &= \begin{bmatrix} -\hat{Y} \\ \hat{X} \end{bmatrix} r_y + \begin{bmatrix} M \\ N \end{bmatrix} \Phi^p v \\ &\quad + \begin{bmatrix} M \\ N \end{bmatrix} \Phi^p \left(Q + (Q\hat{M} - Y)\Pi \begin{bmatrix} -\hat{Y} \\ \hat{X} \end{bmatrix} \right) r_y, \quad (162) \\ \Phi^p &= \left(I - (Q\hat{M} - Y)\Pi \begin{bmatrix} M \\ N \end{bmatrix} \right)^{-1}. \end{aligned}$$

Theorem 15. Given the plant model (1) and controller (161), setting

$$\bar{v} = \left(I - (Q\hat{M} - Y) \Pi \begin{bmatrix} M \\ N \end{bmatrix} \right)^{-1} v, \quad (163)$$

$$Q = \left(I + \hat{M} \Pi \begin{bmatrix} -\hat{Y} \\ \hat{X} \end{bmatrix} \right)^{-1} Y \Pi \begin{bmatrix} -\hat{Y} \\ \hat{X} \end{bmatrix}, \quad (164)$$

and Π ensuring

$$\left(I - \Pi \begin{bmatrix} -\hat{Y} \\ \hat{X} \end{bmatrix} \right)^{-1} \in \mathcal{RH}_\infty, \quad (165)$$

$$\left(I + \hat{M} \Pi \begin{bmatrix} -\hat{Y} \\ \hat{X} \end{bmatrix} \right)^{-1} \in \mathcal{RH}_\infty, \quad (166)$$

$$\left(I - (Q\hat{M} - Y) \Pi \begin{bmatrix} M \\ N \end{bmatrix} \right)^{-1} \in \mathcal{RH}_\infty \quad (167)$$

results in

$$\begin{bmatrix} u \\ y \end{bmatrix} = \begin{bmatrix} M \\ N \end{bmatrix} \bar{v} + \begin{bmatrix} -\hat{Y} \\ \hat{X} \end{bmatrix} r_y. \quad (168)$$

Proof. The proof follows from (162) immediately. \square

Theorem 15 showcases that the controller (161) enables fully recovering the system performance, as far as we are able to design the privacy filter Π so that the conditions (165)-(167) are satisfied. Herewith, it is worth remarking that the conditions (165)-(166) are necessary conditions for the system stability and the realization of the residual feedback controller Qr_y^p , while the necessity of the condition (167) depends on the use of the reference signal v . For instance, for $v = 0$, the existence of (167) becomes nonrelevant. Below, the realization of the privacy-preserving system with a performance-preserving controller is summarized.

Realization of the privacy-preserving system

- 1) Implement the privacy system (156) (on the plant side), add the auxiliary signal p to y and send y^p to the control station;
- 2) Set the controller (on the control station side) for given v , either as an observer-based state feedback controller

$$u = F\hat{x} + \bar{v} + Qr_y^p,$$

or equivalently

$$u = Ky^p + \left(X + Q\hat{N} \right)^{-1} \bar{v} + Qr_y^p,$$

$$K = -\left(X + Q\hat{N} \right)^{-1} \left(Y - Q\hat{M} \right),$$

where \bar{v} is set according to (163).

3) System-level privacy and privacy filter design: We now attend to designing Π in the regard of system-level privacy. To this end, a measure of system privacy in terms of the similarity between G and G_Δ or equivalently between the image subspaces \mathcal{I}_G and \mathcal{I}_{G_Δ} ,

$$\mathcal{I}_{G_\Delta} = \left\{ \begin{bmatrix} u \\ y \end{bmatrix} : \begin{bmatrix} u \\ y \end{bmatrix} = \begin{bmatrix} M - \hat{Y}\Psi \\ N + \hat{X}\Psi \end{bmatrix} v_\Delta, v_\Delta \in \mathcal{H}_2 \right\}$$

is introduced. As introduced in Subsection III-A, the gap metric between \mathcal{I}_G and \mathcal{I}_{G_Δ} defined by

$$\delta(\mathcal{I}_G, \mathcal{I}_{G_\Delta}) = \left\| \mathcal{P}_{\mathcal{I}_G} - \mathcal{P}_{\mathcal{I}_{G_\Delta}} \right\|.$$

is a well-established mathematical tool serving for such a purpose.

Definition 8. Given the plant model (1) and controller (2), the system-level privacy induced by signal p given in (156) is defined as the gap metric $\delta(\mathcal{I}_G, \mathcal{I}_{G_\Delta})$.

It follows from (47) and (48) immediately that (i) when $\Pi = 0$, privacy level is zero, (ii) if $\mathcal{I}_G \perp \mathcal{I}_{G_\Delta}$, then the maximal privacy level is achieved, i.e. $\delta(\mathcal{I}_G, \mathcal{I}_{G_\Delta}) = 1$. Notice that $\mathcal{I}_G \perp \mathcal{I}_{G_\Delta}$ implies $\forall \begin{bmatrix} u \\ y \end{bmatrix} \in \mathcal{I}_G, \begin{bmatrix} u \\ y^p \end{bmatrix} \in \mathcal{I}_{G_\Delta}$,

$$\left\langle \begin{bmatrix} u \\ y \end{bmatrix}, \begin{bmatrix} u \\ y^p \end{bmatrix} \right\rangle = \sum_{k=0}^{\infty} (u^T(k)u(k) + y^T(k)y^p(k)) = 0. \quad (169)$$

Consequently, it is impossible to identify the model $G = NM^{-1}$, or equivalently (A, B, C, D) , by means of the data (u, y^p) belonging to \mathcal{I}_{G_Δ} . Generally speaking, the gap metric between system subspaces is a system-theoretic privacy metric, quantifying how much additional information that the augmented signal y^p reveals about the system dynamic.

Remark 10. Generally speaking, system identification algorithms are computations using process data collected over a finite time interval. On the other hand, the inner product (169) is defined over $[0, \infty)$. In order to preserve the privacy level, an inner product over finite time interval $[k_0, k_1]$,

$$\left\langle \begin{bmatrix} u \\ y \end{bmatrix}, \begin{bmatrix} u \\ y^p \end{bmatrix} \right\rangle = \sum_{k=k_0}^{k_1} (u^T(k)u(k) + y^T(k)y^p(k)),$$

is to be defined. As a result, time-varying (normalized) coprime factorizations that lead to time-varying post- and pre-filters are applied. This issue will not be addressed in this work. The reader is referred to [52], [61] for the corresponding concepts and computation algorithms.

Next, we study the computation of the gap metric induced privacy-level and design of the privacy filter (156). It is known in the literature that

$$\vec{\delta}(\mathcal{I}_G, \mathcal{I}_{G_\Delta}) = \inf_{Q \in \mathcal{RH}_\infty} \|I_{G_0} - I_{G_{0,\Delta}} Q\|_\infty, \quad (170)$$

$$I_{G_0} = \begin{bmatrix} M_0 \\ N_0 \end{bmatrix}, I_{G_{0,\Delta}} = \begin{bmatrix} M_0 - \hat{Y}_0 \Psi_0 \\ N_0 + \hat{X}_0 \Psi_0 \end{bmatrix} \Theta_0, \quad (171)$$

where (M_0, N_0) is the normalized RCP of G , (\hat{X}_0, \hat{Y}_0) the corresponding RCP of the controller, and

$$\Psi_0 = \left(I - \Pi \begin{bmatrix} -\hat{Y}_0 \\ \hat{X}_0 \end{bmatrix} \right)^{-1} \Pi \begin{bmatrix} M_0 \\ N_0 \end{bmatrix}$$

with the pre-filter $\Theta_0 \in \mathcal{RH}_\infty$ normalizing $I_{G_{0,\Delta}}$, i.e. $I_{G_{0,\Delta}}^* I_{G_{0,\Delta}} = I$.

The optimization (170) is an MMP whose solution requires considerable computational effort. Remembering our final goal of designing the privacy filter (156), solving the MMP (170)

remarkably complicates the design procedure. For our purpose, the subsequent known results are presented, which provides us with a tight lower bound of the gap metric $\delta(\mathcal{I}_G, \mathcal{I}_{G_\Delta})$. On account of the fact that the privacy level $\delta(\mathcal{I}_G, \mathcal{I}_{G_\Delta})$ should be larger than zero and $\delta(\mathcal{I}_G, \mathcal{I}_{G_\Delta})$ is smaller than one due to the relation between \mathcal{I}_G and \mathcal{I}_{G_Δ} , below only the case $0 < \delta(\mathcal{I}_G, \mathcal{I}_{G_\Delta}) < 1$ is addressed.

Lemma 2. [48] *Given the normalized SIRs and SKRs,*

$$I_{G_i} = \begin{bmatrix} M_i \\ N_i \end{bmatrix}, K_{G_i} = \begin{bmatrix} -\hat{N}_i & \hat{M}_i \end{bmatrix}, i = 1, 2,$$

and assume that $0 < \delta(\mathcal{I}_{G_i}, \mathcal{I}_{G_j}) < 1, i \neq j$, then it holds

$$\delta(\mathcal{I}_{G_i}, \mathcal{I}_{G_j}) \geq \|K_{G_i} I_{G_j}\|_\infty = \inf_{Q \in \mathcal{RL}_\infty} \|I_{G_i} - I_{G_j} Q\|_\infty. \quad (172)$$

It is known [48] that $\inf_{Q \in \mathcal{RL}_\infty} \|I_{G_i} - I_{G_j} Q\|_\infty$ is the gap metric measuring the similarity between two ℓ_2 image subspaces

$$\mathcal{I}_{G_i}^{\mathcal{L}_2} = \left\{ \begin{bmatrix} u \\ y \end{bmatrix} : \begin{bmatrix} u \\ y \end{bmatrix} = \begin{bmatrix} M_i \\ N_i \end{bmatrix} v, v \in \ell_2 \right\},$$

$i = 1, 2$. We denote it by $\delta^{\mathcal{L}_2}(\mathcal{I}_{G_i}, \mathcal{I}_{G_j})$. The equation in (172) means that

$$\delta^{\mathcal{L}_2}(\mathcal{I}_{G_i}, \mathcal{I}_{G_j}) = \|K_{G_i} I_{G_j}\|_\infty.$$

In this context, the concept of system-level \mathcal{L}_2 -privacy is introduced.

Definition 9. *Given the plant model (1) and controller (161), the gap metric,*

$$\delta^{\mathcal{L}_2}(\mathcal{I}_G, \mathcal{I}_{G_\Delta}) = \inf_{Q \in \mathcal{RL}_\infty} \|I_{G_0} - I_{G_{0,\Delta}} Q\|_\infty,$$

is called \mathcal{L}_2 -privacy induced by signal p given in (156).

Theorem 16. *Given the plant model (1) and controller (161), the \mathcal{L}_2 -privacy preserved by means of the privacy filter (156) is given by*

$$\delta^{\mathcal{L}_2}(\mathcal{I}_G, \mathcal{I}_{G_\Delta}) = \left\| \Pi_0 \begin{bmatrix} M_0 \\ N_0 \end{bmatrix} \right\|_\infty, \quad (173)$$

$$\Pi_0 = R_N \left(\begin{bmatrix} -\hat{N}_0 & \hat{M}_0 \end{bmatrix} - \Pi \right), \quad (174)$$

$$R_N^* R_N = \left(\left(\begin{bmatrix} -\hat{N}_0 & \hat{M}_0 \end{bmatrix} - \Pi \right) \left(\begin{bmatrix} -\hat{N}_0 & \hat{M}_0 \end{bmatrix} - \Pi \right)^* \right)^{-1}.$$

Proof. Denote the normalized SKR of G_Δ by $K_{G_{0,\Delta}}$. According to Lemma 2,

$$\delta^{\mathcal{L}_2}(\mathcal{I}_G, \mathcal{I}_{G_\Delta}) = \|K_{G_{0,\Delta}} I_{G_0}\|_\infty.$$

We now determine $K_{G_{0,\Delta}}$. Observe that

$$\begin{bmatrix} M_0 - \hat{Y}_0 \Psi_0 \\ N_0 + \hat{X}_0 \Psi_0 \end{bmatrix} = \left(I - \begin{bmatrix} -\hat{Y}_0 \\ \hat{X}_0 \end{bmatrix} \Pi \right)^{-1} \begin{bmatrix} M_0 \\ N_0 \end{bmatrix}.$$

It is apparent that

$$\begin{aligned} K_{G_\Delta} &:= R_N \left[\begin{bmatrix} -\hat{N}_0 & \hat{M}_0 \end{bmatrix} \left(I - \begin{bmatrix} -\hat{Y}_0 \\ \hat{X}_0 \end{bmatrix} \Pi \right) \right] \\ &= R_N \left(\begin{bmatrix} -\hat{N}_0 & \hat{M}_0 \end{bmatrix} - \Pi \right) \end{aligned}$$

is an SKR of G_Δ , where $R_N \in \mathcal{RH}_\infty$ is a post-filter to be selected. Now, let R_N satisfy

$$\begin{aligned} R_N^* R_N &= \left(\left(\begin{bmatrix} -\hat{N}_0 & \hat{M}_0 \end{bmatrix} - \Pi \right) \left(\begin{bmatrix} -\hat{N}_0 & \hat{M}_0 \end{bmatrix} - \Pi \right)^* \right)^{-1}, \\ \Pi_0 &= R_N \left(\begin{bmatrix} -\hat{N}_0 & \hat{M}_0 \end{bmatrix} - \Pi \right) =: K_{G_{0,\Delta}} \end{aligned}$$

so that Π_0 is the normalized SKR of G_Δ , i.e. $\Pi_0 \Pi_0^* = I$. As a result,

$$\|K_{G_{0,\Delta}} I_{G_0}\|_\infty = \|\Pi_0 I_{G_0}\|_\infty.$$

□

Remark 11. *As an SKR of G_Δ , $\left[\begin{bmatrix} -\hat{N}_0 & \hat{M}_0 \end{bmatrix} - \Pi \right]$ is stable and right invertible. By a spectral factorization [44]*

$$\left(\begin{bmatrix} -\hat{N}_0 & \hat{M}_0 \end{bmatrix} - \Pi \right) \left(\begin{bmatrix} -\hat{N}_0 & \hat{M}_0 \end{bmatrix} - \Pi \right)^* = \Theta_0 \Theta_0^*,$$

where Θ_0 is invertible over \mathcal{RH}_∞ , we have $R_N = \Theta_0^{-1}$.

Theorem 16 considerably simplifies the design of the privacy filter (156) and enables us to perform the selection of Π_0 . To this end, let us firstly parametrize Π_0 as

$$\Pi_0 = \begin{bmatrix} \Pi_{0,1} & \Pi_{0,2} \end{bmatrix} \begin{bmatrix} X_0 & Y_0 \\ -\hat{N}_0 & \hat{M}_0 \end{bmatrix}.$$

It turns out

$$\Pi_0 I_{G_0} = \Pi_{0,1}, \Pi_0 \begin{bmatrix} -\hat{Y}_0 \\ \hat{X}_0 \end{bmatrix} = \Pi_{0,2}.$$

Recall the conditions (165)-(167) in Theorem 15 for the system stability, and settings of Q, \bar{v} . Attributed to Corollary 1, they are further written as

$$\begin{aligned} \left(I - \Pi \left(\begin{bmatrix} -\hat{Y}_0 \\ \hat{X}_0 \end{bmatrix} R_0 + \begin{bmatrix} M_0 \\ N_0 \end{bmatrix} \bar{R}_0 \right) \right)^{-1} &\in \mathcal{RH}_\infty, \\ \left(I + \hat{M} \Pi \left(\begin{bmatrix} -\hat{Y}_0 \\ \hat{X}_0 \end{bmatrix} R_0 + \begin{bmatrix} M_0 \\ N_0 \end{bmatrix} \bar{R}_0 \right) \right)^{-1} &\in \mathcal{RH}_\infty, \\ \left(I - (Q \hat{M} - Y) \Pi \begin{bmatrix} M_0 \\ N_0 \end{bmatrix} T_0^{-1} \right)^{-1} &\in \mathcal{RH}_\infty \end{aligned}$$

with \bar{R}_0, R_0 and T_0 defined in Corollary 1. Substituting

$$\Pi = (I - \bar{\Pi}_{0,2}) \left[\begin{bmatrix} -\hat{N}_0 & \hat{M}_0 \end{bmatrix} - \bar{\Pi}_{0,1} \begin{bmatrix} X_0 & Y_0 \end{bmatrix} \right], \quad (175)$$

$$[\bar{\Pi}_{0,1} \quad \bar{\Pi}_{0,2}] = R_N^{-1} [\Pi_{0,1} \quad \Pi_{0,2}],$$

$$\hat{\Pi}_{0,2} = (I - \bar{\Pi}_{0,2}) R_0 \quad (176)$$

into them allow us to express the conditions (165)-(167) respectively by

$$\left(I - \hat{\Pi}_{0,2} - \bar{\Pi}_{0,1} \bar{R}_0 \right)^{-1} \in \mathcal{RH}_\infty, \quad (177)$$

$$\left(I + \hat{M} \left(\hat{\Pi}_{0,2} - \bar{\Pi}_{0,1} \bar{R}_0 \right) \right)^{-1} \in \mathcal{RH}_\infty, \quad (178)$$

$$\left(I + (Q \hat{M} - Y) \bar{\Pi}_{0,1} T_0^{-1} \right)^{-1} \in \mathcal{RH}_\infty. \quad (179)$$

Consequently, the design of the privacy filter (156) is equivalently formulated as

$$\sup_{\Pi_{0,1}} \delta^{\mathcal{L}_2}(\mathcal{I}_G, \mathcal{I}_{G_\Delta}) = \sup_{\Pi_{0,1}} \|\Pi_{0,1}\|_\infty \quad (180)$$

$$\text{s.t. (177)-(179).} \quad (181)$$

It is of interest to notice that $\delta^{\mathcal{L}_2}(\mathcal{I}_G, \mathcal{I}_{G_\Delta})$ reaches its maximum for $\Pi_{0,2} = 0$. In that case, $\Pi_{0,1}$ normalizes $[X_0 \ Y_0]$, i.e.

$$\Pi_{0,1} [X_0 \ Y_0] \begin{bmatrix} X_0^* \\ Y_0^* \end{bmatrix} \Pi_{0,1}^* = I.$$

On the other hand, setting $\Pi_{0,2} = 0$ leads to, for instance,

$$I - (I - \bar{\Pi}_{0,2}) R_0 - \bar{\Pi}_{0,1} \bar{R}_0 = I - R_0 - \bar{\Pi}_{0,1} \bar{R}_0,$$

which implies, the condition (177) is probably not satisfied. Nevertheless, this observation inspires the subsequent algorithm for a practical sub-optimal solution of the design problem (180)-(181).

Privacy filter design: a sub-optimal solution

- 1) Select a sufficiently small $0 < \varepsilon \ll 1$ and set

$$\bar{\Pi}_{0,2} = \varepsilon I \implies \Pi_{0,2} = \varepsilon R_N \quad (182)$$

so that the conditions (177)-(179) are satisfied;

- 2) Compute $\hat{\Pi}_{0,1}$ that normalizes $[X_0 \ Y_0]$ by a spectral factorization,

$$[X_0 \ Y_0] [X_0 \ Y_0]^* = \hat{\Pi}_{0,1}^{-1} (\hat{\Pi}_{0,1}^{-1})^*$$

and set

$$\Pi_{0,1} = \sqrt{(1 - \varepsilon^2)} \hat{\Pi}_{0,1}; \quad (183)$$

- 3) Set Π according to (175).

We now examine the condition $\Pi_0 \Pi_0^* = I$ and (180). It holds

$$\begin{aligned} \Pi_0 \Pi_0^* &= \varepsilon^2 R_N \begin{bmatrix} -\hat{N}_0 & \hat{M}_0 \end{bmatrix} \begin{bmatrix} -\hat{N}_0^* \\ \hat{M}_0^* \end{bmatrix} R_N^* \\ &\quad + (1 - \varepsilon^2) \hat{\Pi}_{0,1} [X_0 \ Y_0] \begin{bmatrix} X_0^* \\ Y_0^* \end{bmatrix} \hat{\Pi}_{0,1}^* \\ &\quad + \varepsilon \sqrt{(1 - \varepsilon^2)} (\Xi + \Xi^*) = I + \varepsilon \sqrt{(1 - \varepsilon^2)} (\Xi + \Xi^*), \\ \Xi &= \hat{\Pi}_{0,1} [X_0 \ Y_0] \begin{bmatrix} -\hat{N}_0^* \\ \hat{M}_0^* \end{bmatrix} R_N^*. \end{aligned}$$

Considering that

$$\left\| \begin{bmatrix} \hat{\Pi}_{0,1} X_0 & \hat{\Pi}_{0,1} Y_0 \\ -\hat{N}_0 & \hat{M}_0 \end{bmatrix} \right\|_\infty \leq \sqrt{2},$$

for sufficiently small ε , $\Pi_0 \Pi_0^*$ can be well approximated by $\Pi_0 \Pi_0^* \approx I$. As a result, we have a sub-optimal solution

$$\delta^{\mathcal{L}_2}(\mathcal{I}_G, \mathcal{I}_{G_\Delta}) = \sqrt{(1 - \varepsilon^2)} \left\| \hat{\Pi}_{0,1} \right\|_\infty.$$

Concerning the conditions (177)-(179), whether they hold depends on $(\hat{M}_0, R_0, \bar{R}_0, T_0)$, or equivalently the parameters (F, L, V, W) of the applied controller. To illustrate this claim, we present the following example.

Example 2. Suppose that (F, L, V, W) are set equal to

$$(F, L, T, W) = (F_0, L_0, V_0, W_0)$$

$$\implies (M, N) = (M_0, N_0), (\hat{M}, \hat{N}) = (\hat{M}_0, \hat{N}_0).$$

Here, we would like to mention the interpretation of the normalized SIR and SKR as an LQ controller and an LS estimator, respectively [43]. It follows from Corollary 1, Lemma 1 and (182) that

$$\begin{aligned} \bar{R}_0 &= 0, R_0 = I, T_0 = I, \hat{M} = \hat{M}_0, \hat{\Pi}_{0,2} = (1 + \varepsilon) I \implies \\ (I - (I - \bar{\Pi}_{0,2}) R_0 - \bar{\Pi}_{0,1} \bar{R}_0)^{-1} &= \varepsilon^{-1} I \in \mathcal{RH}_\infty, \\ I + \hat{M} (I - \bar{\Pi}_{0,2}) R_0 - \bar{\Pi}_{0,1} \bar{R}_0^{-1} &= I + \hat{M}_0 (1 - \varepsilon). \end{aligned}$$

Since $\left\| \hat{M}_0 \right\|_\infty \leq 1 \implies \left\| \hat{M}_0 (1 - \varepsilon) \right\|_\infty < 1$, it holds $(I + \hat{M}_0 (1 - \varepsilon))^{-1} \in \mathcal{RH}_\infty$. As a result, the conditions (177)-(178) are guaranteed, which assures the system stability and the existence of the controller Qr_y^p . Concerning the condition (179), it is equivalent to

$$\begin{aligned} &\left(I - (Q\hat{M} - Y) \Pi \begin{bmatrix} M_0 \\ N_0 \end{bmatrix} T_0^{-1} \right)^{-1} \\ &= \left(I + (Q\hat{M}_0 - Y_0) R_N^{-1} \Pi_{0,1} \right)^{-1} \in \mathcal{RH}_\infty. \end{aligned} \quad (184)$$

Thus, when (184) is true, v is arbitrarily selectable. Otherwise, v is to be selected properly so that \bar{v} can be realized according to (163).

VI. CONCLUSIONS

In this work, we have leveraged the unified framework of control and detection to explore analysis, simultaneous detection, fault-tolerant and resilient control of cyber-physical control systems under attacks and faults. In a three-step procedure, we have firstly built the control-theoretic foundation for the subsequent work. Specifically, we have introduced, among others, the image, kernel and residual subspaces in the system input-output data space (u, y) , gap metric as the distance between two subspaces, and the Bezout identity-based transformations between (u, y) and (r_u, r_y) as well as the image and residual subspaces, where Theorem 1 and Corollary 1 function as a basic mathematical tool. A further result is the PnP structure that builds an essential system configuration adopted in the proposed fault-tolerant and attack-resilient control schemes. We have then reviewed the MTD, watermark methods, the auxiliary system-based detection method, and characterized zero dynamics attacks in the unified framework. On this basis, the alternative and enhanced forms of these methods have been proposed.

The major part of our endeavours has been devoted to establishing a control-theoretic paradigm, in which analysis, simultaneous detection of faults and attacks, fault-tolerant and attack resilient control of CPCSs are unified addressed. Concerning system analysis, three essential information and structural properties have been revealed. They are the existence of (i) an attack information potential between the plant and control station and (ii) the duality between the faulty dynamic and attack dynamic, and (iii) the interpretation of cyber-attacks as uncertainty in the controller. Aiming at a general and detection method-independent definition of stealthy attacks, the concept of attack detectability has been introduced, which is complemented by the concept of actuability of attacks. The latter is overlooked in the literature, but important for

addressing attack design issues. The proof of the existence conditions of undetectable and actuatable/unactuable attacks have been provided as well. An immediate application of the aforementioned results is the introduction of image attacks as a general form of undetectable (stealthy) attacks that provides a detection method-independent platform for (stealthy) attacks design. The last of part of the system analysis has been dedicated to system vulnerability. To this end, the concept of attack stability margin as a measure of the system vulnerability has been introduced, and a design procedure of image attacks and the proof of a sufficient condition of the system vulnerability under image attacks have been provided.

As the last part of our work, simultaneous detection of faults and attacks as well as fault-tolerant and attack-resilient control have been explored. Specifically, three simultaneous detection schemes have been presented. In the PnP structure, a fault-tolerant and attack-resilient control system has been designed, whose control performance and stability conditions have been analyzed. Concerning system privacy-preserving, we have proposed a subspace-based privacy-preserving scheme whose core is a privacy filter generating an auxiliary signal. For our purpose, the concepts of system-level privacy and \mathcal{L}_2 -privacy based on the similarity of two system subspaces and measured by gap metric have been introduced. In this regard, the \mathcal{L}_2 -privacy-filter design problem has been formulated and solved in the form of an optimization problem.

At the end of this paper, we would like to highlight three key properties that have been for the first time revealed and utilized in this work,

- the attack information potential between the control station and plant,
- the duality between the faulty dynamic and attack dynamic, and
- the two-site control and detection architecture for configuring CPCSSs.

Most of the significant results presented in this paper, including simultaneous detection of faults and attack, fault-tolerant and attack-resilient control, and subspace-based privacy-preserving, vulnerability analysis-aided image attack design schemes, have been achieved based on these three properties. Note that the last two design schemes are indeed the consequence of the duality between the faulty and attack dynamics, although they have not been explicitly introduced in this regard. We are convinced that these three system properties are of enormous potentials to facilitate the development of advanced methods towards secure and safe CPCSSs.

REFERENCES

- [1] S. X. Ding, *Advanced Methods for Fault Diagnosis and Fault-tolerant Control*. Berlin: Springer-Verlag, 2020.
- [2] L. H. Chiang, E. L. Russell, and R. D. Braatz, *Fault Detection and Diagnosis in Industrial Systems*. London: Springer, 2001.
- [3] R. J. Patton, P. M. Frank, and R. N. C. (Eds.), *Issues of Fault Diagnosis for Dynamic Systems*. London: Springer, 2000.
- [4] M. Blanke, M. Kinnaert, J. Lunze, and M. Staroswiecki, *Diagnosis and Fault-Tolerant Control, 2nd Edition*. Berlin Heidelberg: Springer, 2006.
- [5] S. X. Ding, *Model-Based Fault Diagnosis Techniques - Design Schemes, Algorithms, and Tools*. Springer-Verlag, 2008.
- [6] H. Alwi, C. Edwards, and C. P. Tan, *Fault Detection and Fault-Tolerant Control Using Sliding Modes*. Springer-Verlag, 2011.
- [7] A. Teixeira, I. Shames, H. Sandberg, and K. H. Johansson, "A secure control framework for resource-limited adversaries," *Automatica*, vol. 51, pp. 135 – 148, 2015.
- [8] S. M. Dibaji, M. Pirani, D. B. Flamholz, A. M. Annaswamy, K. H. Johansson, and A. Chakrabortty, "A systems and control perspective of CPS security," *Annual Reviews in Control*, vol. 47, p. 394–411, 2019.
- [9] D. Ding, Q.-L. Han, X. Ge, and J. Wang, "Secure state estimation and control of cyber-physical systems: A survey," *IEEE Trans. Syst., Man, and Cybern.: Syst.*, vol. 51, no. 1, pp. 176–190, 2021.
- [10] S. Tan, J. M. Guerrero, P. Xie, R. Han, and J. C. Vasquez, "Brief survey on attack detection methods for cyber-physical systems," *IEEE Systems Journal*, vol. 14, pp. 5329–5339, 2020.
- [11] C. Zhou, B. Hu, Y. Shi, Y.-C. Tian, X. Li, and Y. Zhao, "A unified architectural approach for cyberattack-resilient industrial control systems," *Proceedings of the IEEE*, vol. 109, pp. 517–541, 2021.
- [12] D. Zhang, Q.-G. Wang, G. Feng, Y. Shi, and A. V. Vasilakos, "A survey on attack detection, estimation and control of industrial cyber-physical systems," *ISA Transactions*, vol. 116, pp. 1–16, 2021.
- [13] M. Segovia-Ferreira, J. Rubio-Hernan, A. Cavalli, and J. Garcia-Alfaro, "A survey on cyber-resilience approaches for cyber-physical systems," *ACM Comput. Surv.*, vol. 56, no. 8, p. 37, 2024.
- [14] J. Qin, M. Li, L. Shi, and X. Yu, "Optimal denial-of-service attack scheduling with energy constraint over packet-dropping networks," *IEEE Trans. Autom. Control*, vol. 63, no. 6, pp. 1648–1663, 2018.
- [15] X. Ren, J. Wu, S. Dey, and L. Shi, "Attack allocation on remote state estimation in multi-systems: Structure results and asymptotic solution," *Automatica*, vol. 87, pp. 184–194, 2018.
- [16] J. Giraldo, D. Urbina, A. Cardenas, J. Valente, M. Faisal, J. Ruths, N. O. Tippenhauer, H. Sandberg, and R. Candell, "A survey of physics-based attack detection in cyber-physical systems," *ACM Comput. Surv.*, vol. 51, 2018.
- [17] Y. Mo and B. Sinopoli, "False data injection attacks in control systems," in *Proc. First Workshop on Secure Control Systems (SCS), CPS Week*, 2010, pp. 1–6.
- [18] F. Pasqualetti, F. Doerfler, and F. Bullo, "Attack detection and identification in cyber-physical systems," *IEEE Trans. Autom. Control*, vol. 58, no. 11, pp. 2715–2729, 2013.
- [19] Y. Mo and B. Sinopoli, "On the performance degradation of cyber-physical systems under stealthy integrity attacks," *IEEE Trans. Autom. Control*, vol. 61, pp. 2618–2624, 2016.
- [20] Y. Chen, S. Kar, and J. M. F. Moura, "Cyber-physical attacks with control objectives," *IEEE Trans. Autom. Control*, vol. 63, no. 5, pp. 1418–1425, 2018.
- [21] Q. Zhang, K. Liu, Y. Xia, and A. Ma, "Optimal stealthy deception attack against cyber-physical systems," *IEEE Trans. Cybern.*, vol. 50, no. 9, pp. 3963–3972, 2020.
- [22] X.-X. Ren and G. H. Yang, "Kullback-leibler divergence-based optimal stealthy sensor attack against networked linear quadratic gaussian systems," *IEEE Trans. Cybern.*, vol. 52, no. 11, pp. 11539–11548, 2022.
- [23] J. Shang, D. Cheng, J. Zhou, and T. Chen, "Asymmetric vulnerability of measurement and control channels in closed-loop systems," *IEEE Trans. Contr. Netw. Syst.*, vol. 9, no. 4, pp. 1804–1815, 2022.
- [24] Y. Mo, S. Weerakkody, and B. Sinopoli, "Physical authentication of control systems: Designing watermarked control inputs to detect counterfeit sensor outputs," *IEEE Control Systems Magazine*, vol. 35, pp. 93–109, 2015.
- [25] W. Heemels, K. Johansson, and P. Tabuada, "An introduction to event-triggered and self-triggered control," in *2012 IEEE 51st IEEE Conference on Decision and Control (CDC)*, 2012, pp. 3270–3285.
- [26] H. Sandberg, S. Amin, and K. H. Johansson, "Cyberphysical security in networked control systems: An introduction to the issue," *IEEE Control Systems Magazine*, vol. 35, no. 1, pp. 20–23, 2015.
- [27] S. Shen, C. Zhang, R. Chai, L. Dai, S. Chai, and Y. Xia, "Stabilizing nonlinear model predictive control under Denial-of-Service attack via dynamic samples selection," *Automatica*, vol. 164, p. 111591, 2024.
- [28] L. An and G. Yang, "Improved adaptive resilient control against sensor and actuator attacks," *Information Sciences*, vol. 423, pp. 145–156, 2018.
- [29] Z. Ye, D. Zhang, C. Deng, H. Yan, and G. Feng, "Finite-time resilient sliding mode control of nonlinear UMV systems subject to DoS attacks," *Automatica*, vol. 156, p. 111170, 2023.
- [30] C. Fang, Y. Qi, J. Chen, R. Tan, and W. Zheng, "Stealthy actuator signal attacks in stochastic control systems: Performance and limitations," *IEEE Trans. Autom. Control*, vol. 65, no. 9, pp. 3927–3934, 2020.
- [31] Y. Chen, S. Kar, and J. M. F. Moura, "Cyber-physical attacks with control objectives," *IEEE Transactions on Automatic Control*, vol. 63, no. 5, pp. 1418–1425, 2018.

[32] L. An and G. H. Yang, "Data-driven coordinated attack policy design based on adaptive L_2 -gain optimal theory," *IEEE Trans. Autom. Control*, vol. 63, no. 6, pp. 1850–1857, 2018.

[33] L. Guo, H. Yu, and F. Hao, "Optimal allocation of false data injection attacks for networked control systems with two communication channels," *IEEE Trans. Control Netw. Syst.*, vol. 8, no. 1, pp. 2–14, 2021.

[34] T. Sui, Y. Mo, D. Marelli, X. Sun, and M. Fu, "The vulnerability of cyber-physical system under stealthy attacks," *IEEE Transactions on Automatic Control*, vol. 66, no. 2, pp. 637–650, 2021.

[35] J. Zhou, J. Shang, and T. Chen, "Optimal deception attacks on remote state estimators equipped with interval anomaly detectors," *Automatica*, vol. 148, p. 110723, 2023.

[36] Q. Zhang, K. Liu, A. M. H. Teixeira, Y. Li, S. Chai, and Y. Xia, "An online kullback–leibler divergence-based stealthy attack against cyber-physical systems," *IEEE Trans. Autom. Control*, vol. 68, no. 6, pp. 3672–3679, 2023.

[37] S. Han and G. J. Pappas, "Privacy in control and dynamical systems," *Annual Review of Control, Robotics, and Autonomous Systems*, vol. 1, pp. 309–332, 2018.

[38] Y. Lu and M. Zhu, "A control-theoretic perspective on cyber-physical privacy: Where data privacy meets dynamic systems," *Annual Reviews in Control*, vol. 47, pp. 423–440, 2019.

[39] Y. Kawano and M. Cao, "Design of privacy-preserving dynamic controllers," *IEEE Transactions on Automatic Control*, vol. 65, no. 9, pp. 3863–3878, 2020.

[40] S. X. Ding, L. Li, D. Zhao, C. Louen, and T. Liu, "Application of the unified control and detection framework to detecting stealthy integrity cyber-attacks on feedback control systems," *Automatica*, vol. 142, p. 110352, 2022.

[41] L. Li, S. X. Ding, L. Zhou, M. Zhong, and K. Peng, "The system dynamics analysis, resilient and fault-tolerant control for cyber-physical systems," *arXiv:2409.13370*, 2024.

[42] S. X. Ding, *Unified framework of control and detection: fault diagnosis, tolerant control and secure CPSSs*. (in press), Springer-Verlag, 2026.

[43] T.-T. Tay, I. Mareels, and J. B. Moore, *High Performance Control*. Springer Science + Business Media, 1998.

[44] K. Zhou, J. Doyle, and K. Glover, *Robust and Optimal Control*. Upper Saddle River, New Jersey: Prentice-Hall, 1996.

[45] J. W. Hoffmann, "Normalized coprime factorizations in continuous and discrete time - a joint state-space approach," *IMA Journal of Mathematical Control and Information*, vol. 13, no. 4, pp. 359–384, 1996.

[46] Z. Guo, D. Shi, K. H. Johansson, and L. Shi, "Optimal linear cyber-attack on remote state estimation," *IEEE Transactions on Control of Network Systems*, vol. 4, no. 1, pp. 4–13, 2017.

[47] X. Liu and G.-H. Yang, "Optimal encryption strategy for cyber-physical systems against stealthy attacks with energy constraints: A stackelberg game approach," *Information Sciences*, vol. 610, pp. 674–693, 2022.

[48] G. Vinnicombe, *Uncertainty and Feedback: H_∞ Loop-Shaping and the ν Gap Metric*. World Scientific, 2000.

[49] L. Li and S. X. Ding, "Gap metric techniques and their application to fault detection performance analysis and fault isolation schemes," *Automatica*, vol. 118, p. 109029, 2020.

[50] S. X. Ding, L. Li, and T. Liu, "An alternative paradigm of fault diagnosis in dynamic systems: orthogonal projection-based methods," *Automatica*, vol. 183, p. 112637, 2026.

[51] T. T. Georgiou, "On the computation of the gap metric," *Syst. Contr. Letters*, vol. 11, pp. 253–257, 1988.

[52] A. Feintuch, *Robust Control Theory in Hilbert Space*. New York: Springer-Verlag, 1998.

[53] A. Kanellopoulos and K. G. Vamvoudakis, "A moving target defense control framework for cyber-physical systems," *IEEE Transactions on Automatic Control*, vol. 64, no. 9, pp. 3776–3783, 2019.

[54] S. Weerakkody and B. Sinopoli, "Detecting integrity attacks on control systems using a moving target approach," in *2015 54th IEEE Conference on Decision and Control (CDC)*, 2015, pp. 5820–5826.

[55] C. Schellenberger and P. Zhang, "Detection of covert attacks on cyber-physical systems by extending the system dynamics with an auxiliary system," in *2017 IEEE 56th Annual Conference on Decision and Control (CDC)*, 2017, pp. 1374–1379.

[56] B. D. O. Anderson, "Output-nulling invariant and controllability subspaces," in *IFAC Proceedings*, vol. 8, 1975, pp. 337–345.

[57] A. A. Salah, L. Zhou, L. Li, S. X. Ding, and C. Louen, "Cloud computing-based fault-tolerant control for recovery from performance degradation caused by multiplicative faults," *IEEE Transactions on Control of Network Systems*, pp. 1–11, 2025.

[58] L. Li, H. Luo, S. X. Ding, Y. Yang, and K. Peng, "Performance-based fault detection and fault-tolerant control for automatic control systems," *Automatica*, vol. 99, pp. 389–316, 2019.

[59] H. Luo, X. Yang, M. Kruger, S. X. Ding, and K. Peng, "A plug-and play monitoring and control architecture for disturbance compensation in rolling mills," *IEEE-ASME Trans. on Mechatronics*, vol. 23, pp. 200–210, 2018.

[60] P. Griffioen, S. Weerakkody, and B. Sinopoli, "A moving target defense for securing cyber-physical systems," *IEEE Transactions on Automatic Control*, vol. 66, pp. 2016–2031, 2021.

[61] L. Li, S. X. Ding, M. Zhong, and K. Peng, "Orthogonal projection-based fault detection for linear discrete-time varying systems," *IEEE Transactions on Automatic Control*, 2024.

[62] A. Hoehn and P. Zhang, "Detection of covert attacks and zero dynamics attacks in cyber-physical systems," in *2016 American Control Conference (ACC)*, 2016, pp. 302–307.

[63] D. Mikhaylenko and P. Zhang, "Stealthy local covert attacks on cyber-physical systems," *IEEE Transactions on Automatic Control*, vol. 67, no. 12, pp. 6778–6785, 2022.

[64] R. S. Smith, "Covert misappropriation of networked control systems: Presenting a feedback structure," *IEEE Control Systems Magazine*, vol. 35, pp. 82–92, 2015.

[65] Z. Li, S. X. Ding, L. Li, and Y. Yang, "A novel cyber attack design scheme based on system subspace analysis," *Automatica*, vol. 185, p. 112769, 2026.

[66] J. Wang, F. Yang, T. Chen, and S. L. Shah, "An overview of industrial alarm systems: Main causes for alarm overloading, research status, and open problems," *IEEE Transactions on Automation Science and Engineering*, vol. 13, no. 2, pp. 1045–1061, 2016.

[67] K. Jin and D. Ye, "Optimal innovation-based stealthy attacks in networked LQG systems with attackcost," *IEEE Trans. Cybern.*, vol. 54, pp. 787–796, 2024.

[68] A. Lu and G.-H. Yang, "False data injection attacks against state estimation without knowledge of estimators," *IEEE Trans. Autom. Control*, vol. 67, no. 9, pp. 4529–4540, 2022.

[69] Q. Liu, J. Wang, Y. Ni, C. Zhang, L. Shi, and J. Qin, "Performance analysis for cyber-physical systems under two types of stealthy deception attacks," *Automatica*, vol. 160, p. 111446, 2024.

[70] Q. Zhang, W. Dai, C. Yang, and X. Chen, "Vulnerability analysis for a class of nonlinear cyber-physical systems under stealthy attacks," *Automatica*, vol. 167, p. 111743, 2024.

[71] S. Skogestad and I. Postlethwaite, *Multivariable Feedback Control*. John Wiley and Sons, Ltd, 2005.

[72] K. Manandhar, X. Cao, F. Hu, and Y. Liu, "Detection of faults and attacks including false data injection attack in smart grid using kalman filter," *IEEE Transactions on Control of Network Systems*, vol. 1, no. 4, pp. 370–379, 2014.

[73] N. Ensanefat, M. Kordestani, A. Chaibakhsh, M. Saif, and K. Khorasani, "Secure cyberattack and anomaly detections in the presence of actuators lags and communication delays with application to industrial gas turbines," *IEEE Transactions on Industrial Cyber-Physical Systems*, vol. 2, pp. 130–142, 2024.

[74] K. Zhang, C. Keliris, T. Parisini, and M. M. Polycarpou, "Identification of sensor replay attacks and physical faults for cyber-physical systems," *IEEE Control Systems Letters*, vol. 6, pp. 1178–1183, 2021.

[75] M. Taheri, K. Khorasani, I. Shames, and N. Meskin, "Cyberattack and machine-induced fault detection and isolation methodologies for cyber-physical systems," *IEEE Transactions on Control Systems Technology*, vol. 32, no. 2, pp. 502–517, 2024.

[76] A. Zaman, B. Safarinejad, and W. Birk, "Security analysis and fault detection against stealthy replay attacks," *International Journal of Control*, vol. 95, no. 6, pp. 1562–1575, 2022.

[77] S. Baroumand, A. Zaman, and L. Mihaylova, "Attack detection and fault-tolerant control of interconnected cyber-physical systems against simultaneous replayed time-delay and false-data injection attacks," *IET Control Theory & Applications*, vol. 17, no. 5, pp. 527–541, 2023.

[78] M. Ramadan and F. Abdollahi, "An active approach for isolating replay attack from sensor faults," *European Journal of Control*, vol. 69, p. 100725, 2023.

[79] X. Xue, D. Shen, S. X. Ding, and D. Zhao, "Dual detection framework for faults and integrity attacks in cyber-physical control systems," *arXiv:2510.14052*, 2025.

[80] Y. Kawano, K. Kashima, and M. Cao, "Modular control under privacy protection: Fundamental trade-offs," *Automatica*, vol. 127, p. 109518, 2021.